Synthesis and design of CMOS mixers with carrier feed-through cancellation and output power modulation for wireless communication systems.

By

Alejandro Israel Bautista Castillo

A Dissertation submitted to the academy of Electronics of the Instituto Nacional de Astrofísica Óptica y Electrónica in partial fulfillment of the requirements for the degree of:

MASTER OF SCIENCE ON ELECTRONICS

Instituto Nacional de Astrofísica Óptica y Electrónica

February, 2014

Santa María Tonantzintla, San Andrés Cholula, Puebla, México

Under the supervision of:

Dr. Alejandro Díaz Sánchez

Dr. Luis Abraham Sánchez Gaspariano

"Las ideas de los matemáticos
como las de los pintores o los poetas,
deben ser bellas.
La belleza es el primer requisito:
no hay lugar permanente en el mundo
para unas matemáticas feas... "

Godfrey Harold Hardy.

RESUMEN

TÍTULO:

Síntesis y diseño de mezcladores CMOS con cancelación de portadora y modulación de potencia de salida para sistemas de comunicación inalámbrica.

AUTOR:[1] Alejandro Israel Bautista Castillo

PALABRAS CLAVE:

DESCRIPCIÓN:

El presente trabajo trata sobre la síntesis y diseño de un mezclador pasivo en tecnología CMOS con cancelación de portador y modulacion de potencia de salida, satisfaciendo las exigencias establecidas por los estándares; Bluetooth, banda ultra ancha (UWB) y servicios de comunicación de implantes médicos (MICS).

La simulación en *Mentor Graphics® ICstudio* 2008.2*b* del mezclador armónico para los estándares Bluetooth y UWB con la tecnología UMC 0.18μm Modo Mixto y RF ha sido llevado a cabo. Además, fue diseñado y fabricado un mezclador pasivo en una tecnología de 0.5μm CMOS de MOSIS para el estándar MICS.

Para las propuestas de diseño de la tecnología UMC de 0.18μm tenemos dos diseños, el primero es de salida unica y el segundo es de salida diferencial, ambas propuestas tienen un rendimiento idéntico en Gc con $-6.05dB$, IIP3 de $15.5dBm$ y una variación del ángulo de conducción del 40% al 7%. Sin embargo, el mezclador de salida diferencial tiene un NF de $9.73dB$ que es superior en comparación con el mezclador de salida unica el cual tiene un NF de $7.7dB$. La principal ventaja del mezclador diferencial es que elimina todos los armónicos de f_{LO} y aumenta el rango dinámico. El mezclador propuesto trabaja con el tercer armónico de la fuente de LO, esto ayuda a reducir la frecuencia de la LO para llegar a la banda de Bluetooth. El segundo diseño es para el estándar UWB, en el cual, el comportamiento de los mezcladores propuestos para UWB

[1]INAOE, Coordinación de Electrónica. Diseño de circuitos integrados.

tiene prestaciones idénticas, en Gc con $-6.63dB$, IIP3 del $16.26dBm$ y una variación del ángulo de conducción del 28% al 7%. Sin embargo, el mezclador diferencial tiene $8.6dB$ de NF y el mezclador de salida unica tiene $6.7dB$ de NF. El mezclador propuesto trabaja con el cuarto armónico de la fuente LO, esto ayuda a reducir la frecuencia de LO para llegar a la banda de UWB. En el caso del prototipo fabricado para la tecnología CMOS de $0.5\mu m$ tiene un área de $619.5\mu m$ X $236.5\mu m$. El PCB que se utiliza para la medición fue diseñado y fabricado con un material estándar FR4. El circuito funciona con una señal LO de $393.5MHz$ y una excursion de $\pm 1.65V$, mientras que BB tiene una frecuencia de $10MHz$ con una amplitud de $660mV$. El circuito está polarizado con $\pm 1.65V$ y la f_{BB} es $@10MHz$. La modulación de la potencia de salida se consigue con una tensión de control entre $450mV$ y $1.9V$, obteniendo un mínimo de potencia de salida de $-28dBm$ y una potencia máxima de $5dBm$. Del mismo modo, se demostró que el mezclador de salida unica y el mezclador de salida diferencial tienen el mismo comportamiento en Linealidad, Gc y la modulación de la potencia de salida.

SUMMARY

TITLE:

Synthesis and design of CMOS mixers with carrier feed-through cancellation and output power modulation for wireless communication systems.

AUTHOR:[2] Alejandro Israel Bautista Castillo

KEY WORDS:

DESCRIPTION:

The present work is about the synthesis and design of a passive mixer in CMOS technology with carrier feed-through cancellation and output power modulation, which satisfies the demands established by Bluetooth, Ultra Wideband (UWB) and Medical Implant Communication Service (MICS).

The simulation in *Mentor Graphics® ICstudio* 2008.2*b* of the harmonic mixer for the Bluetooth and UWB standards with the UMC $0.18\mu m$ Mixed Mode and RF CMOS technology have been carried out. Furthermore, was designed and fabricated a passive mixer in a double poly three metal layers $0.5\mu m$ CMOS technology from MOSIS foundry for MICS standard. For the proposed designs for the UMC $0.18\mu m$ technology we have two designs, the first is single-ended and second is differential both proposals have identical performance in Gc with $-6.05dB$, IIP3 of $15.5dBm$ and a variation of the conduction angle from 40% to 7%. However, the differential mixer has an NF of $9.73dB$ which is superior compared to the NF of $7.7dB$ of the single-ended mixer; but the principal advantage of the differential mixer is that it removes all the harmonics of f_{LO} and increases the dynamic range. The proposed mixer works with the third harmonic of the LO source, this helps to reduce the frequency of the LO to reach the Bluetooth band. The second design is for the UWB standard, in the wich, the behavior of the proposed mixers for UWB have identical performance in Gc with $-6.63dB$, IIP3

[2]INAOE. Electronic Department. Integrated circuit design.

of 16.26dBm and a variation of the conduction angle from 28% to 7%. However, the differential mixer has an NF 8.6dB and the NF of the single-ended mixer is 6.7dB. The proposed mixer works with the fourth harmonic of the LO source, this helps to reduce the frequency of LO to reach the band UWB. In the case of the fabricated prototype for 0.5μm CMOS technology the area was 619.5μm X 236.5μm. The PCB used for measurements was designed and fabricated with an standard FR4 material. The circuit works with LO signal of 393.5MHz with a excursions of $\pm 1.65V$, while that BB has a frequency of 10MHz with amplitude of 660mV. The circuit is biased with $\pm 1.65V$ and the f_{BB} is @10MHz. The modulation of the output power is achieved with a control voltage between 450mV to 1.9V, obtaining a minimum power of output of $-28dBm$ and a maximum power of 5dBm. Similarly, it was shown that the differential mixer and single-ended mixer have the same behavior in Linearity, Gc and modulation of the output power.

Contents

List of Figures

List of Tables

Chapter 1

Introduction

Commonly, there are two assumptions in circuit analysis: linearity and time invariation. In general, circuits which don't fulfill these assumptions are not desirable. However, the functionality of any wireless communication system depends on the use of at least one non-linear or time variant circuit, e.g., the mixer. Every transceiver has a mixer whose aim is the frequency translation of the signals involved in the system. Linear and time invariant systems are not capable to generate the translation of the spectral components. So, the mixer must, necessarily, to use either, non-linear or time variant circuits [1].

1.1 Mixer

A mixer is conformed by one output and two input ports, as shown in Figure 1.1. The signal to be translated in frequency is $v_{in}(t)$, and $v_{LO}(t)$ is a square wave or a sinusoidal signal, which is generated in the transceiver (TRX), by a local oscillator (LO). A local oscillator is a device that generates a signal with a given frequency. The frequency translation is accomplished by the multiplication in time domain of $v_{in}(t)$ and $v_{LO}(t)$. By doing this, we obtain:

$$\omega_{RF} \mathrm{x} \omega_{LO} \Rightarrow \omega_{BB} \text{ (down conversion)}$$

$$\omega_{IF} \mathrm{x} \omega_{LO} \Rightarrow \omega_{RF} \text{ (up conversion)}$$

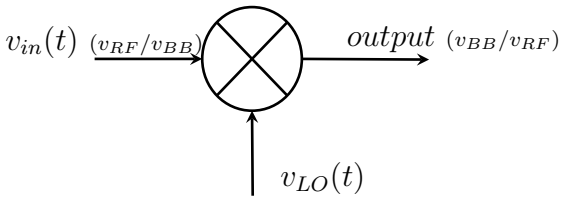

Figure 1.1: Block diagram of a mixer.

where ω_{RF} is the tone at radio frequency, ω_{LO} is the tone of LO and ω_{BB} is the baseband frequency. Thus,

$$output = (Acos(\omega_1 t))(Bcos(\omega_2 t)) = \frac{AB}{2}\left[cos(\omega_1 - \omega_2)t + cos(\omega_1 + \omega_2)t\right] \tag{1.1}$$

where $v_{LO}(t) = Acos(\omega_1 t)$ and $v_{in}(t) = Bcos(\omega_2 t)$, and $\omega_2 \neq \omega_1$

Note that the result yields in a sum and a substraction of $v_{in}(t)$ and $v_{LO}(t)$, with an amplitude proportional to the product of those signals. When the $(\omega_1 + \omega_2)t$ is the component of interest, the circuit is used as an *up-converter* (UC), which in turn is employed in transmitters (TXs). On the other hand, when the component of interest is $(\omega_1 - \omega_2)t$, the circuit is occupied as a *down-converter* (DC), whose function is useful in receivers (RX). Therefore, in (1.1) there is an extra component that is necessary to cancel. In case of an UC, the $(\omega_1 - \omega_2)t$ must be suppressed mean while $(\omega_1 + \omega_2)t$ has to be eliminated on the DC. The unwanted signal in UC or DC mixers is usually called the *image*, and tend to be troublesome, especially in DCs. For a better understanding of this phenomenon, let's take a look of the following trigonometric identity:

$$cos(a - b) = cos(a)cos(b) + sen(a)sen(b) \tag{1.2}$$

if $a = 0$, then

$$cos(-b) = cosb \tag{1.3}$$

In (1.3), it can be noticed that it does not matter if the argument is positive or negative the result will be the same. Terefore, the following relationship arises:

$$Acos(\omega_{IF}t) = Acos((\omega_{in} - \omega_{LO})t) = Acos((\omega_{LO} - \omega_{in})t) \tag{1.4}$$

Thus, if $(\omega_{in}-\omega_{LO})t$ is either, positive or negative, it produces the same intermediate frequency, and consequently when two different tones upper and lower with respect to LO are fed to the DC, the downconversion will contain both overlaped tones, which produces interference in the communication link, and it is prohibitive. Even though each wireless standard imposes restrictions to the emissions produced by the TX, it does not have control over the signals present in the communication channel. Then, the power of image may be larger than the power of the signal, of interest. Therefore, the image frequency is located in

$$\omega_{im} = \omega_{in} + 2\omega_{IF} = 2\omega_{LO} - \omega_{in} \tag{1.5}$$

In consequences the use of circuits which eliminate the image is very important. There are four cases of interest of the image frequency in heterodyne RXs [2]; these are illustrated in Figure 1.2.

1.2 Mixer Metrics

The five Figures of merit (FOMs) of a mixer are [3]:

- Conversion Factor
- Noise Figure
- Ports isolation
- Linearity
- Power consumption

In the following subsections we delve into these.

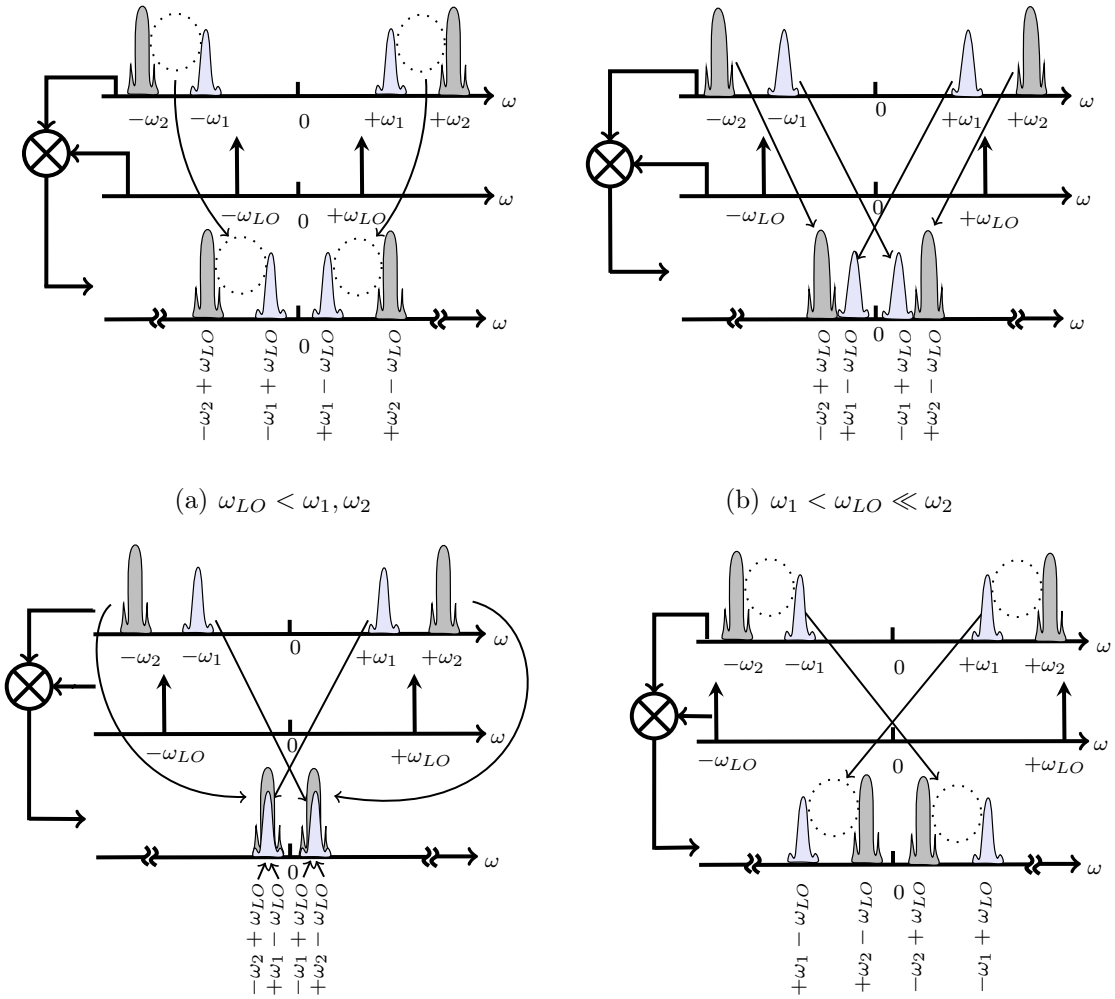

(a) $\omega_{LO} < \omega_1, \omega_2$

(b) $\omega_1 < \omega_{LO} \ll \omega_2$

(c) $\omega_1 < \omega_{LO} < \omega_2$

(d) $\omega_1, \omega_2 < \omega_{LO}$

Figure 1.2: Problem of image in heteroyne down conversion.

1.2.1 Conversion Factor

Conversion Factor is defined as the ratio of the IF output with respect to the input signal value RF. Specifically [3]:

$$Voltage\ \ Conversion\ \ Gain = \frac{r.m.s.\ \ voltage\ \ of\ \ the\ \ output\ \ signal}{r.m.s.\ \ voltage\ \ of\ \ the\ \ input\ \ signal} \tag{1.6}$$

$$Power\ \ Conversion\ \ Gain = Gc = \frac{Power\ \ delivered\ \ to\ \ the\ \ load}{Available\ \ power\ \ from\ \ the\ \ source} \tag{1.7}$$

From the multiplication described in (1.1), the conversion gain is $\frac{B}{2}$, or half the LO amplitude. A high gain conversion is desirable to minimize the noise impact over further stages, ensuring the fed of the signal to the subsequent stages with more power compared with the noise produced by the circuits involved. However, from the point of view of linearity, a large gain is not convenient. Being aware of this trade-off, it is necessary to realize a good design for having a good balance between noise and linearity [4].

1.2.2 Noise Figure

Any communication system is limited by noise [5]. Consider the simplified block diagram of a communication system, as shown in Figure 1.3. The function of a TX is to encode the emmited signals from the source, with the aim of preserve the integrity of the information during its propagation across the channel. In its simpliest form, a channel is a medium which connects the TX and RX. The function of the RX is to extract useful information of the signal and turn it into an adequate form for its use. The first task to be performed, in the RX path, is the amplification of the signal, since it is notoriously attenuated during the propagation. Assume an ideal source (without noise). The signal passing through the channel is only contaminated by the noise from the channel. This, often is a result of the interference, the vanishing of the signal, or the fact that the path of the link may be too long. Therefore, the signal is reduced and weak signals at the RX must be, first, amplified. However, the signal and the noise may have the same energy. A form of measure of the defference of power between the signal and noise, is with the signal-to-noise ratio (SNR), which is calculated by dividing the signal power between the noise power. This is an important datum to take into account in a communication system. For example, the typical requirements of the SNR for various applications are [5]:

- +15 dB for radar.

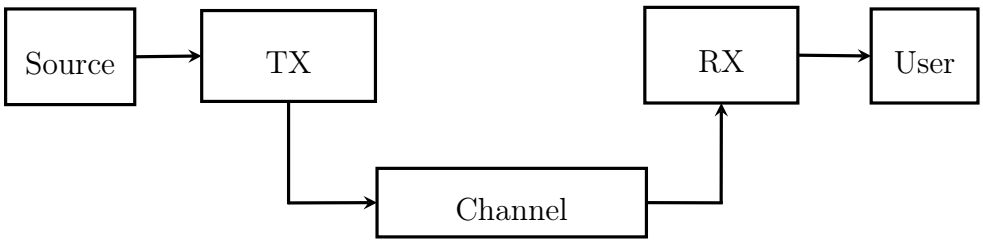

Figure 1.3: Simplified diagram of a communications system.

- +18 dB for cellular telephony.
- +30 dB for broadcast communication.

Hence, in any communications system, the intrinsic and extrinsic noise has double importance and it is necessary to establish: A minimal level of signal that is able to be processed, and consequently the maximum range of the communication system; The capacity of the channel, i.e., the highest ratio at which the information can be transmitted with zero error probability, that strongly depends on its output SNR [5].

The magnitude of noise can be expressed by means of the noise factor (F), it is a single value that characterizes the noise of a two-ports system, provided that the impedance of the source is given. Without this information, this parameter is worthless, since the noise factor is conceptually based upon the comparison between the noise of the two-ports system and the noise of the source signal [6]. F is obtained from dividing the input SNR_{in} by the output SNR_{out}. F indicates how degraded is the SNR_{in} due to the channel, RX and TX [2]. Mathematically, the noise factor is determined as follows [5]:

$$F = \frac{SNR_{in}}{SNR_{out}} = \frac{S_i}{N_i}\frac{N_o}{S_o} \tag{1.8}$$

where S_i, S_o are the available power from the signals at the input and output ports. Similarly, N_i and N_o represent the available noise power at the input and output ports.

If the system is noiseless, then SNR_{in}=SNR_{out}. This is because both, the input signal and the noise signal are amplified by the same factor and any additional noise does not

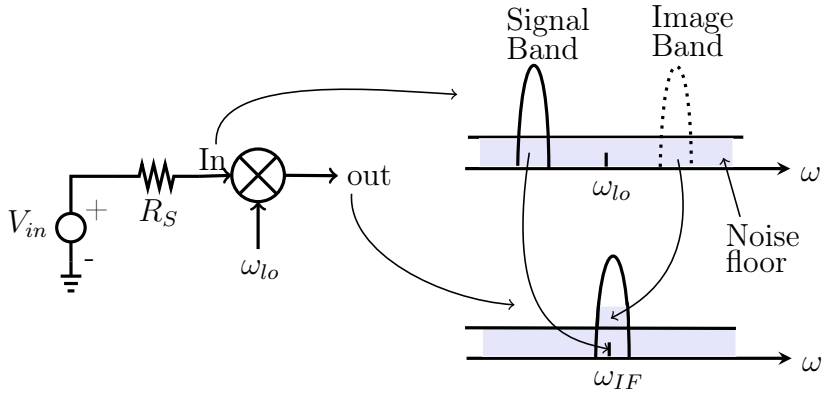

(a) Single sideband (SSB) NF.

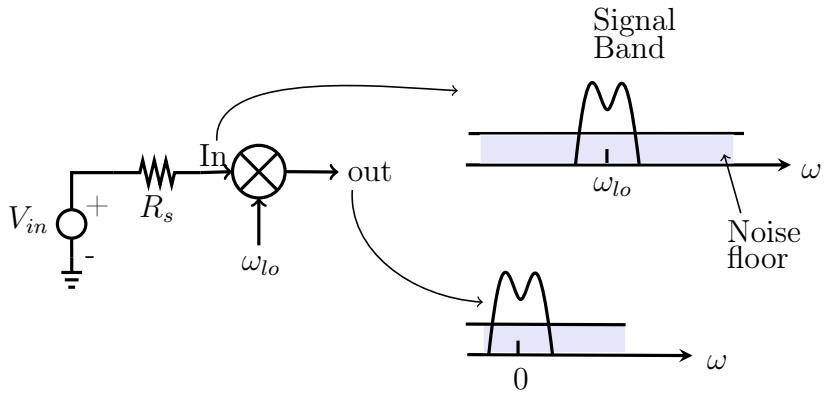

(b) Double sideband (DSB) NF.

Figure 1.4: Noise Figure in a mixer.

interfer. In this way, ideally, the noise factor would be:

$$F = 1, \qquad NF = 0dB \tag{1.9}$$

where F is noise factor while NF is the Noise Figure and is given in decibels (dBs). The NF analysis of a mixer is commonly confusing. To simplify the analysis it is considered an ideal unity gain mixer (noiseless), as shown in Figure 1.4(a). The spectrum at the input of the mixer consists of a signal component accompanied by thermal noise, which can be modeled by the source impedance (R_S); the noise can be considered constant along the electromagnetic spectrum. Therefore, in the signal band as in the image band, the noise has the same magnitude [7]. When the frequency translation is performed, the signal, the signal band noise and the image band noise are translated

to ω_{IF}. Consequently, SNR_{out} is the double of SNR_{in}. Therefore, the noise figure of an ideal mixer is $3dB$ [8]. This quantity is obtained from a single band case. Now, consider the mixer shown in Figure 1.4(b). In this case, only the noise in the signal band is translated to the baseband, thereby yielding equal input and output SNR when the mixer is noiseless. The NF is thus equal to $0dB$. This quantity is called the double sideband noise figure to emphasize that the input signal resides on both sides of ω_{LO}. In summary, the SSB NF of a mixer is $3dB$ higher than its DSB NF if the signal and image bands experience equal gains at the output port of the mixer.

1.2.3 Linearity

Most of the blocks of a communication system are purely non-linear, some of them more than others, generating different distortion levels. The distortion occurs when the output signal does not have a linear relation with respect to the input signal. For example, If the input signal in a system is a sinusoidal signal, ideally the output signal will also be a pure sine, i. e.

$$V_{in}(t) = V_{in}Sin(\omega_0 t + \varphi) \quad \Rightarrow \quad V_{out}(t) = \alpha V_{in}Sin(\omega_0 t + \varphi) \tag{1.10}$$

where α is the gain. Nevertheless, due to the fact that the system is not linear, we have:

$$V_{out}(t) = \alpha_1 Acos(\omega t + \varphi) + \alpha_2 A^2 cos^2(\omega t + \varphi) + \alpha_3 A^3 cos^3(\omega t + \varphi) + ... \tag{1.11}$$

It is important to mention that the expression 1.11 is valid for a memoryless weak nonlinear system. By applying a Taylor series decomposition to (1.11), it is obtained

$$V_{out}(t) = \frac{\alpha_2 A^2}{2} + \left(\alpha_1 A + \frac{3\alpha_3 A^3}{4}\right) cos(\omega t + \varphi) + \frac{\alpha_2 A^2}{2} cos(2\omega t + 2\varphi) + \frac{\alpha_3 A^3}{4} cos(3\omega t + 3\varphi) + ... \tag{1.12}$$

where $cos(\omega t + \varphi)$ is the desired component, and $cos(n\omega t + n\varphi)$ (with $n = 2, 3, 4...$) are the harmonics that generate unwanted frequency components, i.e distortion. Figure

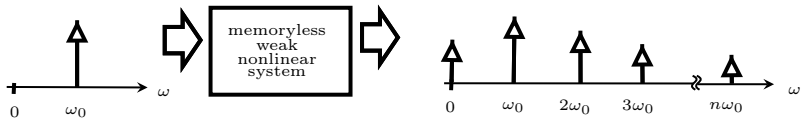

Figure 1.5: Frequency components produced by a memoryless weak nonlinear system.

1.5 depicts the spectrum at the input and output of a nonlinear system expressed in (1.12). Not just this, but also we see that $cos(\omega t + \varphi)$ is affected by one portion of the energy in $cos(3\omega t + 3\varphi)$. Therefore, the linearity is an important parameter that specifies the ability of a circuit to manage large signal swings.

The mixer is one of the most frequency product generators due to the multiplication performed to translate the signals in frequency. The most important distortion component in the mixer is the intermodulation (IM) distortion, which is generated by the unwanted product of two or more frequencies, i. e. , when two or more different tones are fed to the input port, the distortion generated by these, contains IM distortion. This is illustrated in Figure 1.6, it can be seen that the frequencies $(2\omega_1 - \omega_2)$, $(2\omega_2 - \omega_1)$ are the third order IM (IM3), which are of particular interest because they transferred some energy to the fundamental, hence, by increasing the power of the input signal more energy will be transferred to the fundamental, which causes a large distortion in the signal of interest. Moreover , these harmonics are the closest to the fundamental and if they have too much energy around it, this could interfer the fundamental signal; for this reason, it is defined a parameter to characterize this behaviour, denominated third order Intersection Point (IP3). This parameter is measured using two pure sinusoidals with equal amplitudes applied to the input. The amplitude of the output of the IM products is normalized in terms of the fundamental at the output. The result can be expressed as:

$$Relative \;\; IM = 20log\left(\frac{3}{4}\frac{\alpha_3}{\alpha_1}A^2\right) dBc \tag{1.13}$$

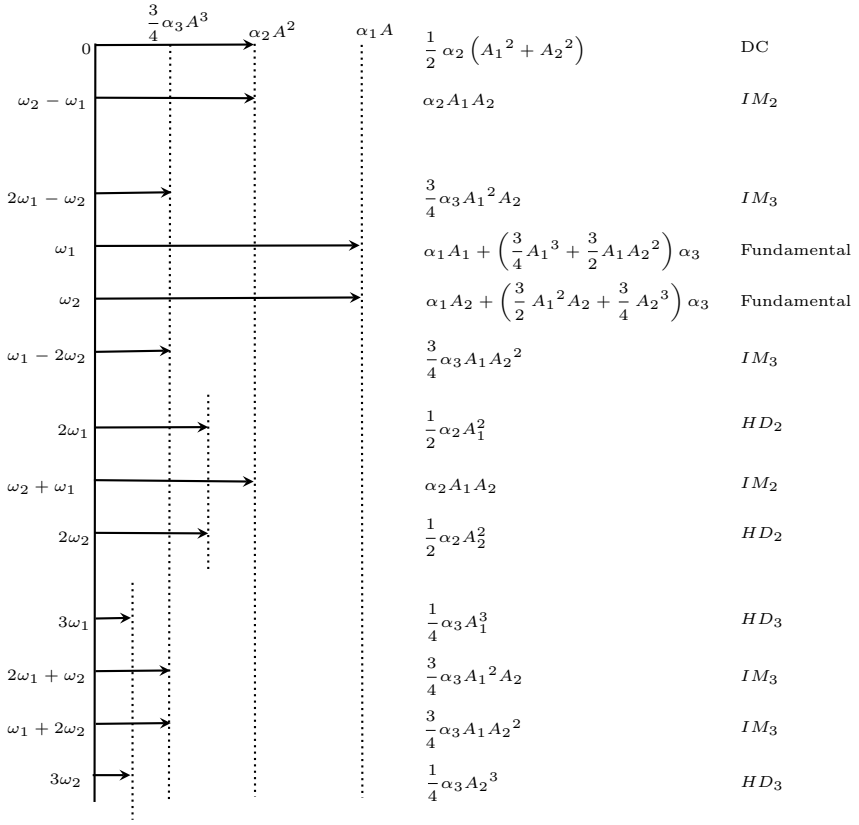

Figure 1.6: Frequency components of a two tones input in a memoryless weak nonlinear system.

The IP3 is defined as the intersection of the two lines as shown in Fig. 1.7. The horizontal coordinate is the input IP3 (IIP3) and the vertical one is the output IP3 (OIP3).

To determine the IIP3, we make:

$$|\alpha_1 A_{IIP3}| = \left|\frac{3}{4}\alpha_3 A_{IIP3}^3\right| \tag{1.14}$$

obtaining

$$A_{IIP3} = \sqrt{\frac{4}{3}\left|\frac{\alpha_1}{\alpha_3}\right|} \tag{1.15}$$

This ratio is very helpful for checking distortion levels in simulations and measurements [2].

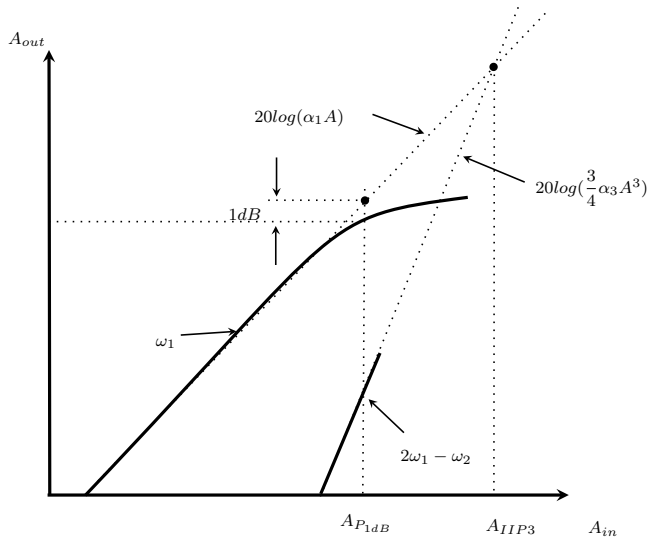

Figure 1.7: Definition if IP3 (for voltage quantities).

1.2.4 Ports isolation

Every device has parasitics elements which can create direct paths from one point to another. In the mixer, coupling between the RF, LO and BB ports generates different effects, the most important are [2]:

- LO-to-RF leakage, which will cause self-mixing problem in direct conversion. Due to the nonzero reverse gain of low noise amplifier, the LO leakage may even reach the antenna through the low noise amplifier.
- LO-to-IF feed through may cause desensitization of the blocks in front of the mixer.
- RF-to-LO feed through allows interferers and spurs present in the RF signal interact with the LO.
- RF-to-IF feed through may cause problems in direct conversion architecture due to the low-frequency even-order inter-modulation product.

As can be noted in Figure 1.8 there are six possible paths between the three ports, however, as shown in Table 1.1 there are four possible combinations with respect to

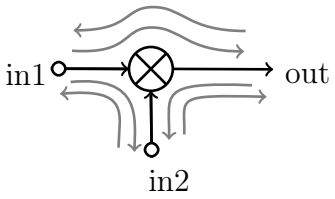

Figure 1.8: Ports isolation concept.

Table 1.1: Ports isolation.

isolation	down conversion	up conversion
in2-in1	LO ⇒ RF	LO ⇒ BB
in1-in2	RF ⇒ LO	BB ⇒ LO
in1-out	RF ⇒ IF	BB ⇒ RF
in2-out	LO ⇒ IF	LO ⇒ RF

conversion. Depending on the conversion type, only two are of interest. Basically, the signal having the higher frequency is the one that will have influence on the other two, and this can be negative if the the presence of this frequency is undesirable.

1.2.5 Power consumption

The power consumption of a mixer is defined as the power provided by the bias supply in order to perform the frequency translation of the signals involved. This parameter is delimited by the applications in which is goin to be used. For example, if the mixer is used in mobile applications, the consumption must be low, to ensure a long life battery. Also, a mixer with a high NF increases the requirements of gain of the low noise amplifier, then, its power consumption is increased [6].

1.3 Mixer in modern wireless technologies

As seen in the previous sections, the performance of the mixer is determined by noise, lineality, losses, power consumption and isolation ports. Nevertheless, as technology

evolves, this requirements are under stringent demands. However, requirements change depending on the communication standard on which the mixer will be applied. For example, The design of ultra wideband (UWB) transceivers faces the following issues [9]:

1. The need for broadband circuits and matching
2. Gain switch in the low-noise amplifier without degrading the input match
3. Broadband transmit/receive switch at the antenna
4. Desensitization due to Wireless local area networks (WLAN) interferers

With a $528MHz$ channel bandwidth, the RX and TX paths of UWB systems may naturally employ direct conversion. Typical direct-conversion issues plague the receive path, except that flicker noise negligibly affects the signal. Also, the TX side is free from injection pulling of the oscillator by the output stage because the transmitted level falls below $41dBm/Hz$. Therefore, the characteristics of the RX depending on the bit rate, MBWA specifies RX sensitivities ranging from $84dBm$ (for $55Mb/s$) to $73dBm$ (for $480Mb/s$). With a required SNR of about $8dB$, these specifications translate to an NF of $6-7dB$. The RX must provide a maximum voltage gain of approximately $84dB$ so as to raise the minimum signal level to the full scale of the baseband A/D converter. Also, based on the interference expected from IEEE 802.11a/g transmitters, a 1-dB compression point (P_{1dB}) of $-23dBm$ (in the high-gain mode) is necessary.

All these requirements are due to the high bandwidth. In contrast, if we analyze the requirements of the design of transceivers for implantable medical devices, we find [10]:

1. Low power consumption during $400MHz$ communication is required. Implant battery power is limited, and the impedance of implant batteries is relatively high. This combination limits peak currents that may be drained from the supply. During communication sessions, current should be limited to $< 5mA$ for most implantable devices.

2. Limiting medical implant communication service (MICS) devices to a maximum of $-16dBm$ equivalent isotropically radiated power (EIRP) in a reference bandwidth of $300kHz$ to prevent interference to meteorological aids

3. To avoid a false activation, the implanted device should use techniques such as requiring activation by a strong magnetic field

MedRadio devices operating in the 401-406 MHz range have a bandwidth limitation of up to $300kHz$, a maximum range of $> 2m$ because the MICS band is designed to improve upon the very-short-range inductive link. The implanted unit has a power into Antenna of $-2dBm$ with a TX power at the surface of the skin of $-33dBm$ and an SNR of $14dB$. Therefore, there is a noise on the order of $-121dBm$, leading to a $9dB$ of NF. Another example would be BLUETOOTH, this standard has a operating frequency of $2.4GHz$, bandwidth of $1MHz$, noise figure of $10dB$ and a power transmission of $10dBm$. The linearity requirement is calculated using the maximum level of co-channel interference and the adjacent channel blockers [11]. It adds a margin of 3 dB, giving a requirement equal to-16dBm IIP3.

In table 1.2 different parameters of diverse standards are shown. It can be observed that the lowest TX power is the UWB, this means that the NF must be lower than $3dB$. on the other hand, BLUETOOTH has much higher power and consequently may be more flexible with the NF. However the NF in MedRadio is very important because its transmission power is very low. therefore, the signal is close to the noise floor. For this reason it is necessary that the device contributes to least amount of noise. Moreover, the bandwidth of UWB is much larger than the one for BLUETOOTH and MedRadio. Therefore, lineality is a very important issue in UWB. The power consumption is more importan in MedRadio because the battery long life requirement. Summarizing, UWB needs a mixer with a high gain conversion. a high lineality and a low noise figure. On the contrary, BLUETOOTH requirements are not so demanding. For the case of MedRadio, most important demands are power consumption and NF.

Table 1.2: Salient features of diverse wireless technologies.

Technologies	Standard	Protocol	Range	Applications	Band RF	Channel number	Modulation Type	EIRP	BER	Data rate	Duplex Mode	Multiple Access
BLUETOOTH	802.15.1	PPP,TCP/IP, OB EX WAP	1 a10m	Multimedia among Mobile Devices	2.4 GHz	79	FHSS:GFSK	0 a 20 dBm	0.1-0.01 %	1 a 24 Mb/s	TDD	TDMA
UWB	802.15.3a 802.15.4a	NA	10m	Radars videoconferencing Military Applications	3.1 a 10.6 GHz	14	PPM PAM ASK	-41 dBm/Hz	10e-5	480 MB/s	OFDM	CDMA OFDM
RFID	ISO 18000	NA	3m	identification	2.4 GHz	1	FSK	-90 dB	10e-5	106 kb/s	FDD	Varios
WIFI	802.11	NA	70 a 150m	Internet	2.4 GHz	11	64QAM 16QAM B-PSK QPSK	20 dBm	10e-5	300 Mbps	FDD	
WIMAX	802.16		70km	Internet TV Telephony	10-66 GHz	20 a 100	QPSK 16QAM 64QAM	30 dBm	10e-5	124 Mb/s	TDD FDD	OFDM OFDMA
3G	IMT-2000	UMTS, HSDPA EDGE CDMA2000	25km	Cell Phones	850, 1700, 1900 y 2100 MHz	640 a 1520	QPSK	3-12 dBm	10e-5	2 Mb/s	FDD TDD	TDMA
MBWA	802.20	TCP/IP	2.5km	Internet	5.5 GHz	520833 a 2083333	64QAM	8-12 dBm	10e-5	64 Mb/s	FDD TDD	SDMA
GEO	NA	NA	Global	Telephony TV Military	C Ka	1800	QPSK FM FDM	-49 dBW	10e-5	32 Mb/s	OFDMA	FDMA TDMA
LEO	NA	NA	Global	Telephony tracking	C Ka, L	800	QPSK	-49.4 y -53 dBW	10e-5	200 Mb/s	TDD	NA
MEO	NA	NA	Global	Telemetry GPS	C Ka, Ku	1800	QPSK	-49 y -53 dBW	10e-5	64 Mb/s	TDD	NA

1.4 Conclusion

The mixer is a complex circuit whose important features include; Gain conversion, Noise Figure, Lineality, Port Isolation and Power Consumption. This five FOMs are important, however, the mixer is an element that generates a lot of distortion, therefore it is necessary to take special care if the mixer if it is used in broadband systems. Nevertheless, if it occupied in systems where the TX power is low, the NF is very important. In sum, before designing a mixer, it is necessary to know the requirements of the standard in which it is going to be placed, because there are diverse trade-offs among each of the FOMs, which can not be ignored.

Chapter 2

Harmonic Mixer

2.1 Introduction

As mentioned in the previous chapter, only nonlinear or time variant systems can function as a mixer. In other words, there exist two ways to implement a mixer: by means of non-linear devices, which is the case of active mixers or using switched circuits, like in passive mixers. On one hand, active mixers present a higher gain compared to passive mixers but their linearity is more degraded. On the other hand, passive mixers exhibit a better linearity than their active counterparts; unfortunately, due to the lack of gain in the switches, their conversion factor is rather low. However, simplicity and higher frequency operation is inherent to passive structures. Thus, they have good characteristics for multiple communication standards ranging from a few MHz to tens of GHz.

2.2 Passive mixers

In passive mixers all transistors work as switches. Then, the multiplication of the signals is performed only with time-variant systems. Some structures of the passive mixers operate in the continuous time domain and some structures operate in the sampled data domain [12]. A passive mixer that operates in the continuous time mode

is denoted as a switching mixer. On the other hand a passive mixer that operates in sampled data domain is called a sampling mixer. Because of its sampling nature, a sampling mixer can also operate in the subsampling mode. Structurally a switching mixer is usually terminated with a resistor and may or may not have a capacitor. On the contrary, a sampling mixer is always terminated only with a capacitor. A variant of the passive mixer are the harmonic mixer, such mixer has the ability to transfer information to the frequencies established by LO. Another variant is the subharmonic mixer, and this kind of mixer has the same function as the harmonic mixer, with the advantage that they have a transconductance stage.

2.3 Harmonic Mixer

If the two inputs of a mixer are denoted by ω_1 and ω_2, the output signal consists of two main components, the sum for up-conversion and subtraction for down-conversion.

$$\omega_{out} = \omega_1 \pm \omega_2 \tag{2.1}$$

In contrast, the harmonic mixers provide the sum or difference frequency at harmonic multiples of one of the two inputs. Hence [13].

$$\omega_{out} = n\omega_1 \pm \omega_2 \tag{2.2}$$

where $n = 1, 2, \ldots, N$ is an integer number. As a special case when $n = 1$, it is obtained the fundamental, and ω_1 is LO, i. e. a harmonic mixer is a device where a band limited signal is mixed with one of the high order harmonics generated by the local oscillator. An output signal is obtained whose frequency is the sum/difference between a harmonic of the local-oscillator and the BB/RF signal [14]. This is why it is necessary that LO contains a large amount of energy distributed along the electromagnetic spectrum. Therefore, it is desirable that LO be a square wave. Figure 2.1 shows the spectrum obtained from a harmonic mixer.

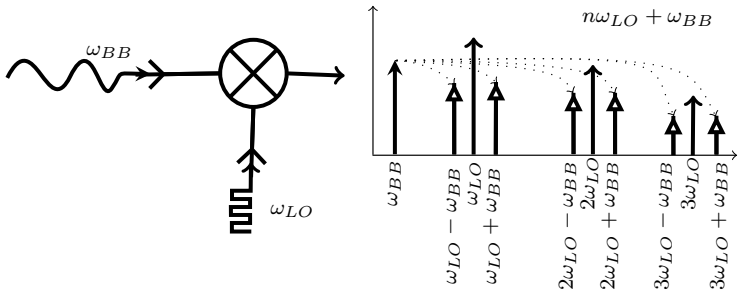

Figure 2.1: Spectrum of a harmonic up-conversion mixer.

Historically, harmonic mixer has been used primarily at the high frequencies where reliable and stable LO sources are either not available or prohibitively expensive. Sometimes, these devices are used in frequency-multiplier design by means of phase loop oscillators (PLOs) or as external mixers of spectrum analyzers [15]. Although theoretically any LO harmonic can be used, second and third order are the most common, since the conversion loss is increased with higher orders [14].

2.3.1 Unbalanced Harmonic Mixer

The operating principle of the harmonic mixer can be explained using Figure 2.2. As can be seen, it is a switch which is controlled by V_{LO}, as a result, the signal is transmitted intermittently from the input to the output node of the switch. Since the switch passes or interrupts the signal, this action can be expressed as

$$V_{LO}(t) = \begin{cases} 1, & 0 < t \leq \dfrac{T}{2} \\ 0, & \dfrac{T}{2} < t \leq T \end{cases} \tag{2.3}$$

From equation 2.3, if we make the assumption that half of the period of V_{LO} the switch is on and the other half it is off, 2.3 can be expressed in a Fourier series. Consequently, the output of the switch is the signal that is multiplied by the input control signal, i.e. [12]:

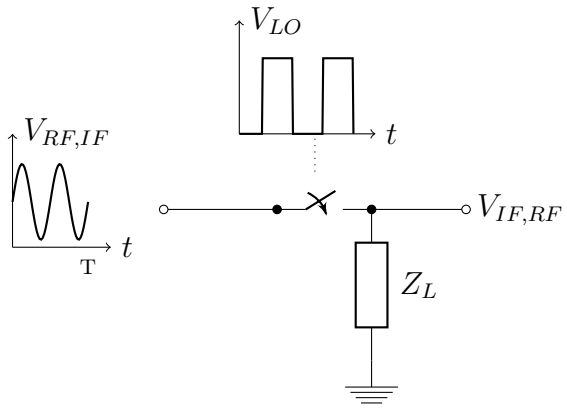

Figure 2.2: Ideal harmonic mixer.

$$V_{IF,RF}(t) = \underbrace{V_{RF,IF}cos(\omega_{RF,IF}t)}_{V_{RF,IF}} \underbrace{\left(\frac{1}{2} + \sum_{n=1}^{\infty} \frac{sin\left(\frac{n\pi}{2}\right)}{\frac{n\pi}{2}} cos(n\omega_{LO}t)\right)}_{V_{LO}} \tag{2.4}$$

From Equation 2.4, it can be noted that V_{LO} contains an infinite number of harmonics. Therefore, because LO contain an infinite number of harmonics spread across the spectrum, the signal which is multiplied by LO is translated along the spectrum. Products of interest for up-conversion and down-conversion are:

$$\underbrace{V_{IF} = \frac{2V_{RF}}{n\pi} cos(\omega_{RF} - n\omega_{LO})}_{down-conversion} \qquad \underbrace{V_{RF} = \frac{2V_{IF}}{n\pi} cos(\omega_{IF} + n\omega_{LO})}_{up-conversion} \tag{2.5}$$

Linearity

The harmonic mixer has rather linear elements. Therefore, the frequency conversion is done by a time variant circuit, in this case the switch [12]. In the previous chapter, it was established that the $IIP3$ is the measure which characterizes the linearity of a device, for three main reasons. First, the IM3 is the harmonic closest to the fundamental harmonic. Second, The IM3 grows cubically in contrast to the fundamental harmonic. Finally, 9/4 of the energy of the IM3 is ceded to the fundamental harmonic. Because of all these reasons it is needed to know where the IM3 is located. It was also defined,

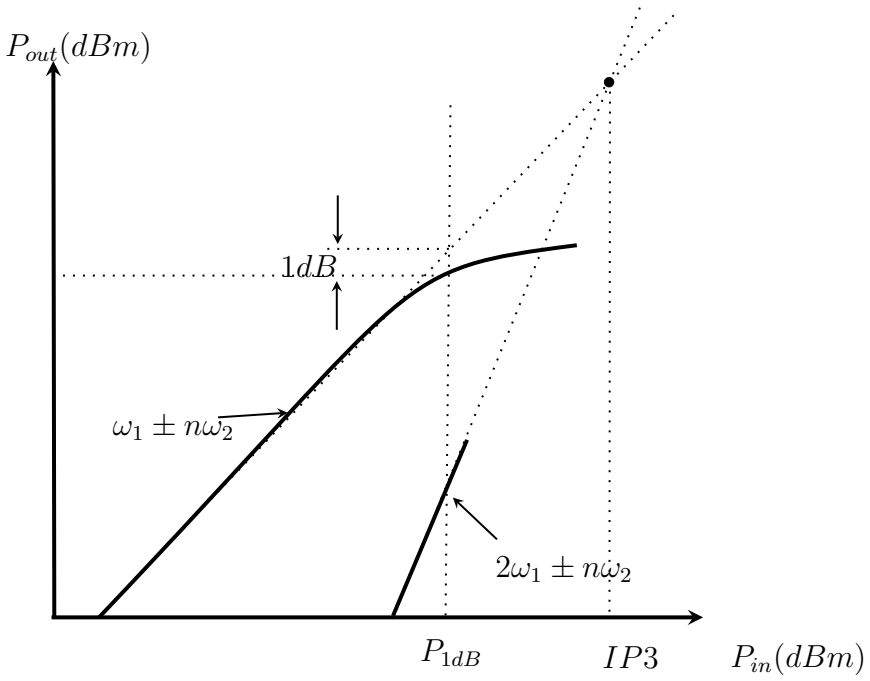

Figure 2.3: IP3 definition for a harmonic mixer.

as the products of third-order intermodulation:

$$IM_3 = 2\omega_1 \pm \omega_2 \qquad or \qquad 2\omega_2 \pm 2\omega_1 \tag{2.6}$$

where ω_2 is LO. Therefore, in the harmonic mixer, the IM3 is given acording to n. Hence:

$$IM_3 = 2\omega_1 \pm n\omega_2 \qquad or \qquad \omega_1 \pm (1+n)\omega_2 \tag{2.7}$$

where n is the n-th harmonic component. Thus, the graph from which the $IIP3$ is obtained is shown in Figure 2.3.

Conversion factor

The harmonic mixer does not exhibit gain since there is no active elements on it. In fact, it presents losses who increase as long as n increases [13]. If we apply (1.7) we obtain for the circuit on Figure 2.2:

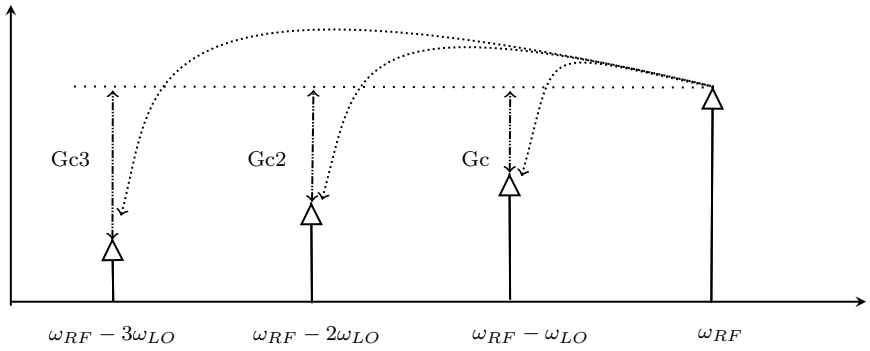

Figure 2.4: Spectrum of down conversion harmonic mixer with Gc.

$$G_c = \frac{2}{n\pi} \tag{2.8}$$

Then, if we occupy the first harmonic (n=1) Gc will have a minimum loss, as shown in Figure 2.4.

Noise figure

The noise factor is a measure of the degradation of the SNR of the input port of a system caused by the components. Since the harmonic mixer presents a conversion loss, special care with noise must be taken due to the significant degradation it implies [16]. The noise factor is calculated using (1.8), by doing the maths, it is obtained:

$$F = 1 + \frac{Nmix}{Nin\ G_c} \tag{2.9}$$

where N_{in} is the input noise of the mixer, N_{mix} is the noise generated by the mixer and G_c is the conversion factor. Thus, substituting (2.8) into (2.9) we have

$$F = 1 + \frac{Nmix\ n\pi}{2Nin} \tag{2.10}$$

Therefore, the F increases as the harmonics are increased. So, it is not recommendable to use very high order harmonics due to the increment in NF. Similarly, the losses are large. However, the linearity performance is good because the system does not

increase the non-linearity, so it is recommendable to use the first three harmonics to not degrade the performance of the mixer [17].

A drawback of the harmonic mixer in TX is the need to filter the low-order tones. This because these components can interfere with other bands. For this reason, a bandpass filter is necessary in the output of the harmonic mixer.

Single-Device based Harmonic Mixer

Figure 2.5 shows the circuit diagram of a harmonic mixer which is implemented with a diode D [15]. On the input port, V_{RF} is fed to a short-circuited stub[1] labeled as $(\frac{\lambda}{4}@RF)$, which allows to pass the signal through at the same time that stops V_{IF}. Similarly, the ports labeled as V_{LO} and V_{IF} have an open-circuited stub labeled as $(\frac{\lambda}{4}@LO)$, which allows V_{LO} and V_{IF} to pass through, but signal is not received at V_{RF}. A diplexer is composed of two filters, a low pass filter implemented with $L1$, $L2$, $L3$, and $C3$, and a high-pass filter implemented with $C1$, $C2$ and $Tlin$. This is used to inject the V_{LO} signal and to extract it from V_{IF}. An inductance ($L3$) to ground in the low pass filter is used as the return of DC.

Despite the fact that the diode is a nonlinear element, the mix is made using a time variant system. This is because the diode can function as a switch which passes a signal if it is forward biased or interrupt the passage of the signal if it is reverse biased. With this result, if V_{LO} has enough energy to make the diode change from one state to another, V_{RF} is intermittently in the cathode of the diode [15].

The port isolation, depends basically on the diplexer and the $\frac{\lambda}{4}@RF$ and $\frac{\lambda}{4}@LO$, stubs. So, the isolation between LO and IF ports is better than 47 dB thanks to the diplexer, and more than 50 dB of LO to RF isolation [15]. The NF of this mixer is inversely proportional to its Gc and directly proportional the noise generated by the devices [15], Thus, the diode is the only element that generates noise, which is modeled by [5]:

[1] In microwave and radio-frequency engineering, a stub is a length of transmission line or waveguide that is connected at one end only. The free end of the stub is either, an open-circuit or (especially in the case of waveguides) a short-circuited [18]

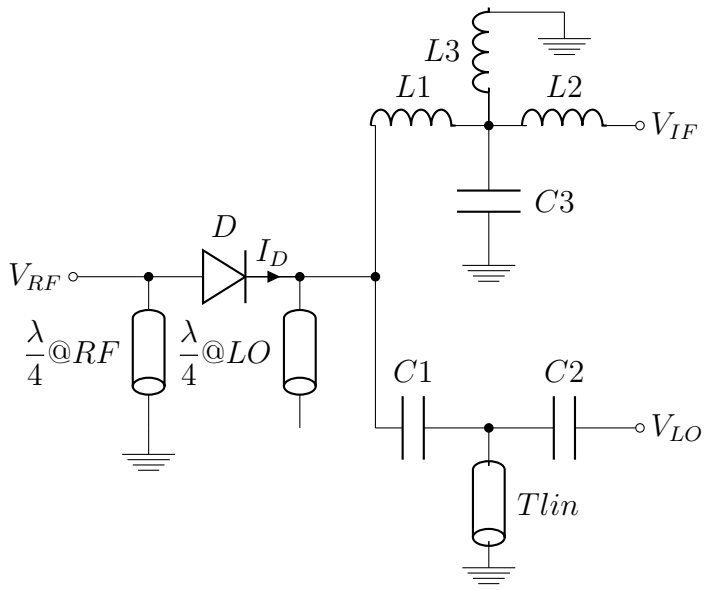

Figure 2.5: Harmonic mixer scheme.

$$V_{n_D}^2 = 2kTr_D \tag{2.11}$$

where $V_{n_D}^2$ is the noise generated by the diode, k is the Boltzmann constant ($k \approx 1,3806504x10^{-23}J/K$), T is the temperature in Kelvin degrees (at room temperature $T \approx 298K$) and r_D is the resistance of the diode, which is given by

$$r_D = \frac{kT}{qI_D} \tag{2.12}$$

where q is the magnitude of the charge of an electron (the elementary charge) and I_D is the current flowing through the diode and is given by

$$I_D = Is\left(e^{\frac{V_{RF}-V_{LO}}{nVt}} - 1\right) \tag{2.13}$$

and Is is the saturation current (approximately $10^{-12}A$); n is the coefficient of emission, dependent on the manufacturing process of the diode and that tends to take values between 1 (for germanium) and the order of 2 (for silicon); Vt is the thermal voltage

Table 2.1: MOSFET capacitances in different regions.

Operating region	C_{GB}	C_{GD}	C_{GS}
Cutoff	$C_{ox}WL$	C_{ov}	C_{ov}
Triode	C_{ovB}	$1/2C_{ox}WL$	$1/2C_{ox}WL$
Saturation	C_{ovB}	C_{ov}	$2/3C_{ox}WL$

($\approx 25.85mV$) at $300K$. Therefore, the noise generated by the mixer is proportional to the voltage difference applied in the mixer.

The mixer diode is frequently used in cost-critical applications such as radio or television receivers, where low cost is more important than a good performance [19]. The diode mixer is suitable for microwave applications, such as speed guns and automatic doors shopping centers. The diode in the RX is simply mounted on the antenna.

Figure 2.6 shows a harmonic mixer implemented with CMOS technology [12]. The principle of operation is similar to the mixer shown in Figure 2.5. With the result that, if V_{LO} is positive, the transistor passes the signal, so that $V_{IF} = V_{RF}$. When V_{LO} is zero, the transistor is turned off, therefore, $V_{IF} = 0$. This mixer still satisfies (2.5). Hence, the conversion factor is inversely proportional to the number of harmonics employed. When V_{LO} is positive, the MOS transistor behaves like a linear resistor, so that this element does not contribute with nonlinearities to the circuit. One advantage of this topology is that a diplexer is not necessary to separate the signals. However, the port isolation is troublesome since there is no resonant network which helps to avoid parasitic coupling. The MOS transistor may be modeled by their parasite elements as shown in Figure 2.7. Where the capacitances of interest are C_{GS} and C_{GD}, which are those that create direct paths between the three ports of the MOS. The value of these capacitances depends on the region of operation and the size of the transistor. Table 2.1 shows the equations of these capacitances.

As shown in the table, the equations of the capacitances of interest when the transistor is turned off, depends on the overlap capacitance, C_{ov}, which may be negligible. Hence, in this region the coupling between the ports is null. However, when the transis-

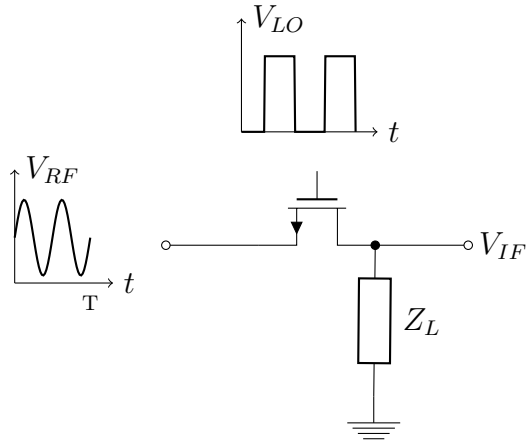

Figure 2.6: Unbalanced harmonic mixer.

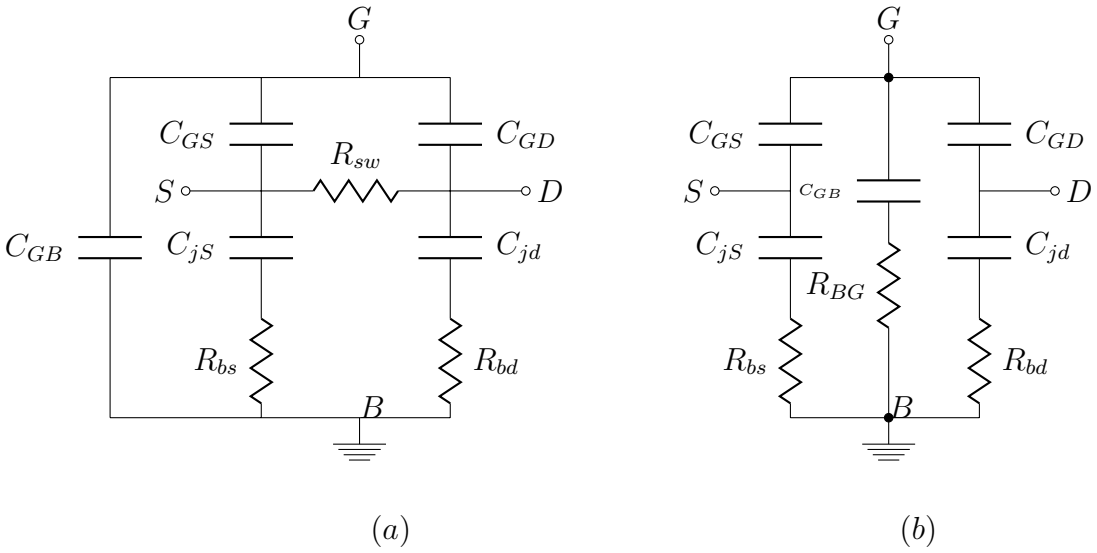

Figure 2.7: Equivalent circuit of a MOS switch; a) on b) off.

tor is conducting, the capacitances are directly proportional to the area of the transistor, this is why one has to take special care with the design of the harmonic mixer with MOS transistors.

With respect to the noise generated, it is found that the noise model of the MOS transistor in the linear region is [5]:

$$V_{n,th}^2 = 4kT\frac{1}{g_{DS}} \tag{2.14}$$

where $V_{n,th}^2$ is the noise generated by the MOS transistor in the linear region, and $\frac{1}{g_{DS}}$ is the resistance of the MOS transistor, which is given by

$$g_{DS} = \mu C_{ox}\frac{W}{L}(V_{GS} - V_{th}) \tag{2.15}$$

where W is the width and L is the length of the transistor, C_{ox} is the capacitance of the gate, μ is the mobility of the electrons, V_{th} in the threshold voltage and V_{GS} is the voltage difference between gate and source terminals. Hence, it is inferred that the noise generated by the transistor is directly proportional to its length and inversely proportional to the width of the transistor and the V_{GS}, as a result, to reduce noise is favorable to work with, V_{GS} large and minimum lengths and large widths.

With respect to linearity, the MOS transistor operates in the linear region, in this region the device can be modeled as a resistance whose value is given by

$$R_{SW} = \frac{1}{\mu C_{ox}\frac{W}{L}(V_{GS} - V_{th})} \tag{2.16}$$

For this reason, the mixer implemented with transistors in the linear region does not contribute with distortion. Hence, the harmonic mixer has superior performance in terms of linearity.

2.3.2 Balanced Harmonic Mixer

Of all the harmonics that are present at the output of the mixer only one is of interest, for upconversion it is $(\omega_{LO} + \omega_{BB})t$ and for downconversion it is $(\omega_{LO} - \omega_{RF})t$. This means that there are minimum three harmonics that will not be utilized (ω_{LO}, ω_{RF} and $(\omega_{LO} - \omega_{RF})t$ for upconversion and $(\omega_{LO} + \omega_{RF})t$ for downconversion); therefore, it's necessary a filter at the output of the mixer to remove the unwanted harmonics, this represents extra costs in terms of area and price. A solution for not using filters is to balance the mixer. This will eliminate some of the unwanted harmonics [20]. The

balanced mixer uses differential signals, the differential signals have a difference of 180^0 with respect to each other. The final signal value is obtained by subtracting these signals, i. e.

$$V_{out}(t) = \alpha_1 A cos(\omega t + \phi) + \alpha_2 A^2 cos^2(\omega t + \phi) + \alpha_3 A^3 cos^3(\omega t + \phi) \tag{2.17}$$

where α is the gain of the system and A the amplitude of the signal. If we subtract equation (2.17) by itself but with a different phase, then:

$$\begin{aligned} y(t) = \left(-\frac{3}{4}\,\alpha_3 A^3 - \alpha_1 A\right)\cos(\omega\, t + \phi_2) + \left(\alpha_1 A + \frac{3}{4}\,\alpha_3 A^3\right)\cos(\omega\, t + \phi_1) \\ + \frac{1}{2}\,\alpha_2 A^2 \cos(2\,\omega\, t + 2\,\phi_2) - \frac{1}{2}\,\alpha_2 A^2 \cos(2\,\omega\, t + 2\,\phi_1) \\ - \frac{1}{4}\,\alpha_3 A^3 \cos(3\,\omega\, t + 3\,\phi_1) + \frac{1}{4}\,\alpha_3 A^3 \cos(3\,\omega\, t + 3\,\phi_2) \end{aligned} \tag{2.18}$$

if $\phi_1 = 0$ and $\phi_2 = 180^0$, we have

$$\left(\frac{3}{2}\,\alpha_3 A^3 + 2\,\alpha_1 A\right)\cos(wt) + \frac{1}{2}\,\alpha_3 A^3 \cos(3\,wt) \tag{2.19}$$

Since

$$\cos(n\pi + \alpha) = -\cos\alpha \qquad if \;\; n \;\; is \;\; odd \tag{2.20}$$

and

$$\cos(n\pi + \alpha) = \cos\alpha \qquad if \;\; n \;\; is \;\; even \tag{2.21}$$

According to (2.19), we can see that the use of differential signals help to eliminate some of the unwanted harmonics. Since the mixer is an element of two input ports, there are two possible cases that can occur

The two input signals are differential $\Rightarrow$ Achieved by removing all the even harmonics of the two signals.

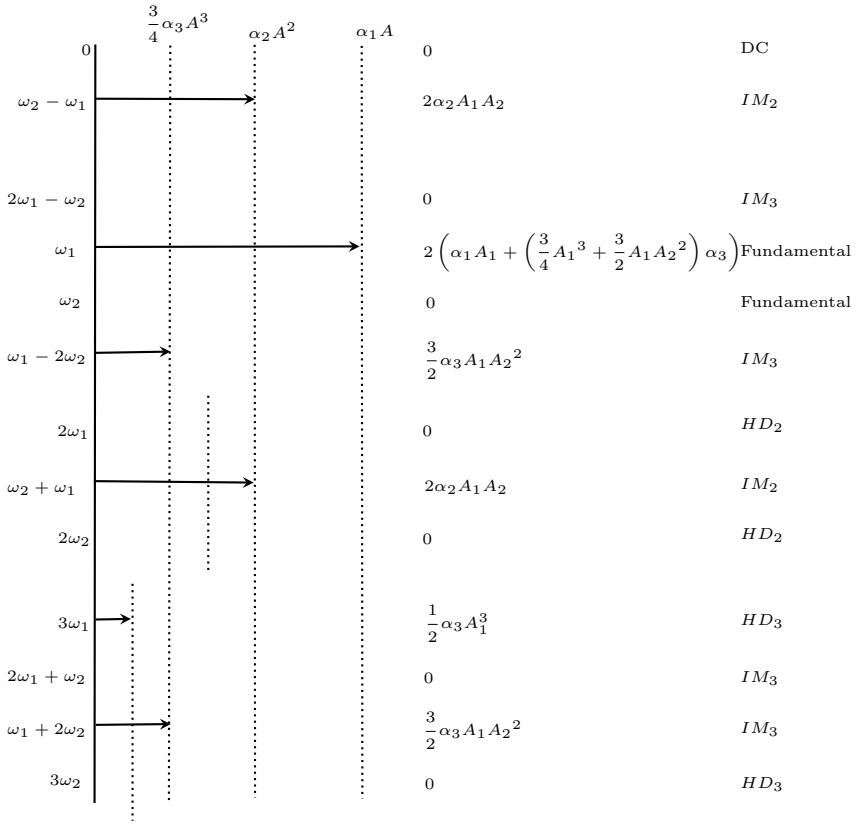

Figure 2.8: Frequency components when two input tones are used and one of them, ω_1, is differential, into a memoryless weak nonlinear system.

Only one signal is differential $\Rightarrow$ Removes all even harmonics of the differential signal and eliminates the presence of harmonics of the signal that is not introduced differentially.

In Figure 2.8 the spectrum is shown for the case of two differential tones. ω_1 is the signal that is introduced differentially into the mixer. Note that ω_2 is removed as well as all even harmonics of ω_1 along with the products of intermodulation that contain even harmonics of ω_1. Therefore, we can conclude that the use of differential signals helps to have a less populated spectrum, which helps to improve the linearity and enhance the port isolation

There are two types of balanced mixer:

Single-Balanced: Combines two identical single-ended mixers to produce better RF/LO

Table 2.2: Advantages and Disadvantages of mixers with balancing.

Advantages and Disadvantages of double balanced mixer compared to single balanced mixer	
Advantages	Disadvantages
Increased linearity	Higher level LO drive level required
Better suppression of spurious products all even order products of the LO and RF inputs are suppressed	At least two baluns are required within he design these add cost and complexity
Isolation between all ports.	

isolation. The balanced mixer using a 90^o of phase generates good RF voltage standing wave ratio, but poor RF/LO isolation, while using a 180^o of phase suppresses all even harmonics of the LO.

Double Balanced: Uses two phase of 180^o. Like the 180^o phase balanced mixer, it has good RF/LO isolation, but poor input voltage standing wave ratio. It suppresses all even harmonics of both the LO and RF signals, thus yielding a very low conversion loss.

While single-balanced mixers provide many advantages over unbalanced designs, double balanced mixers are the most common [20]. However, there are a number of advantages and disadvantages to consider in a single balanced mixer. Table 2.2 detail those.

The possibility a mixer with a single balanced circuit is shown in Figure 2.9. It can be noted that LO has two phases, which means that when M1 behaves like a resistor M2 does as an open circuit. Thus, when LO is zero $+RF$ is present in the node labeled as V_{IF}, and when LO is positive, $-RF$ is present in the node labeled as V_{IF}. Therefore, the mixer multiplies the RF signal by ± 1. As a result, all even harmonics are eliminated, along with the IM that contains even harmonics. Thus, the balanced harmonic mixer helps to increase the linearity. Because the third-order intermodulation product is given by

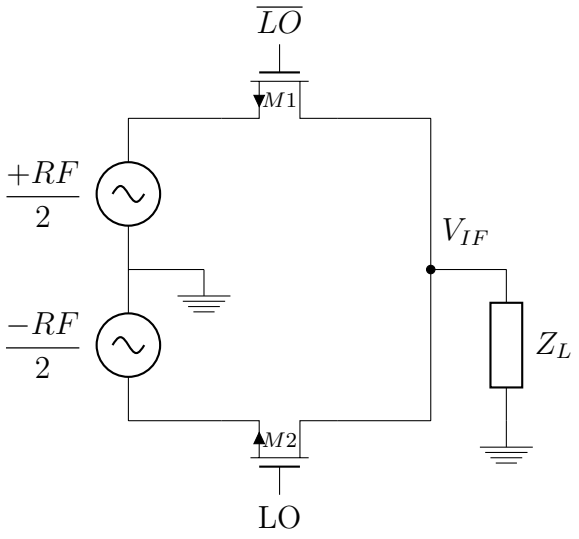

Figure 2.9: Single Balanced Harmonic Mixer.

$$IM_3 = 2\omega_1 \pm \omega_2 \qquad or \qquad \omega_1 \pm 2\omega_2 \tag{2.22}$$

it contains even harmonics, if ω_1 is the differential signal, $2\omega_1 \pm \omega_2$ is the product removed and this is the closer to the fundamental signal.

The noise from this mixer is the double of the unbalanced mixer. However, the Gc remains the same. This implies that NF increases with respect to the unbalanced mixer.

In the same way in which it has been created a single-balanced mixer, it can be created a double-balanced mixer. That is, if connecting the four unbalanced mixer, it is obtained a double-balanced mixer. Figure 2.10 shows a double balanced harmonic mixer. $M1$ and $M2$ are the first single-balanced mixer, $M3$ and $M4$ are the second single-balanced mixer. Therefore, in V_{+IF} it is obtained the multiplication of V_{RF} by ± 1 whereas in V_{-IF}, it is obtained the multiplication of V_{RF} by ∓ 1. In this mixer, LO and RF are differential signals. As a result, all even harmonics are eliminated. therefore, The IM_3 are suppressed and the linearity is increased.

The noise from this mixer, is the double with respect to the single-balanced mixer. However, the Gc increases due to the subtraction of V_{+IF} and V_{-IF}. This is equivalent

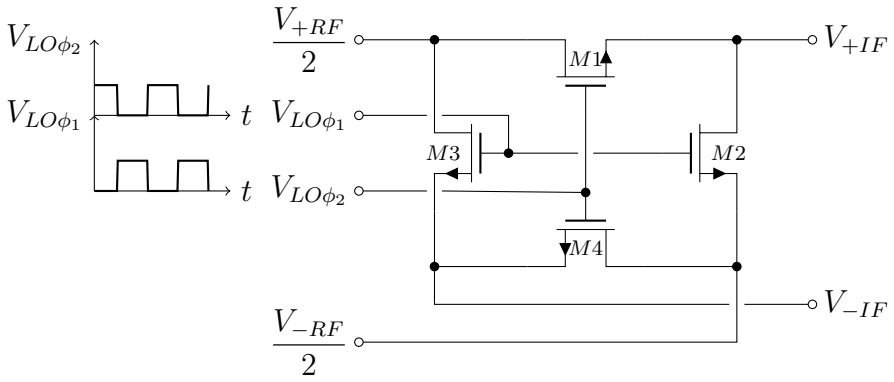

Figure 2.10: Double Balanced Harmonic Mixer.

to twice the Gc of the single-balanced mixers. Therefore, the double balanced mixer has a better performance in NF with respect to the single-balanced one.

The topologies shown in Figures 2.9 and 2.10 have the problem that are implemented with a unique NMOS transistors and their main problem using them as a switch is that it can transmit completely a negative value, however, the positive values are delimited by the threshold voltage. Therefore, the maximum amplitude available is.

$$V_{IF} = V_{RF} - Vth \tag{2.23}$$

This may cause a degradation in the signal swing, which can be seen as a distorted signal. The solution to this problem is to use P-type complementary transistors. These transistors are optimal to drive positive values, however, the maximum swing for the negative amplitudes is bounded by the threshold voltage. In conclusion, N transistors are good conductors of negative signal swings and P transistors are good conductors of positive signal swings.

A double-balanced harmonic mixer which solves the problem of the excursion of the signal is the H-Bridge Ring Mixer shown in Figure 2.11 [21]. $M1$ and $M3$ are P-type transistors, $M2$ and $M3$ are N-type transistors. When V_{LO} is zero, $M1$ behaves like a resistance, and $M2$ as an open circuit. Therefore, V_{+RF} is present at node labeled as V_{+IF}. Considering now that LO is positive, $M2$ behaves like s resistance, and $M1$ as

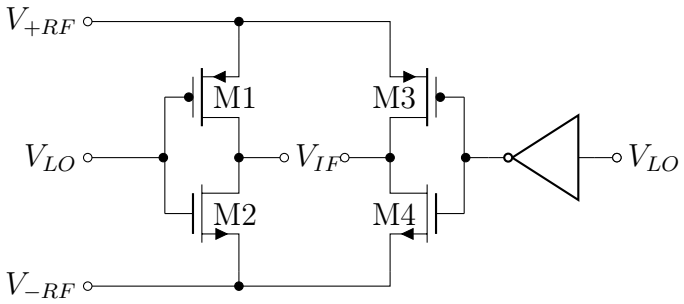

Figure 2.11: H-Bridge Ring Mixer.

an open circuit. Therefore, V_{-RF} is present at node labeled as V_{+IF}. Thus $M1$ and $M2$ behave like a single-balanced mixer but with a better dynamic range.

The harmonic mixer implemented with MOS transistors has a good performance in linearity. However, you have to be careful in terms of NF, because the Gc always indicates losses. Therefore, the only option for reducing the NF is to increase the size of the transistors. However, increasing the dimensions deteriorates the ports isolation. That is why before designing a mixer it is necessary to know the standard in which the mixer will be used in order to correctly decide the features of the circuit.

2.4 Subharmonic mixer

One problem of the harmonic mixer is that the Gc indicate losses which affects the NF. It is necessary to increase the Gc to decrease the NF. The solution is to introduce a gain stage to increase Gc. In this way subharmonic mixer works with a transconductance stage at the input. In Figure 2.12, it is shown a subharmonic mixer; $M1$, $M2$, $M3$, and $M4$ are switches. $M5$ and $M6$ work in the saturation region, which implies that

$$V_{out} = g_m R_L 2RF \tag{2.24}$$

consequently, the mixer has a gain given by

$$G_c = \frac{2g_m R_L}{n\pi} \tag{2.25}$$

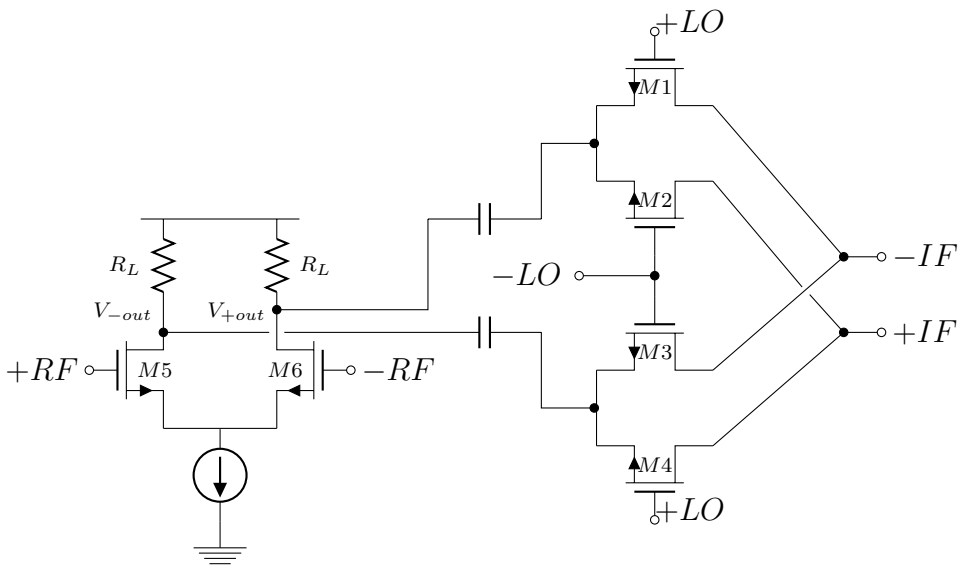

Figure 2.12: Quad Mixer.

Therefore, degradation of Gc to a higher order of n is lesser due to $2g_mR_L$. However, linearity is affected since $M5$ and $M6$ operate in the saturation region and in this region the current of MOS transistor is quadratic. Although this circuit acts like a double-balanced mixer, it is possible to eliminate the IM3, consequently linearity is refereed to IM5. The IM5 is a harmonic further away and has lesser energy than the fundamental. Thus; the linearity is almost unaffected.

2.5 Conclusion

The harmonic mixer is a variant of the passive mixer which has the advantage that the devices employed in its architecture do not contribute to the degradation of the linearity of the circuit in comparison to the active mixer. This is due to two main reasons: first, because the mixer behaves like a resistive circuit, and these resistors have a linear behavior; therefore, the output current has a linear behavior; this is valid if LO has enough energy to completely turn on and off the transistors and its transitions are abrupt; on the other hand, the balanced the mixer eliminates IM3, which alleviates the linearity because this harmonic is which more energy gives to the fundamental. This

kind of mixer is reliable when the LO has not to perform at high frequencies. However, an special issue is the NF due to losses in the output port. Although the harmonic mixer has a minimum contribution of noise with respect to the active mixer.

Therefore, based on the information presented, it can be concluded that the harmonic mixer may be used in broadband systems such as UWB or MBWA, because they have a good linearity performance. However, UWB has an effective isotropic radiated power transmitted to the receiver in the order of $-41dBm/Hz$ and a noise floor in the band in the order of $-84dBm/Hz$. These two data limited the conversion factor and have minimum losses. The losses reduce the energy of the signal, making it approaches to the noise floor level. In contrast, MBWA has a TX power of $43dBm/MHz$ and a noise floor within the band of $-174.5dBm$. This implies that MBWA has a higher dynamic range compared to UWB. Therefore, there are no complications if Gc has losses. In sum, it is necessary to know all the features and needs of the standard in order to propose the best design and performance.

Chapter 3

Proposed CMOS mixer

3.1 Introduction

As mentioned in the previous chapter, the passive mixer that operates in the continuous time mode is denoted as a switching mixer. It has as main advantage a high linearity performance. In this thesis, we propose a new type of harmonic mixer, which still behaves as a switching mixer. The difference between a switching mixer and a harmonic mixer is the number of the harmonic from LO used as the carrier. In switching mixers, the harmonic that is used to translate the frequency is the fundamental while in harmonic mixers, the harmonic used is the higher order of the LO harmonic component. Therefore, the FOMs are slightly different. On the other hand, NF increases as Gc decreases, this is due to the fact that high order harmonics have lower energy with respect to the fundamental. On the other hand, ports isolation is improved because LO has minimal presence in the other two ports. Regarding to linearity and power consumption, the harmonic mixer and the switching mixer have the same behavior. Therefore, the passive mixer that operates in the continuous time mode can function as a switching mixer or as a harmonic mixer. Depending on the application and the demands of the standard, it can be selected the most suitable mixer. For example, if the noise requirements are of interest, which is the case in downconversion mixers (DCM), it is preferable to use the switching mixer. At the same time, if the ports isolation

requirements are of interest and the RF power is much higher than the noise present in the system, it is recommended to use a harmonic mixer. On the other hand, in up-conversion mixers (UCM), the linearity is important since these are on the transmission path and the linearity of the overall transmitter is one of the most stringent demands to satisfy [22]. Consequently, UCMs are preferable to produce as few distortion as possible. Moreover, carrier feedthrough is also a relevant issue in UCMs. This phenomenon occurs when a DC component in the BB is mixed with the fundamental frequency of the local oscillator (LO). Both, linearity and carrier feedthrough, can be minimized by using UCMs based on passive topologies [2]. In addition, differential architectures improve the linearity of the UCM by cancelling the even-order harmonic components.

A CMOS UCM and DCM with the capacity to adjust by means of a DC voltage control the pulse width of the waveform at its output port as well as regulating its output power, is introduced in this chapter. Simulations are performed with the aim of the parameters of the UMC $0.18\mu m$ Mixed-Mode and RFCMOS $1.8V$ Twin-Well technology.

3.2 Single ended mixer

The principle of operation of a switching mixer is explained by referring to the square wave shown in Figure 3.1. When V_{LO} is zero the mixer is on, and $V_{in} = V_{out}$. When V_{LO} is positive the mixer is off, and consequently $V_{out} = 0$. Therefore, V_{LO} can be expressed as

$$V_{LO}(t) = \begin{cases} 1, & \text{if } -\dfrac{T_{LO}}{2} < t < 0 \\ \\ 0, & \text{if } 0 < t < \dfrac{T_{LO}}{2} \end{cases}$$

where, T_{LO} is the period of the LO. Note that we assume a 50% duty cycle of the LO square wave. If we expand $V_{LO}(t)$ into its Fourier series, the adove expression can be written as [23]

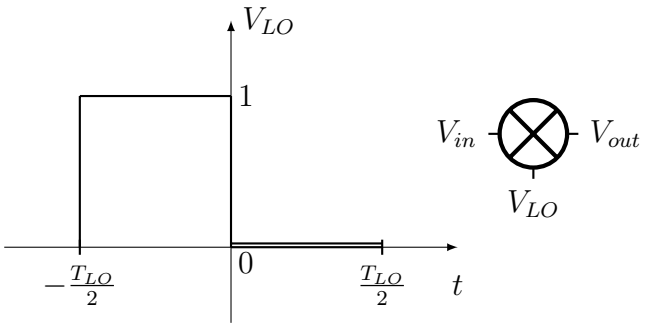

Figure 3.1: Local Oscillator waveform used as the *on/off* mechanism in a mixer.

$$V_{LO}(t) = \frac{1}{2} - 2\sum_{n=0}^{\infty} \frac{sin(\omega_{LO}(2n+1)t)}{(2n+1)\pi} \tag{3.1}$$

where $n = 0, 1, 2, \ldots, \infty$

The proposed mixer uses MOSFET transistors type N and P, this with the purpose of increasiny the dynamic range. For a high logic value of LO, the mixer is OFF and when LO has a low logic value, the mixer is ON. Therefore, the LO signal at the mixer output will be given by

$$1 - V_{LO}(t) = \frac{1}{2} + 2\sum_{n=0}^{\infty} \frac{sin(\omega_{LO}(2n+1)t)}{(2n+1)\pi} \tag{3.2}$$

We can see that when $V_{LO}(t)$ has a value of *1* the result will be logical value of *0* and when $V_{LO}(t)$ has a value of *0* the result is a logical value of *1*.

3.2.1 Verification of frequency translation

The proposed circuit for the frequency translation is shown in the Figure 3.2. It consists basically of a CMOS inverter which is controlled by $V_{LO}(t)$. When $V_{LO}(t)$ has a *low* logic value, C_L is charged at $Vb + Vpcos(\omega_{in}t)$ through M_p. When $V_{LO}(t)$ has a *high* logic value, C_L is discharge, through M_n. Hence, at the output of the inverter, the signal can be written as

$$V_{out} = \left(\frac{1}{2} + 2\sum_{n=0}^{\infty} \frac{sin(\omega_{LO}(2n+1)t)}{(2n+1)\pi}\right)(Vb + Vpcos(\omega_{in}t)) \tag{3.3}$$

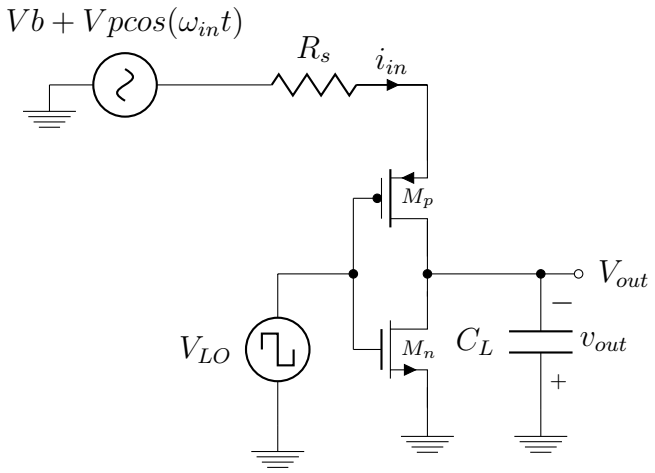

Figure 3.2: Proposed CMOS mixer circuit.

expanding (3.3), we have

$$V_{out} = \overbrace{\frac{Vb}{2}}^{DC} + \overbrace{\frac{Vpcos(\omega_{in}t)}{2}}^{Signal} + \overbrace{2Vb\sum_{n=0}^{\infty}\frac{sin(\omega_{LO}(2n+1)t)}{(2n+1)\pi}}^{LO} + \underbrace{2Vp\sum_{n=0}^{\infty}\left(\underbrace{\frac{sin((\omega_{LO}(2n+1)-\omega_{in})t)}{(2n+1)\pi}}_{down\ \ conversion\ \ case} + \underbrace{\frac{sin((\omega_{LO}(2n+1)+\omega_{in})t)}{(2n+1)\pi}}_{up\ \ conversion\ \ case}\right)}_{Frequency\ \ Conversion} \tag{3.4}$$

We can see that one of the components is DC (Vb), the rest are the signal of interest, both, the upconversion and the downconversion cases, and the local oscillator (LO) signal. Therefore, we see that mathematically the circuit behaves like a mixer. The spectrum at the output of the mixer is detailed in Figure 3.3 for downconversion (left-hand-side) and upconversion (right-hand-side).

3.2.2 Linearity

Linearity can be easily estimated with the aid of (3.4). If we take the difference of power ($\triangle P$) between the component of interest, $(\omega_{LO} \pm \omega_{in})t$, and the closest high order IM

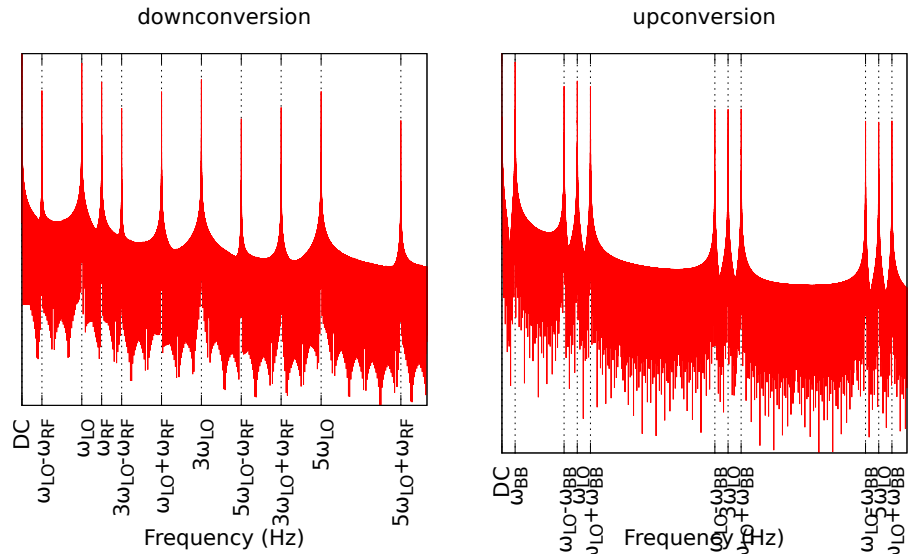

Figure 3.3: Frequency Conversion of the proposed single ended mixer.

product, which in this case is $(3\omega_{LO} - \omega_{in})t$, the input third intercept point (IIP3) is expressed as [2]

$$IIP_3 = \frac{\triangle P|_{dB}}{2} + P_{in}|_{dBm} \tag{3.5}$$

where P_{in} is the input power of the $Vb+Vpcos(\omega_{in}t)$ and $\triangle P$ is the power difference between $(\omega_{LO} \pm \omega_{in})t$ and $(3\omega_{LO} \pm \omega_{in})t$.

3.2.3 Power

For the analysis of the power consumption, is used equivalent model of the proposed mixer shown in Figure 3.4, by considering the *rms* value of the cosine waves at ω_{in}, the average energy stored in the load capacitor, C_L, during half period of the LO is given by [24]

$$E_{CL} = \frac{C_L\left(V_b^2 + \frac{V_p^2}{2}\right)}{2} \tag{3.6}$$

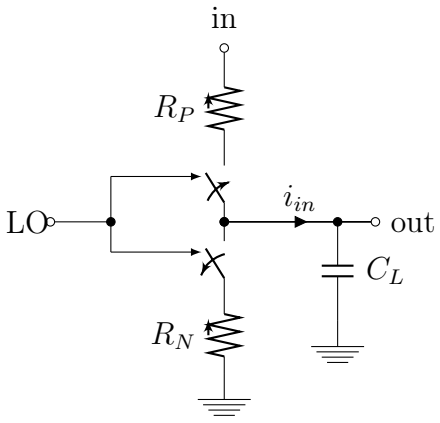

Figure 3.4: Equivalent circuit for the charge and discharge of C_L in the mixer.

Thus, in a complete switching cycle of the LO, the average power delivered to both load capacitors, P_{out}, is expressed as [25]

$$P_{out} = f_{LO} C_L \left(V_b^2 + \frac{V_p^2}{2} \right) \tag{3.7}$$

where f_{LO} is the fundamental frequency of the LO. In a similar way, it can be proved that the average power provided by the ω_{in} source, P_{in} is given by

$$P_{in} = f_{LO} 2C_L \left(V_b^2 + \frac{V_p^2}{2} \right) \tag{3.8}$$

Combining (3.7) and (3.8), the conversion factor defined as the ratio between the output and input power, results in

$$Gc = \frac{P_{out}}{P_{in}} \simeq -3dB \tag{3.9}$$

The static power dissipation is proportional to the leakage current when the inverter is not switching, and the short-circuit power dissipation is proportional to t_r and t_f. Ideally, when the CMOS inverter is in either output high (M_p is ON and M_n is OFF in Figure 3.2) or output low (M_p is OFF and M_n is ON) state, there should be no current passing through the two transistors. However, in either state, a small current passes through the OFF-state transistor, hence, causing static power dissipation. The

channel leakage currents can be obtained by calculating the channel resistance in the OFF state. However, the short circuit current is the one that can contribute most to unwanted power consumption. It occurs while one of the two transistors is changing from the ON state to the OFF state and the other transistor from OFF to ON. During the transitions a direct-path current passes through both transistors. The average short-circuit power dissipation is then:

$$P_{sc} = V_{DD} I_{peak} \frac{t_r + t_f}{2} f_{LO} \tag{3.10}$$

and

$$I_{peak} = \frac{\mu_n C_{ox}}{2} \frac{W_n}{L_n} (V_{tb} - V_{tn})^2 \tag{3.11}$$

where V_{tb} is the threshold voltage of the CMOS inverter and V_{tn} is the threshold voltage of the N-channel transistor. In consequence, the total dynamic power dissipation is the sum of the short-circuit power and the power produced by leakage currents.

3.2.4 Ports Isolation

Due to the parasitics of the MOS transistors diverse coupling among the ports of the mixer arise, especially at high frequencies. The value of the parasitics depends on the biasing and the size of the transistors. Therefore, in order to analyze the port isolation of the mixer, the model of the MOS transistors with all its parasitics capacitances is used. The proposed mixer is a time-variant system. However, for analyzing how much energy is transferred from one port to another due to coupling of the parasitic elements, it is necessary to analyze the system as a time-invariant one and by using the Laplace transform we will be able to know how much energy is transferred as frequency increases.

up conversion

The effects of the parasitic elements are present at high frequencies, therefore, in up-conversion LO is the source that has the highest frequency, so that, using Figure 3.5 we obtain how much energy of LO is present in the BB and RF ports. Expression

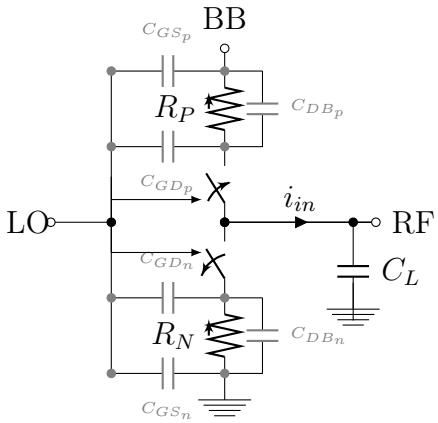

Figure 3.5: Equivalent model of the CMOS switch with parasitic capacitances.

(3.12) shows the amount of signal from LO that is transfered to the RF port, the equation remains in terms of the g_{DSP}, C_{GDP}, C_{DBP} and (C_{GSP}) and this depends on the dimensions. Figure 3.6 shows the plot of (3.12).

$$LO \Rightarrow BB = \frac{g_{DSP}^{-1} C_{GDP} R_S \left(2\, C_{DBP} + C_{GDP}\right) s^2 + 2\, C_{GDP} R_S s}{g_{DSP}^{-1} C_{GDP} R_S \left(2\, C_{DBP} + C_{GDP}\right) s^2 + \left(C_{GDP}\left(2\, R_S + {g_{DSP}}^{-1}\right) + \frac{C_{DBP}}{g_{DSP}}\right) s + 1} \tag{3.12}$$

where

$$\frac{1}{g_{DS_P}} = \frac{1}{k'_P \frac{W}{L}(V_{RF} - |V_{ToP}|)} \tag{3.13}$$

$$C_{GD_P} \approx C_{GS_P} \approx \frac{C_{ox} W L}{2} \tag{3.14}$$

$$C_L = C_{GD_N} + C_{GD_P} + C_{DB_N} + C_{DB_P} \tag{3.15}$$

As can be seen, the isolation worsens while the dimensions and frequency are increased. This is due to the fact that parasitic capacitances are directly proportional to both, dimensions and frequency. As can be observed in Figure 3.6, the worst case is at a frequency of $10G$, where it is obtain a transference of $0dB$, i.e. the energy of LO has been, theoretically, completely transferred to the BB port. On the other hand, when

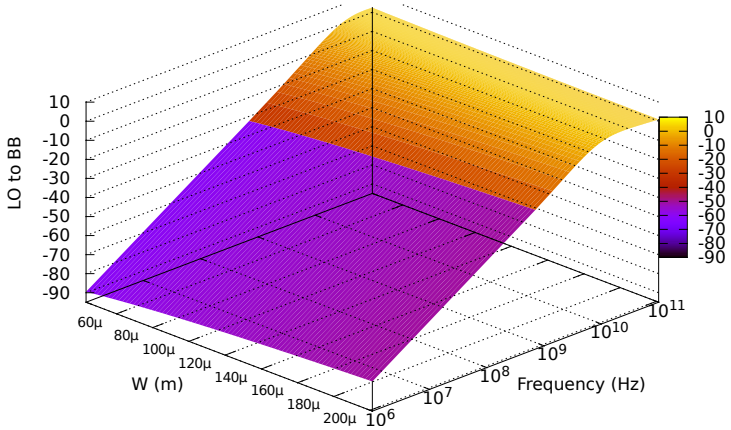

Figure 3.6: Energy transfer from LO to BB in function of the frequency and the size of the transistors.

the frequency of operation is set at $1GHz$, the transference is of $-20dB$.

The other case of interest is how LO affect RF. For this case we have

$$LO \Rightarrow RF = \frac{g_{DSP}^{-1} C_{GDP} R_S \left(C_{GDP} + 2\,C_{DBP}\right) s^2 + \left(2\,R_S + {g_{DSP}}^{-1}\right) C_{GDP} s}{g_{DSP}^{-1} C_{GDP} R_S \left(2\,C_{DBP} + C_{GDP}\right) s^2 + \left(C_{GDP}\left(2\,R_S + {g_{DSP}}^{-1}\right) + \frac{C_{DBP}}{g_{DSP}}\right) s + 1} \tag{3.16}$$

It can be seen that the equations are almost identical, and consequently, the graphs are also alike (Figure 3.7). This is because the parasitic capacitances involved for connecting LO with the others ports are identical ($C_{GDP} = C_{GSP}$). Again, by doing some computation it is obtained a transference from LO to RF of $2dB$ at $10GHz$ whereas for $1GHz$ the number is $-18dB$.

Downconversion

In downconversion RF is the source that has the highest frequency. By using Figure 3.8 we obtain how much of this energy is present in the LO and BB ports. First, we

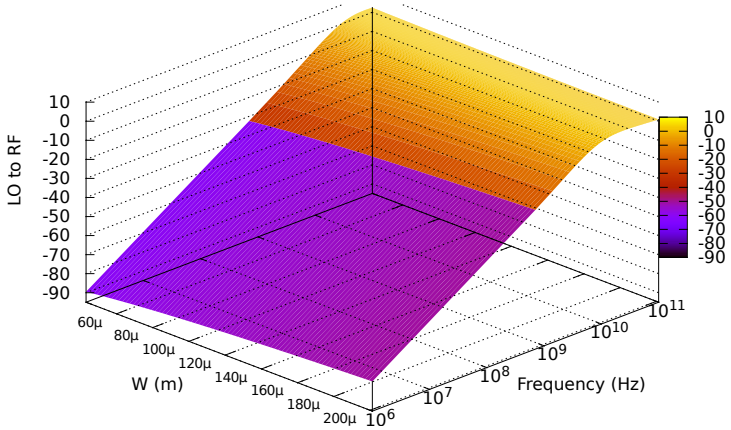

Figure 3.7: Energy transfer from LO to RF in function of frequency and size of the transistors.

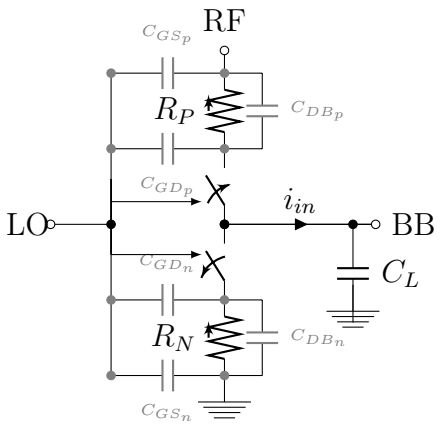

Figure 3.8: Equivalent model of the CMOS switch with parasitic capacitances.

analyze the RF to LO transference, which is given by

$$RF \Rightarrow LO = \frac{g_{DSP}^{-1} C_{GDP} R_S \left(C_{GDP} + 2\,C_{DBP} + C_L\right) s^2 + 2\,C_{GDP} R_S s}{g_{DSP}^{-1} C_{GDP} R_S \left(C_{GDP} + 2\,C_{DBP} + 2\,C_L\right) s^2 + \left(\left(2\,R_S + g_{DSP}{}^{-1}\right) C_{GDP} + \frac{C_{DBP}+C_L}{g_{DSP}}\right) s + 1} \tag{3.17}$$

As shown in Figure 3.9, it is similar the affectation of the LO port due to the RF signal with respect to the LO-BB isolation. This is because it is the same signal path. By doing the mathematics, we calculate a transference of $0dB$ at $10GHz$ and of $-20dB$ at $1GHz$.

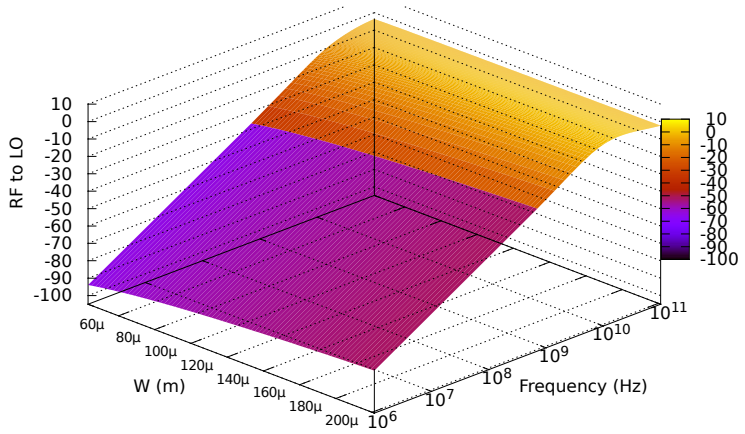

Figure 3.9: Energy transfer from RF to LO in function of frequency and the size of the transistors.

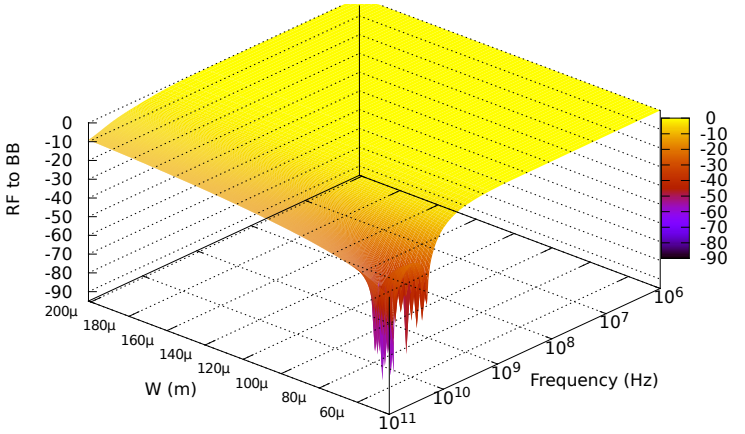

Figure 3.10: Energy transfer from RF to BB in function of frequency and the size of the transistors.

Finally, (3.18) expresses how much from the signal at the input will be present in the output. We are interested in having a good transference since this is the frequency translation of interest. After analizing the circuit, we found:

$$RF \Rightarrow BB = \frac{g_{DSP}^{-1} {C_{GDP}}^2 R_S s^2 + 2\, C_{GDP} R_S s + 1}{g_{DSP}^{-1} C_{GDP} R_S \left(C_{GDP} + 2\, C_L\right) s^2 + \left(\left(2\, R_S + {g_{DSP}}^{-1}\right) C_{GDP} + \frac{C_L}{g_{DSP}}\right) s + 1} \tag{3.18}$$

In this case, the signal will be present without any loss until a frequency as high as

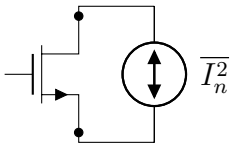

$$Linear \Rightarrow \overline{I_{n,th}^2}(f) = 4KTg_{DS}$$
$$Saturation \Rightarrow \overline{I_{n,th}^2}(f) = 4KT\gamma g_m$$

Figure 3.11: Thermal noise in MOS transistors.

$10GHz$. This is depicted in Figure 3.10.

We can conclude that the ports isolation in the order of GHz is not good. For this reason, we have to be careful with the use of the mixer in systems operating at very high frequencies.

3.2.5 Noise Figure

The transistors conforming the mixer are switched between the cut-off an linear regions. In the former case, it does not exist a channel and hence there is not current flowing from drain-to-source. Consequently, we consider that the transistor does not add up noise to the circuit. on the other hand, there is conduction in the linear region. The channel generates thermal noise. The thermal noise associated with the transistor can be modeled by a current source connected between drain and source, as illustrated in Figure 3.11 [5].

In the Figure 3.12 it is shown the equivalent circuit for performing the noise analysis. Since the mixer is a time variant system, we have two equivalent circuits, one when the transistor P is ON and the transistor N is OFF, and other when the transistor N is ON and the transistor P is OFF. Hence, the noise can be expressed as:

$$\overline{V_{no}^2} = \begin{cases} \overline{I_{nR_{in}}^2} R_{in}^2, & \text{if } 0 < t < \dfrac{T_{LO}}{2} \\ \\ \overline{I_{nR_N}^2} R_N^2, & \text{if } \dfrac{T_{LO}}{2} < t < T_{LO} \end{cases} \tag{3.19}$$

where $R_{in} = R_s + R_P$, $\overline{I_{nR_N}^2}$ is the noise current is generated by transistor N, $\overline{I_{nR_{in}}^2}$

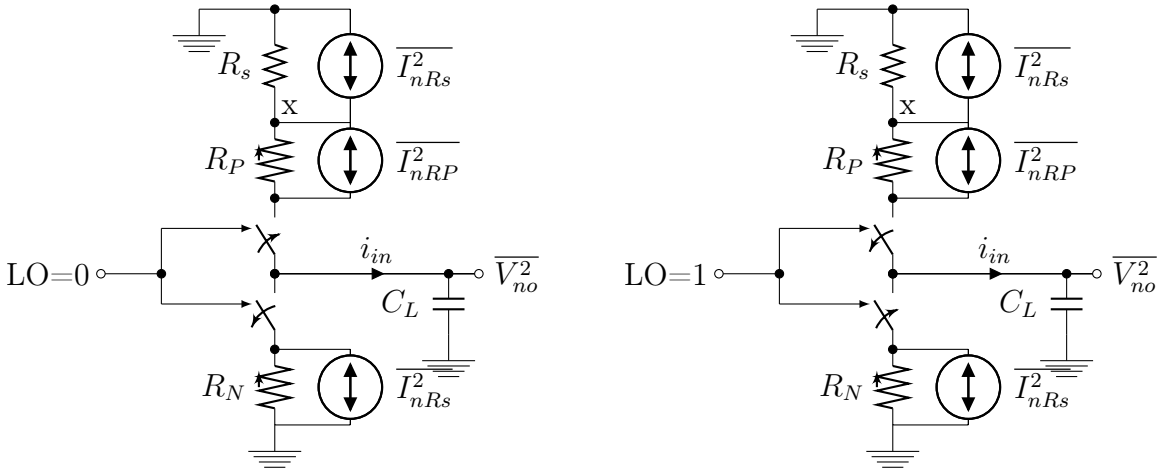

(a) (b)

Figure 3.12: Noise equivalent circuit: a) LO= *low*, b) LO= *high*.

is the noise current is generated by transistor P and the impedance of the source , and

$$\frac{1}{RP} = g_{DS_P} = \mu_P C_{ox} \frac{W}{L} \left(\left(Vb + \frac{Vp}{\sqrt{2}} \right) - V_{THP} \right) \tag{3.20}$$

$$\frac{1}{RN} = g_{DS_N} = \mu_N C_{ox} \frac{W}{L} \left((Vdd) - V_{THN} \right) \tag{3.21}$$

If we expand 3.19 in a Fourier Series and obtain the convergence of the series, we have:

$$\overline{V^2_{no}} \quad = \quad 2kT\left(R_s + R_P\right) \quad + \quad 2kTR_N \quad + \quad \left(4kT\left(R_s + R_P\right) - 4kTR_N\right)\frac{1}{4\pi} \tag{3.22}$$

On the other hand, the noise at the input of the mixer is given by [2]

$$\overline{V_{xn}}^2 = \overline{I^2_{nRS}} * R^2_S \tag{3.23}$$

In order to calculate the Noise Figure, it is neccesary to obtain the power at the input and at the output of the mixer, i. e.

$$V^2_{BB,RF} = \left(\frac{Vp}{\sqrt{2}} \pi \right)^2 \tag{3.24}$$

$$V_x^2 = \left(Vb + \frac{Vp}{\sqrt{2}}\right)^2 \tag{3.25}$$

Using (3.22), (3.23), (3.24) and (3.25), we obtain

$$SNR_{out} = \frac{\left(\frac{Vp}{2\pi}\right)^2}{2kT\left(R_s + R_P\right) + 2kTR_N + \left(4kT\left(R_s + R_P\right) - 4kTR_N\right)\frac{1}{4\pi}} \tag{3.26}$$

$$SNR_{in} = \frac{\left(Vb + \frac{Vp}{2}\right)^2}{4KTR_S} \tag{3.27}$$

and hence

$$NF = \frac{\pi}{4}\left(2 + \pi^{-1}\right) + \frac{\frac{\pi}{4}\left(2 + \pi^{-1}\right)R_P + \frac{\pi}{4}\left(2 - \pi^{-1}\right)R_N}{R_s} \tag{3.28}$$

Figure 3.13 depicts equation (3.28) in function of the dimensions of the transistor and the DC voltage, Vb. It can be seen that with respect to Vb, it does not exist large variations. However, with respect to the transistor dimensions, the NF is reduced conforming the width (W) of the device increases. This is due to the fact that the resistance of MOS transistor is inversely proportional to its length. Therefore, with large sizes, the resistance is reduced. In summary, it is favorable to use large dimensions since the noise that generates the device is minimum, and in consequence, the degradation of the SNR_{in} will be minimized.

3.3 Differential mixer

The principal advantage of the differential mixer, is that all the harmonic components of the local oscillator are removed, resulting that the presence of the LO at the output of mixer is completely null. This assertion will be proved with the analysis realized in this section. Additionally, differential structures also exhibit a large output dynamic range with respect to their single-ended counter parts.

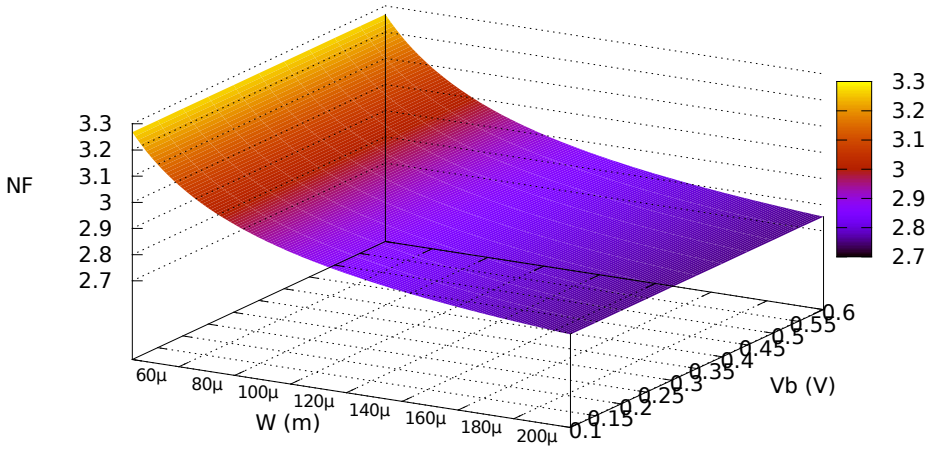

Figure 3.13: Noise Figure as a function of the size of the transistors and the DC (Vb) of the input signal.

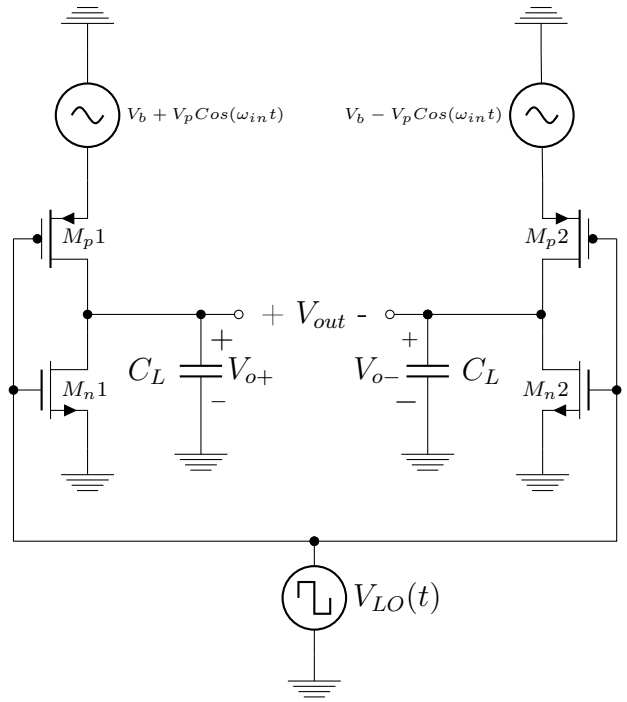

Figure 3.14: Proposed CMOS differential mixer circuit.

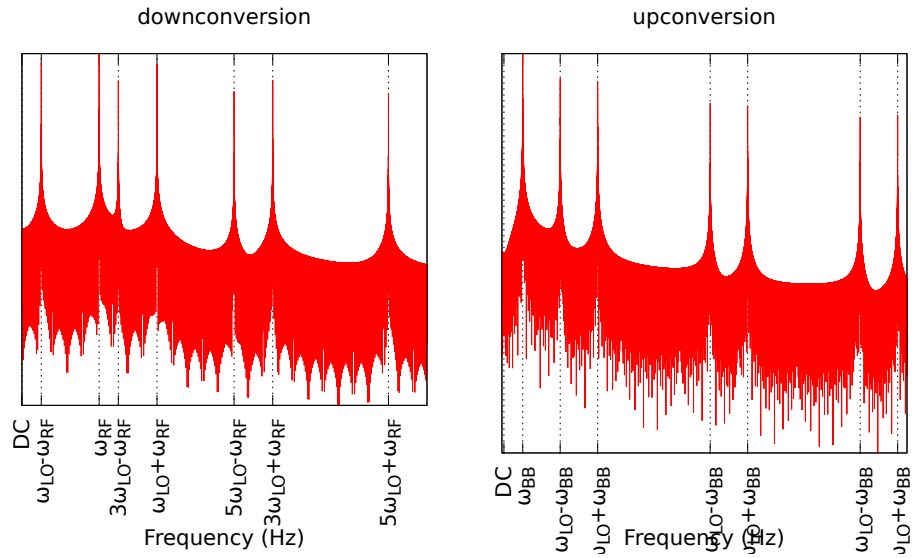

Figure 3.15: Frequency Conversion of the differential mixer.

3.3.1 Verification of frequency translation

The proposed circuit is shown in the Figure 3.14. It comprises two CMOS inverters controlled by LO and fed with the signal to be shifted in frequency. In (3.3) we have the multiplication of the oscillator with the signal of RF/BB, if we apply a shift of 180^o, to the RF/BB signal, we have:

$$V_{out} = Vpcos(\omega_{in}t) + 2Vp\sum_{n=0}^{\infty}\left(\frac{sin((\omega_{LO}(2n+1)-\omega_{in})t)}{(2n+1)\pi} + \frac{sin((\omega_{LO}(2n+1)+\omega_{in})t)}{(2n+1)\pi}\right) \quad (3.29)$$

Thus, the mixer still upconverts/downconverts the BB/RF signal whereas the LO signal is cancelled. However, to ensure the cancellation of LO, it is necessary to realize a careful layout, because the mismatch in the trajectories of the LO affects the cancellation of this signal. Figure3.15 shows the spectrum obtained at the output of the differential mixer.

3.3.2 Linearity

The linearity in this case is the same as for the case of the single-ended mixer. This is due to the fact that with the differential architecture, it is deleted just the LO signal and this does not affect the linearity. So, the IIP3 results also

$$IIP_3 = \frac{\triangle P|_{dB}}{2} + P_{in}|_{dBm} \tag{3.30}$$

where P_{in} is the input power of the $Vb + Vpcos(\omega_{in}t)$ and $\triangle P$ is the power difference between $(\omega_{LO} \pm \omega_{in})t$ and $(3\omega_{LO} \pm \omega_{in})t$.

3.3.3 Power

With respect to the power, if it is considered the *rms* value of the sinusoidal waves at ω_{in}, the average energy stored on each load capacitor, C_L, during a complete switching cycle of the LO, P_{out} is expressed as

$$P_{out} = 2f_{LO}C_L\left(Vb + \frac{Vp}{\sqrt{2}}\right)^2 \tag{3.31}$$

where f_{LO} is the fundamental frequency of the LO. In a similar way, it can be proved that the average power provided by the ω_{in} source, P_{in} is given by

$$P_{in} = 4f_{LO}C_L\left(Vb + \frac{Vp}{\sqrt{2}}\right)^2 \tag{3.32}$$

Combining (3.31) and (3.32), the conversion factor, defined as the ration between the output and input power, results in

$$CF = \frac{P_{out}}{P_{in}} = \frac{2f_{LO}C_L\left(Vb + \frac{Vp}{\sqrt{2}}\right)^2}{4f_{LO}C_L\left(Vb + \frac{Vp}{\sqrt{2}}\right)^2} \approx -3dB \tag{3.33}$$

The value of $Gc = -3dB$ is the maximum conversion factor that can have a passive circuit and if we compare at Gc of the single-ended mixer respect to differential mixer we conclude that both have the same behavior which is somehow favorable.

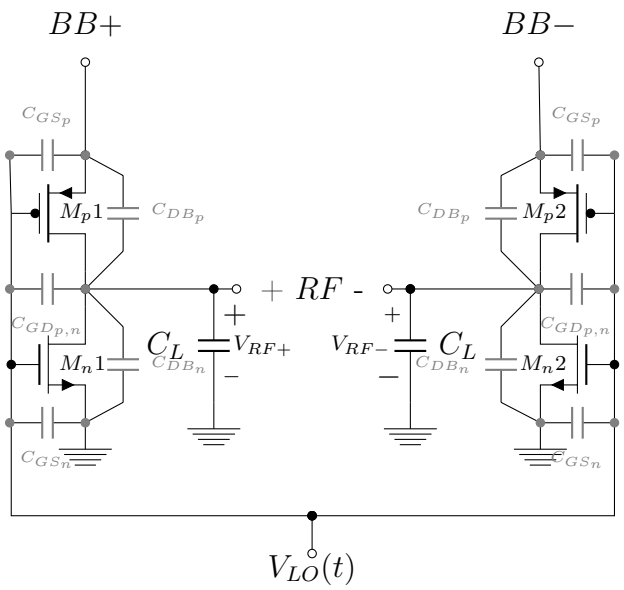

Figure 3.16: Switched CMOS mixer with parasitic elements.

3.3.4 Ports isolation

As explained in the analysis of ports isolation for the single-ended mixer, unwanted signal paths exist, which at high frequencies may cause a wrong function of the mixer. The case of the differential mixer is not exempt from these trajectories. However, the proposed topology has the advantage that LO is not differential which means that by subtracting the output signal, the presence of the LO is eliminated. Thus we can say that the proposed differential mixer eliminates the carrier without the use of a resonant network. This implies that the port isolation between LO and BB in downconversion and LO RF in upconversion, is satisfactory. However, in the upconversion LO can corrupt BB, or in downconversion LO can corrupt RF. Therefore, it is presented the analysis of differential mixer for the upconversion and downconversion case.

up conversion

In upconversion, LO is the larger frequency. So, LO is the one that can be present in the other ports. Analyzing the circuit in Figure 3.16, we found

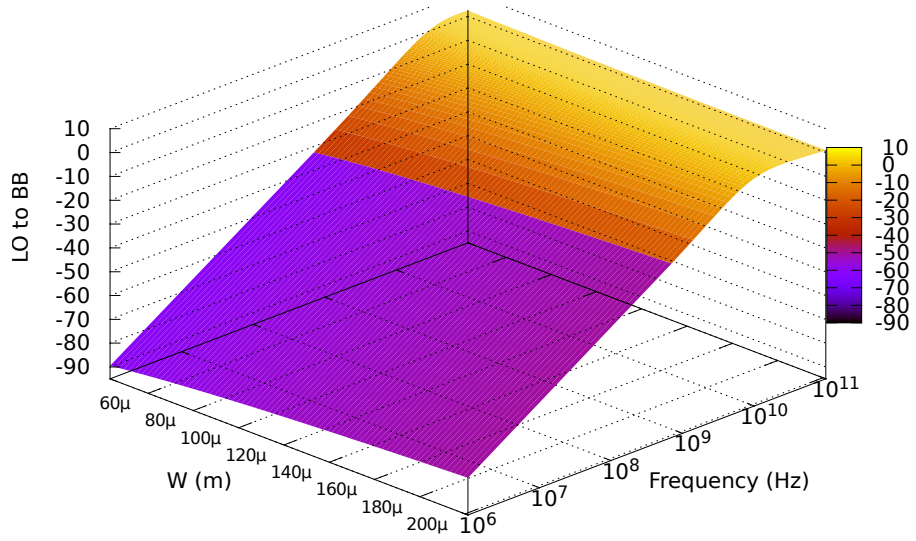

Figure 3.17: Energy transfer from LO to BB in function of frequency and the size of the transistors.

$$LO \Rightarrow BB = \frac{g_{DSP}^{-1} C_{GDP} R_S \left(2\,C_{DBP} + C_{GDP}\right) s^2 + 2\,C_{GDP} R_S s}{g_{DSP}^{-1} C_{GDP} R_S \left(2\,C_{DBP} + C_{GDP}\right) s^2 + \left(C_{GDP}\left(2\,R_S + g_{DSP}{}^{-1}\right) + g_{DSP}^{-1} C_{DBP}\right) s + 1} \tag{3.34}$$

It can be seen in Figure 3.17 that he presence of the LO in the BB port is $-20dB$ at a frequency of $1GHz$. Additionally, even when these is some portion of the energy of LO in $BB+$ and $BB-$, when taking the difference in the output, the presence of the LO is cancelled.

Downconversion

It is of interest to know how it affects the RF signal to the rest of ports. Therefore, the first analysis is to determine how much energy from the RF will be present at the LO port. We found that

$$RF \Rightarrow LO = \frac{g_{DSP}^{-1} C_{GDP} R_S \left(C_{GDP} + 2\,C_{DBP} + C_L\right) s^2 + 2\,C_{GDP} R_S s}{g_{DSP}^{-1} C_{GDP} R_S \left(C_{GDP} + 2\,C_{DBP} + 2\,C_L\right) s^2 + \left(\left(2\,R_S + g_{DSP}{}^{-1}\right) C_{GDP} + g_{DSP}^{-1}\left(C_{DBP} + C_L\right)\right) s + 1} \tag{3.35}$$

As shown in Figure 3.18, it is similar the affectation of the LO port due to the RF

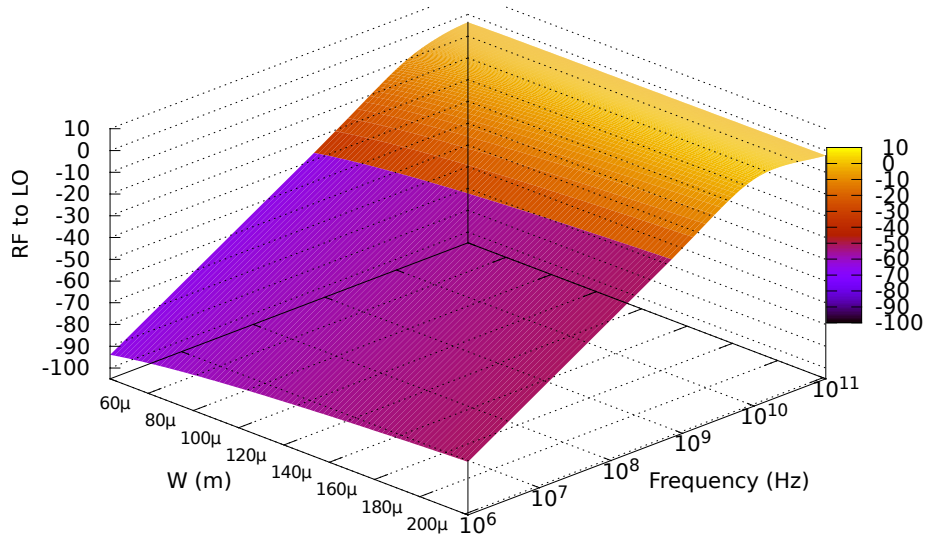

Figure 3.18: Energy transfer from RF to LO in function of frequency and the size of the transistors.

signal with respect to the isolation of LO to BB. This is because it is the same signal path. Finally, (3.36) expresses how much from the signal at the input port will be present in the output port. We are interested in having a good transference since this is the frequency translation of interest. After analizing the circuit, we have:

$$RF \Rightarrow BB = \frac{g_{DSP}^{-1} {C_{GDP}}^2 R_S s^2 + 2\, C_{GDP} R_S s + 1}{g_{DSP}^{-1} C_{GDP} R_S \left(C_{GDP} + 2\, C_L\right) s^2 + \left(\left(2\, R_S + {g_{DSP}}^{-1}\right) C_{GDP} + \frac{C_L}{g_{DSP}}\right) s + 1} \tag{3.36}$$

In this case, as may be seen in Figure 3.19, the signal will be present without any loss until a frequency as high as $10GHz$. We conclude that port isolation is good especially in the up-conversion, this is due to the cancellation of LO. It is important to mention that LO cancellation is achieved more effectively if a careful layout is done.

3.3.5 Noise Figure

In the differential circuits, the outputs are substracted and every DC level is removed. However, this is not the case of noise unless there is correlation. When the channel of

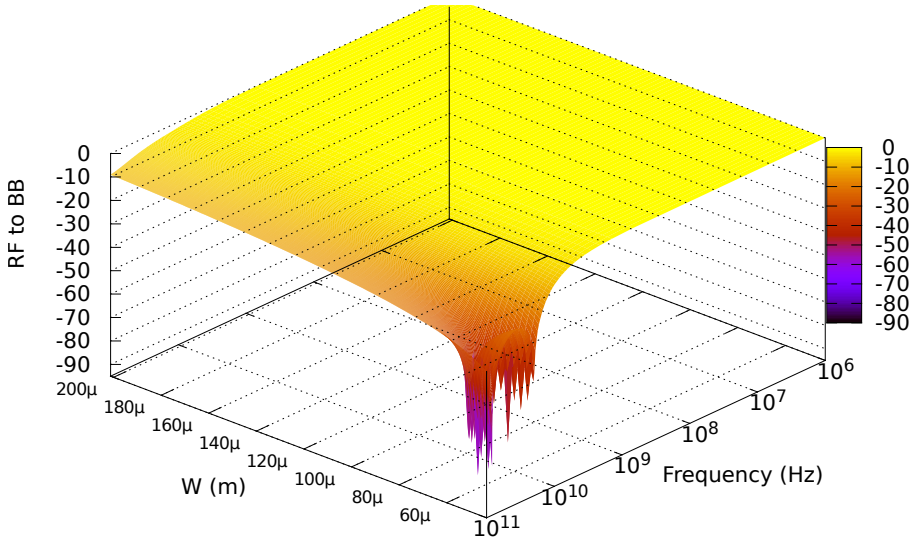

Figure 3.19: Energy transfer the RF to BB with respect to frequency and the size of the transistors.

the MOS transistors operates in linear mode, the charge of the carriers is in thermal equilibrium within the lattice, and from a macroscopic point of view the Ohm law is satisfied. The channel generates thermal noise and an important property of the thermal noise is that two different physical sources (although derived from identical transistors) are uncorrelated [5]. Hence, it can be inferred that the noise can not be subtracted. Therefore, in the differential systems there is the double of noise that in the single-ended ones. According to this, the noise of the circuit shown in Figure 3.20 has the double of noise that the single-ended topology, i. e.

$$\overline{V_{BBn}}^2 = \begin{cases} 2\overline{I^2_{nR_{in}}} * R^2_{in}, & \text{if } 0 < t < \dfrac{T_{LO}}{2} \\ \\ 2\overline{I^2_{nR_N}}, & \text{if } \dfrac{T_{LO}}{2} < t < T_{LO} \end{cases} \tag{3.37}$$

again, $R_{in} = R_s + R_P$, $\overline{I^2_{nR_N}}$ is the noise current is generated by transistor N, $\overline{I^2_{nR_{in}}}$ is the noise current is generated by transistor P and the impedance of the source , and

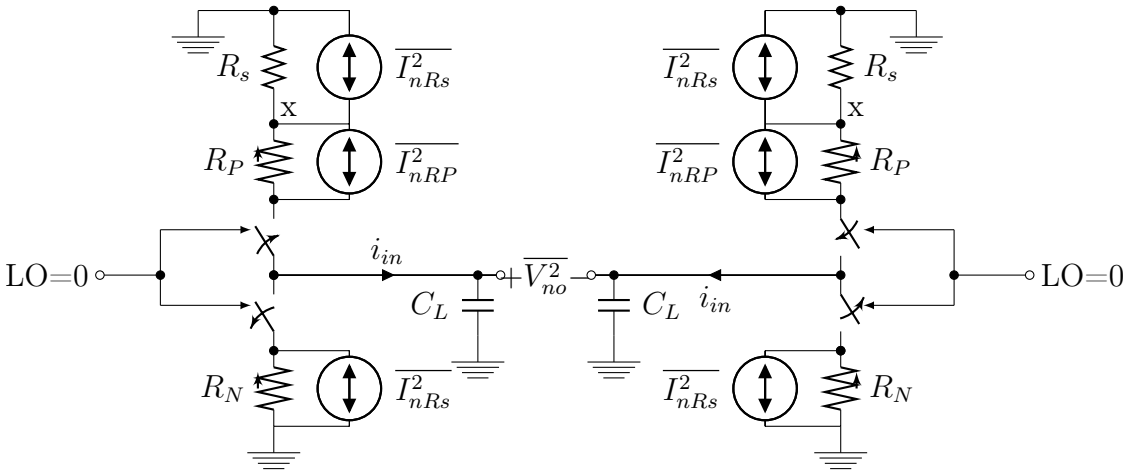

Figure 3.20: Noise equivalent model for the differential mixer.

$$\frac{1}{RP} = g_{DS_P} = \mu_P C_{ox} \frac{W}{L} \left(\left(Vb + \frac{Vp}{\sqrt{2}} \right) - V_{THP} \right) \tag{3.38}$$

$$\frac{1}{RN} = g_{DS_N} = \mu_N C_{ox} \frac{W}{L} \left((Vdd) - V_{THN} \right) \tag{3.39}$$

Developing (3.37) in a Fourier series and obtaining the convergence of the series we can find the total noise at the output of mixer, which is giving by

$$\overline{V^2_{no}} = 4kT\left(R_s + R_P\right) + 4kTR_N + \left(8kT\left(R_s + R_P\right) - 8kTR_N\right)\frac{1}{4\pi} \tag{3.40}$$

The SNR_{in} is given by the ration of the power of $V_{in}(t)$ between the noise power from the source, which is $4KTR_S$. On the other hand, the SNR_{out} is given by the ratio between the output power and the total noise power at the output. Thus

$$SNR_{out} = \frac{\left(\frac{Vp}{2\pi}\right)^2}{4kT\left(R_s + R_P\right) + 4kTR_N + \left(8kT\left(R_s + R_P\right) - 8kTR_N\right)\frac{1}{4\pi}} \tag{3.41}$$

$$SNR_{in} = \frac{\left(Vb + \frac{Vp}{2}\right)^2}{4KTR_S} \tag{3.42}$$

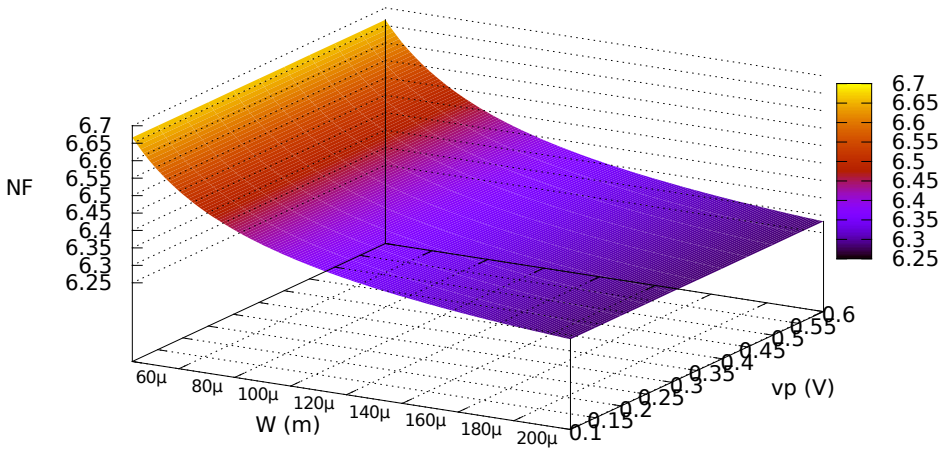

Figure 3.21: Noise Figure of the differential mixer as a function of Vp and size of transistors.

Therefore, the NF is given by

$$NF = \frac{\pi}{4}\left(4 + 2\,\pi^{-1}\right) + \frac{\frac{\pi}{4}\left(4 + 2\,\pi^{-1}\right) R_P + \frac{\pi}{4}\left(4 - 2\,\pi^{-1}\right) R_N}{R_s} \tag{3.43}$$

Comparing the NF of the sigle-ended mixer with the NF of the differential mixer, the NF of the single-ended circuit is better than the NF of the differential approach. Hence, if the noise requirements are stingent, the single-ended topology is a better solution. Therefore, LO cancellation, linearity and Noise Figure are trade-off with the proposed architectures for frequency translation.

Some other important datum is the minimum noise power of a communication channel, which is given by $-174dBm$ [5]. Furthemore, in the $0.18\mu m$ CMOS technology employed for design and simulation, the noise generated by the transistors P and N in the lineal region is shown in Figure 3.22 [26]

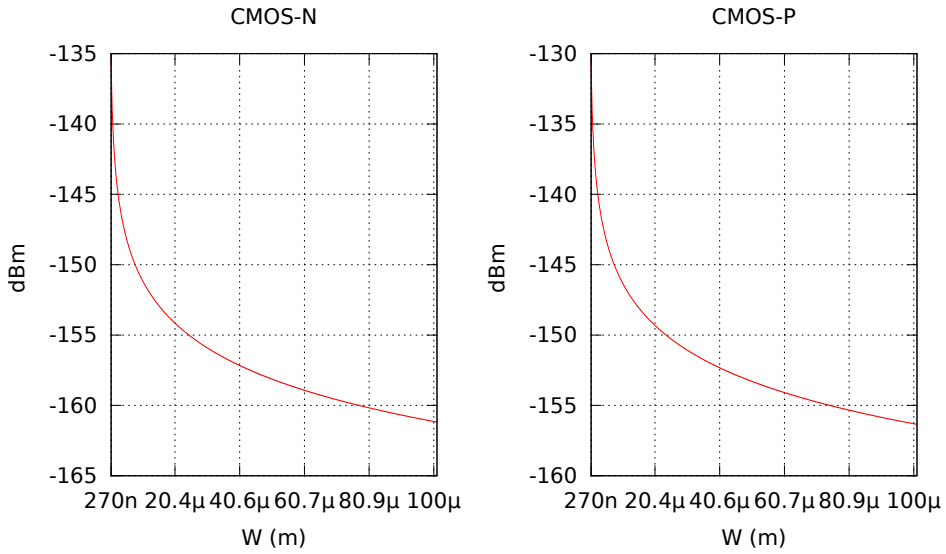

Figure 3.22: Noise generated by transistors in linear region.

3.4 Duty cycle of the inverter

The duty cycle is the fraction of time where the signal of the V_{LO} at the input port is at a high logic value, and is given by

$$D = \frac{\tau}{T} \tag{3.44}$$

Where τ is the time that the signal at the output remains in its maximum value and T is the period of the signal. Now, consider a symmetrical inverter (which means that the output of the inverter switches in the same time with respect to LO) like the one shown in Figure 3.23. When V_{in} is zero V_{out} is Vb. In addition, when the voltage at V_{in} exceeds $Vb/2$, V_{out} is zero. Typically, Vb equals the maximum amplitude of V_{in}. If this is done and the inverter is designed symmetrically, the duty cycle of the input is the same as the duty cycle of the output. Therefore, by varying Vb the duty cycle is modified.

The most common manner to modify the duty cycle is modifying the dimensions of the transistors, nevertheless, once it is made, the duty cycle can not be altered. Other choice is modifying the value of polarization of the inverter, if this value is changed,

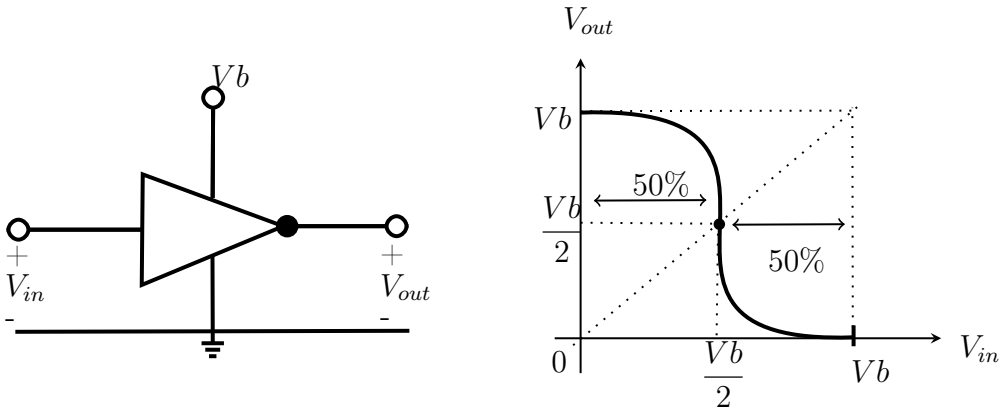

Figure 3.23: DC characteristic of an inverter gate.

the duty cycle can be modified. Figure 3.24 shows the characteristic curve of the duty cycle of the inverter gate in function of the bias supply. It can be appreciated how the duty cycle decreases when the value of polarization decreases.

The modification of the duty cycle, is an important contribution in this work. Since the modification of the duty cycle changes the harmonic content of the spectrum of the signal, by changing the duty cycle, the spectrum also changes. The mechanism by which the duty cycle is modified in the proposed circuit is by means of the peak voltage of the signal at the input port along with its DC component.

The spectrum of the output signal of the mixer as a function of the bias supply of the circuit is detailed in Figures 3.25 and 3.26. $\omega_{LO} \pm \omega_{BB}$ is the harmonics that has more energy with respect to the variation of the duty cycle. We can see also that by varying the duty cycle, some harmonics are suppressed, which is beneficial in terms of linearity.

3.5 Conclusion

Both, single-ended and differential mixers are good. The main advantage that presents the differential architecture is that it cancels the LO. On the other hand, the single-ended mixer has a lower power consumption and a better NF. In addition, by changing

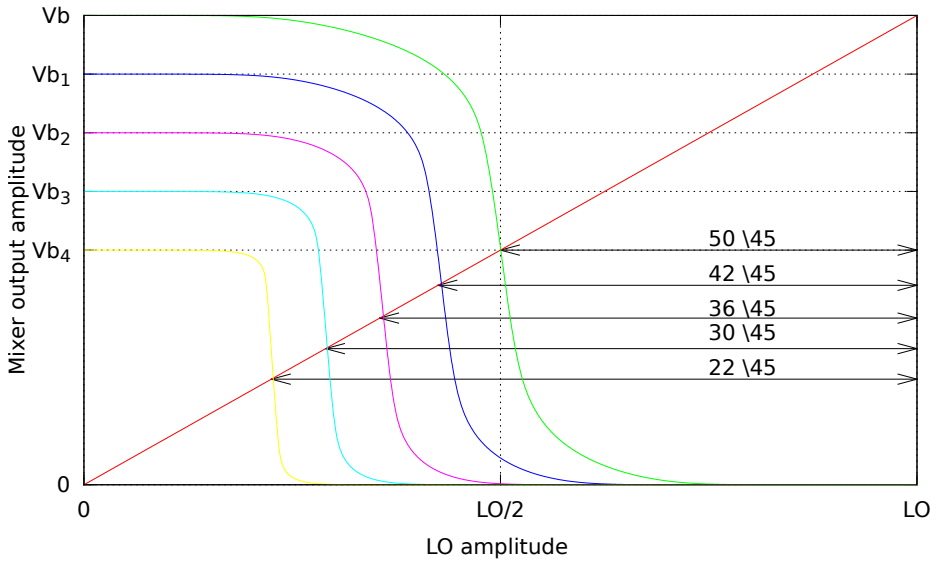

Figure 3.24: Duty cycle variation of the inverter gate.

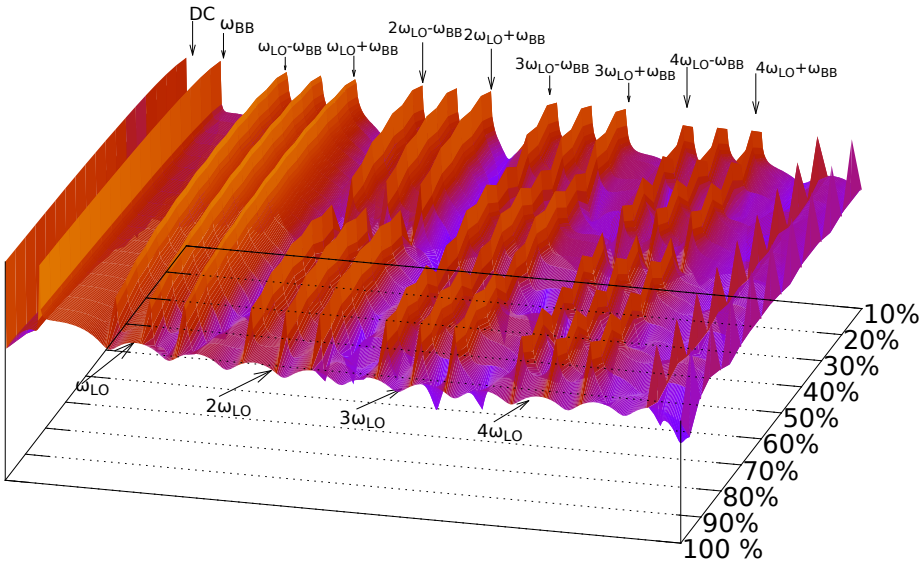

Figure 3.25: Output spectrum of the single-ended mixer with respect to the duty cycle Variation.

the DC level at the input, the duty cycle at the output can be modified and consequently the spectrum of the signal is changed. This may be advantageus in applications where linearity demands are stringent. Some of the mos salient features of the proposed mixer

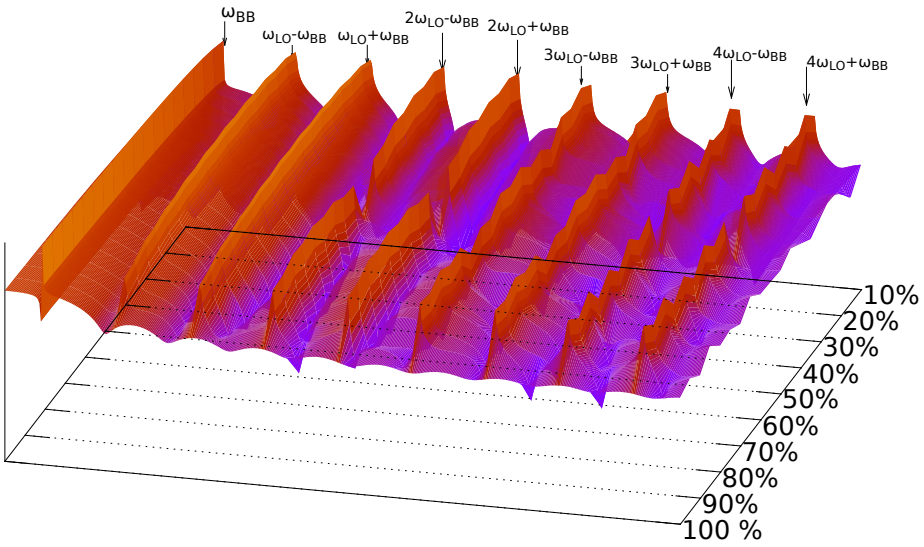

Figure 3.26: Output spectrum of the differential mixer in function of the duty cycle.

are summarized in Table 6.1.

We can see that the linearity achieved is $36dBm$ which is a good number as it indicates that the proposed mixer can work with large signal amplitudes and if working with small signals the $IM3$ shows very little energy. Concerning Gc, it is a typical value for a passive device. However, because the IP3 is high and consequently large signals at the input port can be used, the output signal of the mixer is away from the noise floor. In relation to the ports isolation, it can be seen that in the order of tens of GHz, there is a transference of approximately one hundred of the power of the unwanted signal. However, in the differential mixer the carrier is suppressed. Hence, LO is not present at the output of mixer and consequently the port isolation is, theoretically, perfect. One of the important contributions in this work is the variation of the output power in function duty cycle, considering that the maximum output power is at 50% of the duty cycle and reducing the duty cycle at 5% we have that the output power varies approximately $9.5dB$. This is helpful in systems where linearity is important, because when the output power is changed also the efficiency of the system is modified.

Table 3.1: characteristics of the proposed mixer.

	Sibgle-ended	Differential
Linearity	$36dBm$	
Conversion Factor	$-3dB$	
Noise Figure	$2.7dB$ @ $W = 200\mu m$	$6.25dB$ @ $W = 200\mu m$
Isolation Ports	LO to BB $-20dB$ @ $1HGz$ (UMC) LO to RF $-18dB$ @ $1GHz$ (UCM) RF to LO $-20dB$ @ $1GHz$ (DCM) RF to BB $0dB$ @ $1GHz$ (DCM)	LO to BB $-\infty dB$ (UMC) LO to RF $-20dB$ @ $1GHz$ (UCM) RF to LO $-20dB$ @ $1GHz$ (DCM) RF to BB $0dB$ @ $1GHz$ (DCM)
Power variation of $\omega_{LO} \pm \omega_{in}$ with respect to the duty cycle	$9.5dB$ @ 50% *to* 5%	

Chapter 4

Upconversion Mixer Design

4.1 Introduction

In the previous chapters we surveyed the performance of the harmonic mixer as well as the requirements of different wireless systems standards. In this chapter, a review of the specifications in Bluetooth and UWB is carried out. Then aim is to identify the key factors for designing the proposed mixer structure in those.

4.2 Bluetooth

Bluetooth, supported by the IEEE 802.15.1 standard is based on a wireless radio system designed for short-range devices and cheap to replace cables, such as mice, keyboards, joysticks and printers [11]. The Bluetooth system operates in the 2.4 GHz ISM band. The range of this frequency band is 2400 MHz to 2483.5 MHz, with a channel spacing of 1 MHz. Therefore, the regulatory range is 2.400 to $2.4835GHz$ with RF channels of

$$f = 2402MHz + k, \quad k = 0, \ldots, 78(MHz) \tag{4.1}$$

this characteristic apply in most countries with the exception of France [11]. The reference sensitivity level equals $-70dBm$, with a transmission power of $10dBm$. As a consequence, the NF is $10dB$. The interference performance on co-channel and adjacents of 1 MHz and 2 MHz is measured with the desired signal of 10 dB over the

Table 4.1: Bluetooth Transceiver Performance Requirements

Sensitivity	$< -70 \ dBm$
IIP3	$> -16.5 \ dBm$
Image Rejection	$> 29 \ dB$
Output Power	$-6 \ to \ 4 \ dBm$
Noise Figure	$< 10 \ dB$
Conversion Gain	$> 16 \ dB$

reference sensitivity level. On all other frequencies, the desired signal shall be 3 dB over the reference sensitivity level. Therefore, the linearity requirement is calculated using the maximum level of the co-channel interference and the adjacent channel blockers [11]. A 3dB margin is added, which gives an IIP3 requirement equal to $-16dBm$. It must be taken into account that the Bluetooth trend is to portable devices. These devices operate with batteries. According to the specification, the Bluetooth transceiver has to meet the regulations shown in table 4.1 to satisfy qualyty of signal.

4.2.1 Circuit Design

A drawback of the proposed topology is that the input port, $V_{in}(t)$, is the source of transistor P. Therefore, It is proposed the use of a P type transistor in the input port of the proposed mixer. Figure 4.1 shown the harmonic mixer with transistor P labeled as M_{pin} at the input port. This transistor is able to work in two modes of operation, saturation and triode. In saturation, the transistor operates as a current source controlled by $V_{in}(t)$. Therefore, the mixer could worked as a sub-harmonic mixer if this transistor is used as an amplifier. In the triode region, the transistor operates as a resistor which varies its resistance with respect to $V_{in}(t)$. The main advantage of the linear region is that the transistor does not contribute to the degradation of the IP3. However, in saturation the Gc can present gains which helps reduce NF. Therefore, in systems in which the linearity requirements are high, it is recommended to use the

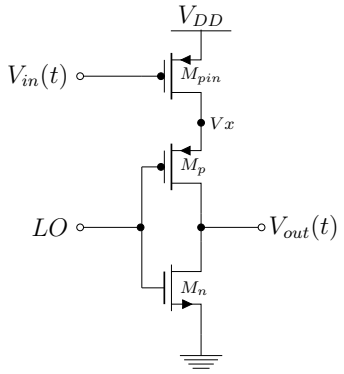

Figure 4.1: Proposed CMOS mixer circuit with transistor P in the input port.

transistor in the linear region, and if the noise is more important, then the use of the transistor in saturation may be better. The transistor can be sized in function of the current which is intended to be delivered to the mixer, for the case of saturation. For the sizing of the transistor in the triode, it is necessary that the resistance of this transistor be as small as possible, This with the aim of not degrading the time constant of the RC circuit which is seen from the input port ($V_{in}(t)$) to the output port ($V_{out}(t)$).

In previous chapters we mentioned that the harmonic mixer has been used primarily at the higher millimeter wave frequencies where reliable and stable LO sources are either not available or prohibitively expensive. For the Bluetooth standard, the frequency of LO for upconversion, if f_{BB} equals $10MHz$, is $2.39GHz$ and $2.41GHz$ for downconversion. Thus, f_{LO} is superior to $2GHz$. For this reason, we propose using the third harmonic of the LO source to achieve the frequency required by the Bluetooth standard. However, it is necessary to filter the low order components that are present in the output port of the mixer, this in order to not interfere with other bands. As shown in the previous chapter, by modifying the conduction angle you can have a control in the power of each one of the harmonics. Therefore, the third harmonic has a stronger presence with 40% of duty cycle. To make the transistors have a switching delay of 10% is used

$$\frac{\left(\frac{W}{L}\right)_n}{\left(\frac{W}{L}\right)_p} = \frac{(Vx - Vi - |V_{TP}|)^2}{(Vi - V_{TN})^2}\frac{\mu_p}{\mu_n} \tag{4.2}$$

Where $\left(\frac{W}{L}\right)_n$ and $\left(\frac{W}{L}\right)_p$ are the ratio of the sizes of the transistors labeled as M_n and M_p respectively; Vx is the maximum voltage excursion of the inverter output; V_{TN} and V_{TP} are the threshold voltages of the transistors and Vi is the threshold voltage of the inverter gate. For example, if a percentage of 50% is desired, Vi would be of $\frac{Vx}{2}$. For the present design the value will be

$$Vi = \frac{2Vx}{5} \tag{4.3}$$

Therefore, substituting (4.3) in (4.2), the relationship of sizes between M_n and M_p is

$$\left(\frac{W}{L}\right)_p = 1.21\left(\frac{W}{L}\right)_n \quad \therefore \quad \left(\frac{W}{L}\right)_p \approx \left(\frac{W}{L}\right)_n \tag{4.4}$$

We now proceed to size the transistors from the harmonic mixer. For this purpose, we use expression (4.5), which is obtained by the forward voltage gain or the parameter $S21$. This equation is obtained from the voltage Vx that is transferred through M_P to C_L, and the discharging voltage stored in C_L through M_n. Accommodating terms as a function of the dimensions, we obtain the aspect ratio of the device M_P, which is expressed as

$$\left(\frac{W}{L}\right)_p = -\frac{4\,\pi^2 f^2 {R_L}^2 {C_L}^2 + 1}{\left(R_L + 2\,\pi^2 f^2 {R_L}^3 {C_L}^2 - \sqrt{{R_L}^2\left(4 + 15\,\pi^2 f^2 {R_L}^2 {C_L}^2\right)}\right)\mu_p C_{ox}\left(V_{GS} - V_t\right)} \tag{4.5}$$

Where R_L and C_L are the load to the output of mixer and f is the translated frequency. For dimensioning M_{pin} we use the time constant (τ) that is equivalent to the time required for charging an discharching C_L. Therefore, Table 4.2 shows the dimensions obtained for the transistors of the harmonic mixer using the third harmonic of LO. As can be observed, M_{pin} is not designed with the minimum dimension allowed by the technology, this with the aim of reducing the mismatch.

Table 4.2: dimensions for the harmonic mixer in Bluetooth

	W	L
Mpin	140 μ	0.36 μ
Mp	70 μ	0.18 μ
Mn	70 μ	0.18 μ

4.3 UWB

UWB can legally operate at frequencies from $3.1GHz$ to $10.6GHz$ with a limited amount of transmission power ($-41dBm/MHz$), which makes it a technology whose range is very short, but more free from interference. Its bandwidth of around $7GHz$ allows channels to have a bandwidth of $500MHz$. It offers an average speed of $500Mbps$, with the condition that the connected devices are in the range of 10 meters or less. The design of transceivers for UWB is not an easy task due to the fact that the circuits has to work at high frequencies and with a wide bandwidth, which makes difficult the coupling. With a channel bandwidth of 528-MHz, the RX and Tx in the UWB systems can use direct conversion TRXs topologies since the flicker noise does not interfere with the signal path [9]. For TRXs design, it is necessary to consider the following specifications: depending on the bit rate, UWB specifies a RX sensitivity ranging from $-84dBm$ (for $55Mb/s$) to $-73dBm$ (for $480Mb/s$); with a SNR requirement of about $8dB$, these translate to an NF of $6-7dB$; the RX must provide a maximum voltage gain of approximately $84dB$, so that it increases the minimum signal level to the full scale of the baseband A/D converter; also, based on the interference expected from IEEE 802.11a/g TXs, an $1-dB$ compression point of $-23dBm$ (in the high-gain mode) is necessary. The UWB transceiver must met the regulations shown in table 4.3 to satisfy quality of signal.

Table 4.3: UWB Transceiver Performance Requirements

Required RX Performance		Required TX Performance	
Sensitivity	-73dBm	Output power	-10dBm
NF	6-7 dB	Output P1dB	-6dBm
Compression Point at 1dB ($P1dB$)	-23 dBm	Carrier Laekage	-30dBc
I/Q Mismatch	6 and 0.6dB	I/Q Mismatch	6 and 0.6dB
Phase Noise	-105 dBc/Hz	Phase Noise	-105 dBc/Hz

4.3.1 Circuit Design

For the UWB standard, the frequency of LO in upconversion, if f_{BB} is $10MHz$, is $3.09GHz$, and in downconversion f_{LO} has a frequency of $3.11GHz$. Hence, the LO frequency is around to $3GHz$. For this reason, we propose to use the fourth harmonic of the f_{LO} in order to achieve the frequency required by the UWB standard. As demonstrated in the previous chapter, by modifying the conduction angle it is possible to have a control in the power of each of the harmonics. Therefore, the fourth harmonic has a stronger energy with a 30% of the duty cycle. For sizing the inverter with a conduction angle of 30%, we used equation (4.2). To obtain the desired duty cycle, we found

$$Vi = \frac{3Vx}{10} \tag{4.6}$$

Therefore, substituting 4.6 in 4.2, the relationship of sizes between the transistors is given by

$$\left(\frac{W}{L}\right)_p = 3.4\left(\frac{W}{L}\right)_n \quad \therefore \quad \left(\frac{W}{L}\right)_p \approx 3\left(\frac{W}{L}\right)_n \tag{4.7}$$

We now proceed to size the transistors from the harmonic mixer. For this purpose, we use expression (4.5), which is obtained of the voltage Vx that is transferred through

Table 4.4: dimensions for the harmonic mixer in UWB

	W	L
Mpin	171 μ	0.36 μ
Mp	85.5 μ	0.18 μ
Mn	28.5 μ	0.18 μ

M_p to C_L, and the discharging voltage stored in C_L through M_n. The aspect ration of the M_p is expressed as

$$\left(\frac{W}{L}\right)_p \approx 475 \tag{4.8}$$

Similarly as in the previous design, it is necessary to reduce the mismatch. For this reason we do not use minimum dimensions in M_{pin}. Table 4.4 shows the dimensions obtained for the transistors of the harmonic mixer using the fourth harmonic of f_{LO}.

4.4 Simulation Results

The proposed mixer is designed with the UMC $0.18\mu m$ Mixed Mode and RF CMOS technology. In this technology there are two main models of transistors. N/P MOSFET $1.8V$ Model and N/P MOSFET $3.3V$ Model. As the name remarks it, we have a maximum bias voltage of $1.8V$ and a $3.3V$, respectively. This design is made with the N/P MOSFET $1.8V$ Model. The simulation is done with the maximum bias voltage that the technology provides, which is $V_{GS} \leq 1.8V(+10\%)$, $V_{DS} \leq 1.8V(+10\%)$ and $-1.8V \leq V_{BS} \leq 0V$. The analyzes considers load capacitance similar to that of an output pad. In UMC the pad has a capacitance of $158.3fF$ with a serie resistor of 1.0190Ω. The simulation was made with *Mentor Graphics® ICstudio* 2008.2*b*.

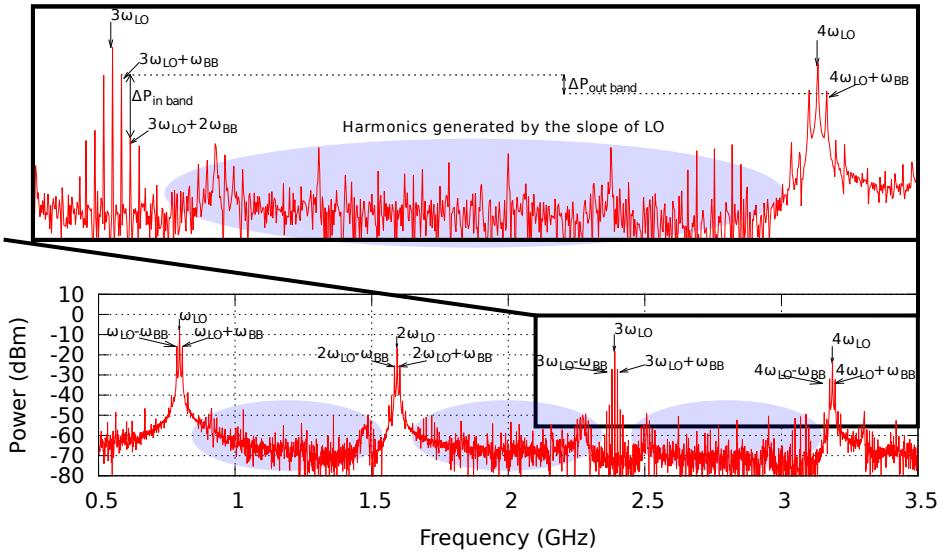

Figure 4.2: Ouput spectrum of a single-ended harmonic mixer in Bluetooth

4.4.1 Harmonic mixer in Bluetooth

For this mixer, we proposed to use the third harmonic of the LO source. Therefore, f_{LO} has a value of $800MHz$ for upconversion and $828.3MHz$ for downconversion when the signal f_{BB} is $10MHz$. The polarization voltage for the circuit is of $V_{DD} = 1.8V$. The power consumption is approximately of $35.7mW$. Figure 4.2 depicts the output spectrum of the single-ended mixer, which is obtained from simulation.

The upconversion for the Bluetooth band of the proposed harmonic mixer is located at $(3\omega_{LO} + \omega_{BB})t$, it has an energy of $-27.14dBm$. The energy at $(\omega_{LO} + \omega_{BB})t$, which is the first upconversion, is of $-15.9dBm$. Therefore we have a loss approximately of $11dBm$ ($\approx 50mW$). Nevertheless, the requirements of LO are reduce to one-third. One of the drawbacks of designing with a conduction angle different from 50% is that it reduces the propagation time from low to high. This can generate new harmonics. In Figure 4.2 are shown shaded in gray, the harmonics generated by the slope of LO. These harmonics have lower energy with respect to the harmonics that are integer multiples of f_{LO}.

On the other hand, in Figure 4.3 is shown the output spectrum of the differential

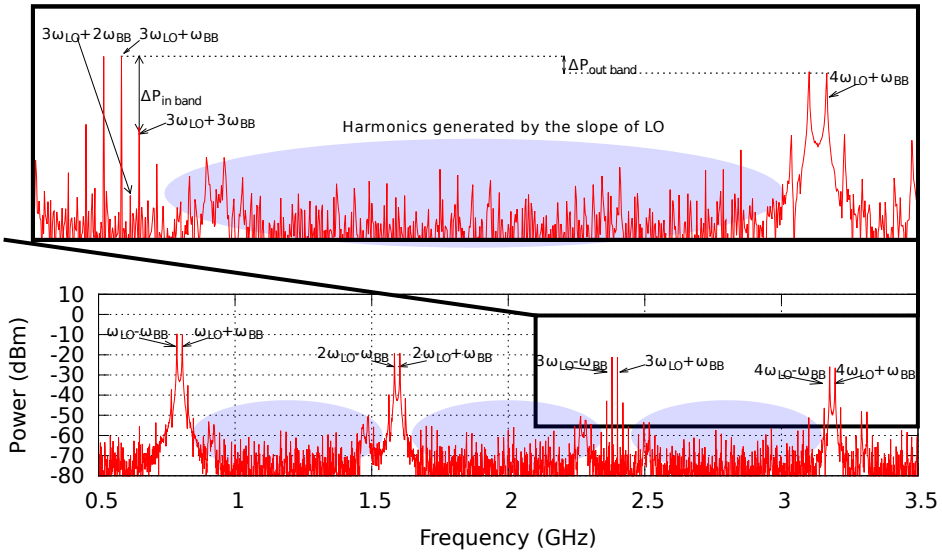

Figure 4.3: Ouput spectrum of a diferential harmonic mixer in Bluetooth

mixer which is obtained from simulation. As can be seen, the harmonics obtained for the differential mixer have the same energy obtained for the single-ended mixer. However, in the spectrum of the differential harmonic mixer, it can be observed that all harmonics generated by LO and all even harmonic of BB are removed.

In the previous chapters it was mentioned that the differential mixer and single-ended mixer have the same behavior in IP3 and Gc. This can be checked in Figures 4.2 and 4.3, which shows that all harmonics contain the same energy. Therefore, to calculate the linearity we used

$$IIP3|_{dBm} = \frac{\triangle P|_{dB}}{2} + P_{in}|_{dBm} \tag{4.9}$$

Where $\triangle P|_{dB}$ is the distance between the $(3\omega_{LO} + \omega_{BB})$ and the $(3\omega_{LO} + 2\omega_{BB})$ for in band or $4\omega_{LO} + \omega_{BB}$ for out band. Therefore, the proposed harmonic mixer with the use of the fourth harmonic for the upconversion has an IP3 of

$$IIP3|_{dBm} = 15.5dBm \tag{4.10}$$

Figure 4.4 shows the conversion factor in function of frequency. As can be seen,

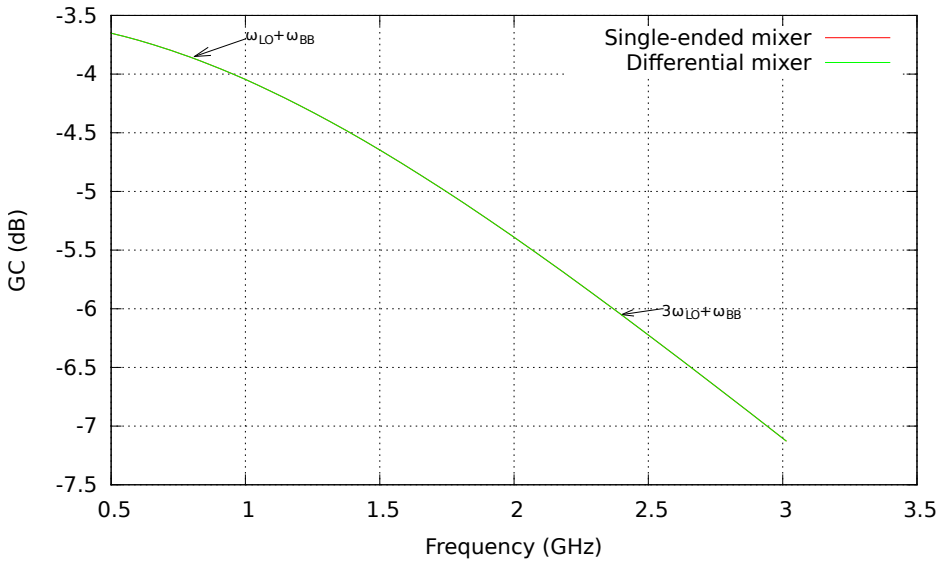

Figure 4.4: Conversion Factor of a differential and single-ended harmonic mixer in Bluetooth

$(\omega_{LO} + \omega_{BB})$, which is the first upconversion, has a Gc of $-3.85dB$, but in the band of Bluetooth Gc turns to be $-6.05dB$. Therefore, by using the third harmonic a loss of approximately $2dB$ with respect to using the fundamental harmonic is present.

As mentioned in previous chapters, the NF is inversely proportional to Gc. In consequently it is expected that NF increases. Figure 4.5 shows NF with respect to frequency. The difference between single-ended mixer and differential mixer with respect to NF is $2dB$. Hence, NF of the single-ended mixer is of $7.7dB$ and NF of the differential mixer is of $9.73dB$.

The modification of conduction angle is an important contribution, with this parameter we can modify the output spectrum and as a consequence, to control the output power of the mixer. Figure 4.6 illustrates the variation of the conduction angle with respect to Vb, this value is the DC level of the BB. As can be seen, there is a manipulation of the conduction angle from 40% to 7% this variation modifies the output power of the mixer. Which varies from $-52dBm$ to $-24dBm$, as shown in Figure 4.7.

Summarizing, we have the design of two harmonic mixers for Bluetooth. Both

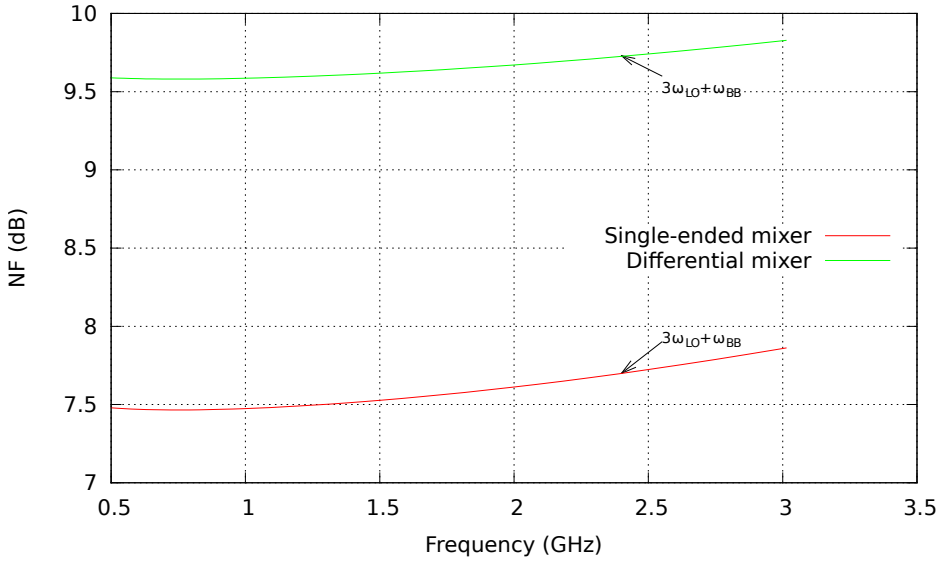

Figure 4.5: NF of the harmonic mixer in Bluetooth

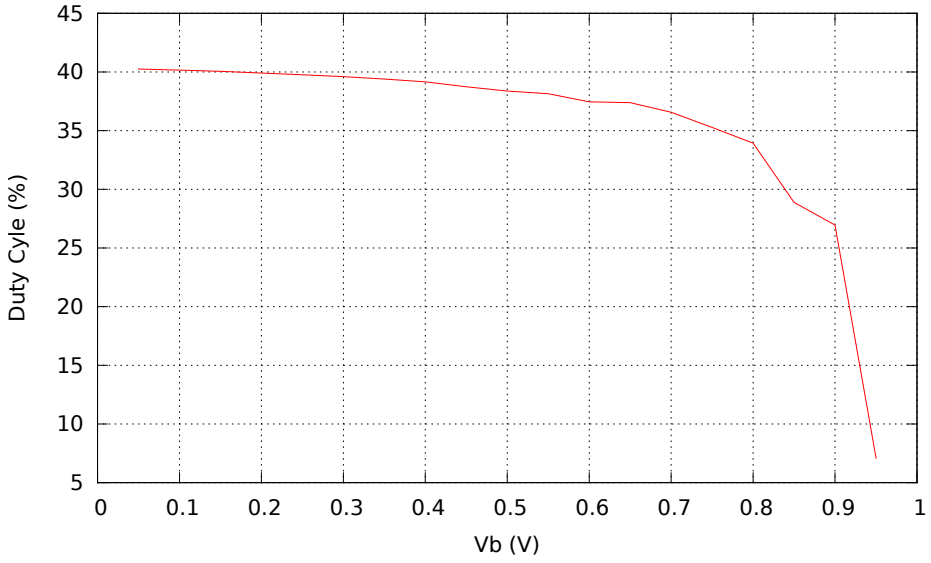

Figure 4.6: Duty Cycle Variation of the single and differential harmonic mixer.

proposals have identical performance in Gc with $-6.05dB$, IIP3 of $15.5dBm$, and a variation of the conduction angle from 40% to 7%. However, the differential mixer has an NF superior compared to the single-ended one, but the principal advantage of the differential mixer is that it removes all harmonics from LO. The proposed mixer works

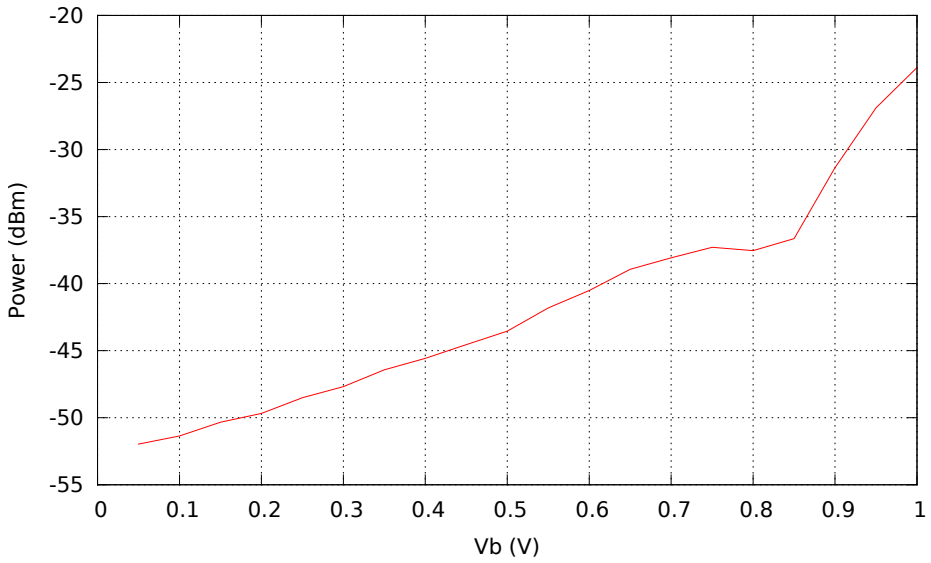

Figure 4.7: Output power tuning in function of Vb of the single and differential harmonic mixer.

Table 4.5: Simulation results of the harmonic mixer for Bluetooth.

RF band	$2.4GHz$-$2.485GHz$
LO Frequency	$800MHz$
BB Frequency	$10MHz$
Power supply	$1.8V$
Power consumption	$15.53dBm$
Conversion Factor	$-6.05dB$
IIP3	$15.5dBm \approx 35mW$
Noise Figure	$7.7dB$
Power output	$-24dB$ **@**$Vb = 1V$
Duty Cycle	40%-7%

with the third harmonic of the LO source, this helps to reduce the frequency of LO to reach the band of Bluetooth. In table 4.5, we present the main characteristics that were obtained from the simulation results.

4.4.2 Simulation Results for UWB

For thw UWB case, it is recommended to use the fourth harmonic of the f_{LO}. Therefore, f_{LO} equals of $772.5MHz$ for upconversion and $2.65GHz$ for downconversion when the f_{BB} equals $10MHz$. The polarization voltage is $V_{DD} = 1.8V$. The power consumption is approximately of $11.85mW$. Figure 4.8 depicts the output spectrum of the single-ended mixer obtained from simulation. The upconversion for the UWB band for the proposed harmonic mixer is located at $(4\omega_{LO} + \omega_{BB})$. It has an energy of $-31.2dB$. The energy at $(\omega_{LO} + \omega_{BB})$ is of $-20dB$. Therefore, we have a loss of approximately $11.2dB$. Nevertheless, the requirements of LO are reduced to a quarter. One of the drawbacks of designing with a conduction angle different from 50% is that it reduces the propagation time from low to high. If the transition from low-to-high is abrupt, the harmonics generated by LO are integer multiples of the fundamental. On the contrary, if the transition from low-to-high has an slope, this generates some other harmonics. Conforming smaller the slope is the harmonics will have more energy. Figure 4.8 shows in shaded gray the harmonics generated by the slope of LO. It can be seen that these harmonics have an energy level approximately equal to that the of IM3. Therefore, it is necessary to take special care with the input power in order to avoid that these harmonics do not add up more energy.

Figure 4.9 illustrates the spectrum at the output of the differential mixer which is obtained from simulation. As can be seen, the IM products obtained from the differential mixer has the same difference in energy between them compared to the single-ended mixer. However, in the spectrum of the differential harmonic mixer it can be observed that all harmonics generated by LO and the even harmonic of BB are removed.

All IM products shown in Figure 4.8 and 4.9 contain the same difference in energy among them. Therefore, the IP3 is the same for single-ended mixer and differential mixer. Hence, the IP3 is

$$IIP3|_{dBm} = 16.26dBm \tag{4.11}$$

Figure 4.10 depicts the conversion factor. As can be seen $(\omega_{LO} + \omega_{BB})$ is the first

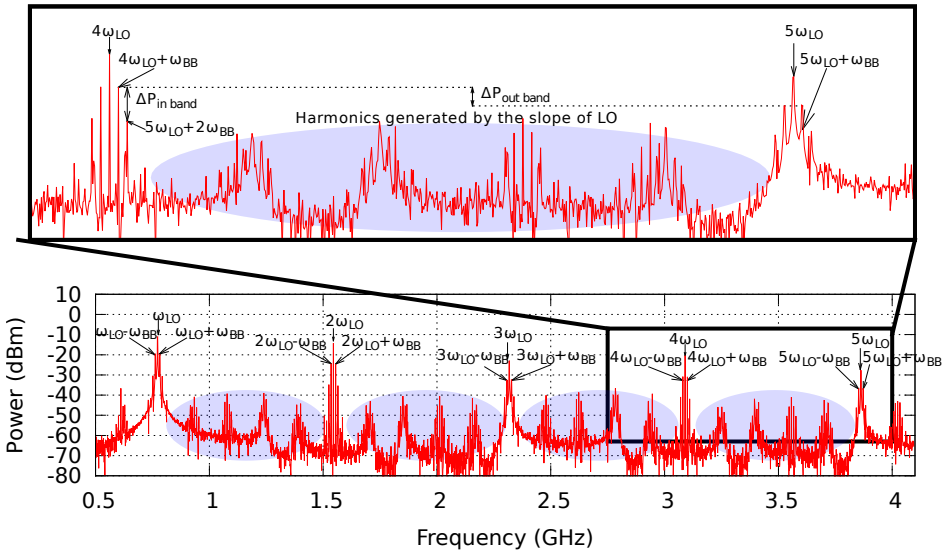

Figure 4.8: Output spectrum of a single-ended harmonic mixer in UWB

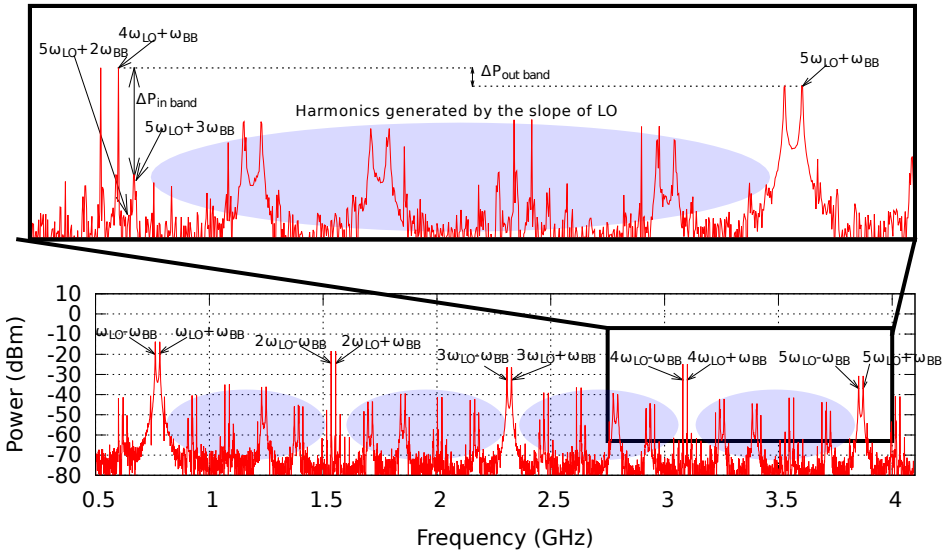

Figure 4.9: Output spectrum of a differential harmonic mixer in UWB

upconversion component, it has a Gc of $-5.7dB$, but in band of UWB it has a Gc of $-6.63dB$. Therefore, by using the fourth harmonic there will be a loss of approximately $1dB$ with respect to the first upconversion component.

As mentioned in the previous chapters, the NF is inversely proportional to Gc.

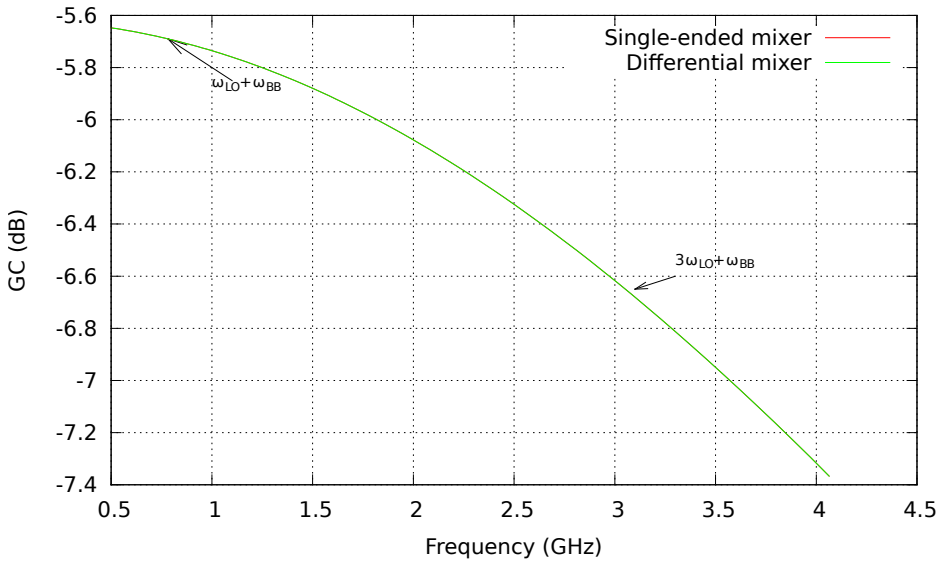

Figure 4.10: Conversion Factor of a diferential and single-ended harmonic mixer in UWB

Hence, as Gc has a double loss with respect to the expected, it is expected that NF increase in the same proportion. Figure 4.11 shows NF with respect to frequency. The difference between the single-ended and the differential mixer with respect to NF is of $2dB$. Hence, the NF of the single-ended mixer is of $6.7dB$ and the NF of the differential mixer is of $8.6dB$.

In Figure 4.12 is shown the variation of the conduction angle with respect to Vb, which is the DC level of the BB. As can be seen, there is a manipulation of the conduction angle from 28% to 7% this variation modify the output power of the mixer from $-38dBm$ to $-21.8dBm$, as shown in Figure 4.13.

Summarizing, we have two design proposals for harmonic mixers, single-ended and differential in UWB. Both proposals have identical performance in Gc with $-6.63dB$, IIP3 of $16.26dBm$ and a variation of the conduction angle from 28% to 7%. However, the differential mixer has a superior NF compared to single-ended mixer, but the principal advantage of the differential mixer is that it removes all the harmonics of f_{LO} and increases the dynamic range. The proposed mixer works with the fourth harmonic of

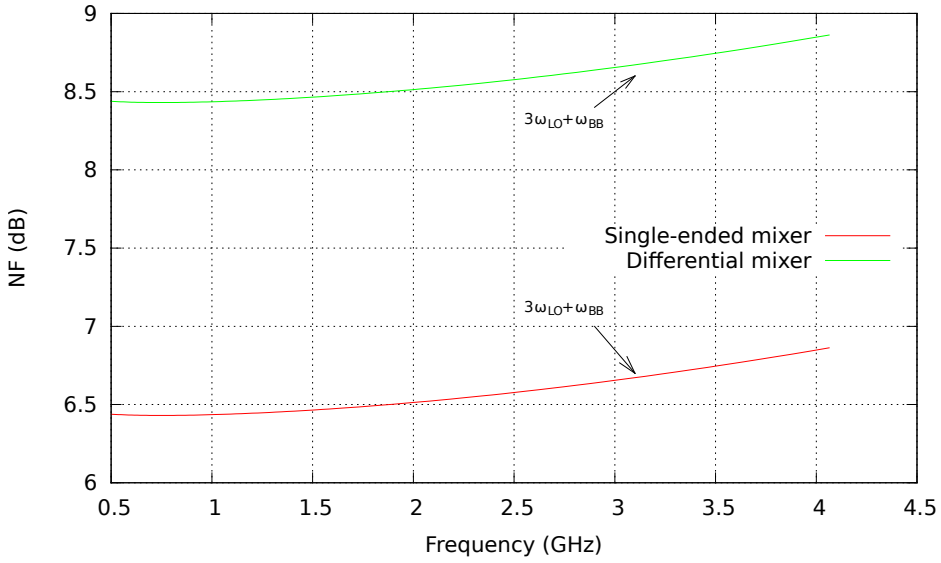

Figure 4.11: Noise figure of the harmonic mixer in UWB

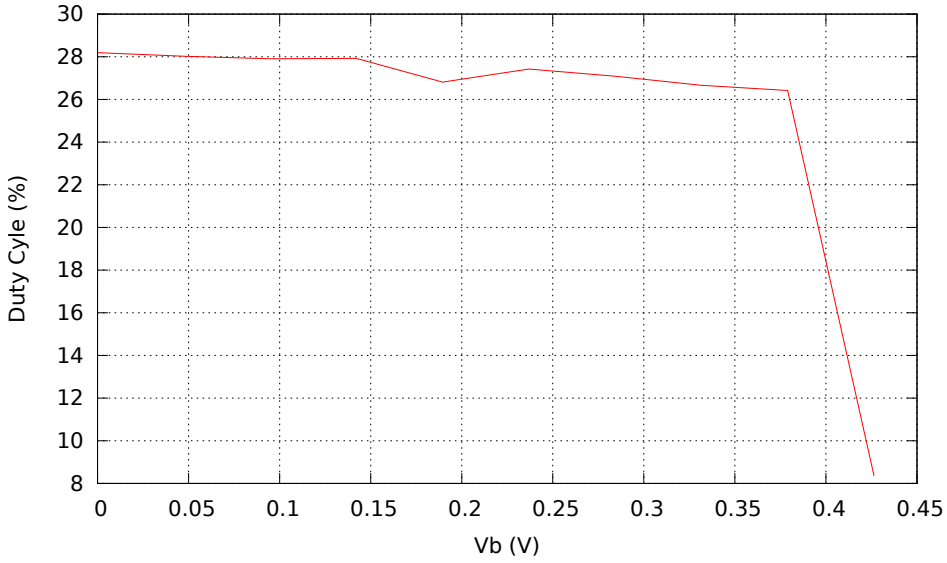

Figure 4.12: Duty Cycle Variation of the harmonic mixer.

the LO source, this helps to reduce f_{LO} to reach the UWB band. Table 4.6 presents the main characteristics from simulation.

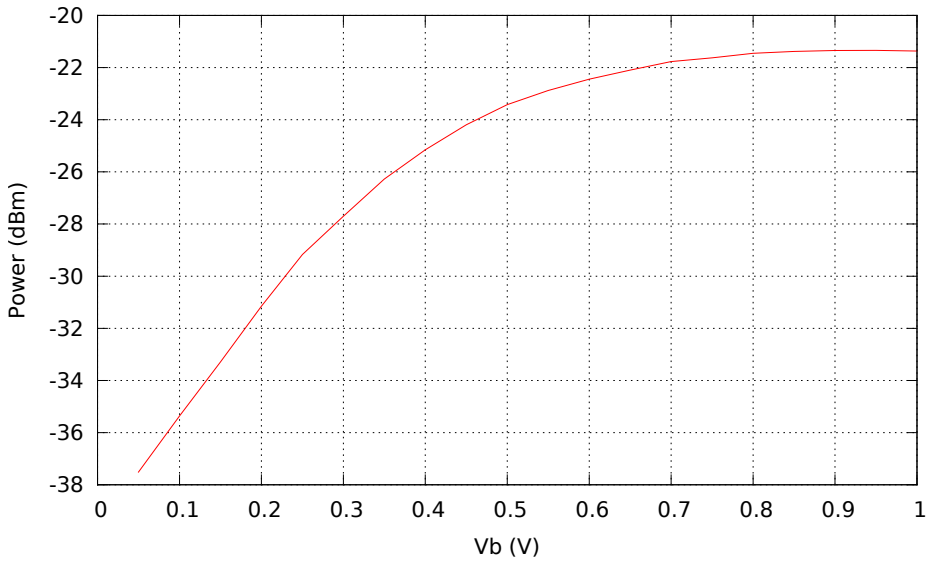

Figure 4.13: Output power tuning in function of Vb

Table 4.6: Simulation results of the harmonic mixer for UWB.

RF band	$3.1GHz$-$10.6GHz$
LO Frequency	$772.5MHz$
BB Frequency	$10MHz$
Power supply	$1.8V$
Power consumption	$11.85mW$
Conversion Factor	$-6.63dB$
IIP3	$16.26dBm$
Noise Figure	$6.7dB$
Output Power	$-21.8dB$ **@**$Vb = 1V$
Conduction Angle	28%-7%

4.5 Conclusion

The simulation in *Mentor Graphics*® *ICstudio* 2008.2*b* of the harmonic mixer for the Bluetooth and UWB standards with the UMC $0.18\mu m$ Mixed Mode and RF CMOS

technology have been carried out. In the first case, two design are presented. Both proposals have identical performance in Gc with $-6.05dB$, IIP3 of $15.5dBm$ and a variation of the conduction angle from 40% to 7%. However, the differential mixer has an NF of $9.73dB$ which is superior compared to the NF of $7.7dB$ of the single-ended mixer; but the principal advantage of the differential mixer is that it removes all the harmonics of f_{LO} and increases the dynamic range. The proposed mixer works with the third harmonic of the LO source, this helps to reduce the frequency of the LO to reach the Bluetooth band. The second design is for the UWB standard, the behavior of the proposed mixers for UWB have identical performance in Gc with $-6.63dB$, IIP3 of $16.26dBm$ and a variation of the conduction angle from 28% to 7%. However, the differential mixer has an NF $8.6dB$ and the NF of the single-ended mixer is $6.7dB$. The proposed mixer works with the fourth harmonic of the LO source, this helps to reduce the frequency of LO to reach the band UWB. The final design is presented in the next chapter, because it was manufactured and characterized.

It can be seen that the NF of the mixer in Bluetooth is greater with respect to the mixer in UWB this is because the mixer that is designed for UWB have a large sizing, accordingly it also provides a lower noise. It was shown that the conduction angle change helps to modify the output power of each of the harmonics. However, it is not advisable to use small angles, because this causes a slower propagation time and therefore more harmonics. We can conclude that the mixer proposed has good performance in terms of noise, linearity and conversion factor, the latter thanks to the manipulation of the conduction angle.

Chapter 5

Experimental results

5.1 Introduction

In the previous chapter we presented two designs proposals of harmonic mixers for two different standards, Bluetooth and UWB. The simulation have been already reported. The experimental results of another one is detailed in this chapter.

The implementation of the harmonic mixer for satisfying the MICS requirements has been developed on a double poly, three metal layers $0.5\mu m$ CMOS technology from ON SEMI foundry. The maximum voltage allowed for biasing the transistors of this particular technology is $5V$. However, $3.3V$ was employed for biasing the prototype. The prototype area is $619.5\mu m \ \ X \ \ 236.5\mu m$ including the output pads. The circuit is designed to operate in the RF band of $402MHz$ to $405MHz$, The main features that are characterized in the MICS band are power consumption ($28.2mW$), Gc ($-6.25dB$) and IIP3 ($28.3dBm$). In the following sections it will be discussed the design of harmonic mixer on MICS and described the test-setup.

5.2 MICS

The Medical Implant Communications Service (MICS) is a mobile-radio service for transmitting data in support of diagnostic or therapeutic functions associated with

Table 5.1: MICS Transceiver Performance Requirements

Implanted Unit	
Frequency Band	402-405 MHz
Receiver noise bandwidth	25kHz
Antenna Gain Tx/Rx	-31.5dBi
Power Into Antenna	-2dBm
Tx Power at the surface of the skin	-33.5dBm EIRP
Required SNR	14dB
Noise Floor	-121dBm
Ambient noise at receiver input	About kTB (due to tissue loss)
Receiver noise figure	9dB

implanted medical devices. The TRXs in the medical implant establish a link with the base station at both frequency bands, $2.45GHz$ and $400MHz$. The higher frequency link sets up a wake-up process to save power since MICS systems spend most of their time asleep and, periodically, the implant should scan for an external programmer which looks for beginning communication [27]. On the other hand, the $400MHz$ link is by which the monitoring activity of the implant is sent to the programmer. Such frequency is well suited for this service because of the signal propagation characteristics in the human body and its international availability [27]. Some of the most salient features of the MICS are summarized in Table 5.1.

5.2.1 Circuit Design

For the MICS standard, the frequency of LO in upconversion, if BB is $10MHz$, is $392MHz$, and in downconversion LO has a frequency of $395MHz$. Hence, the requirements of LO are lower with respect to the two previous standards. Therefore, for this design, it is recommended to use the first harmonic of the LO source for the conversion. Before starting the design it is proposed the use of a P type transistor at the input

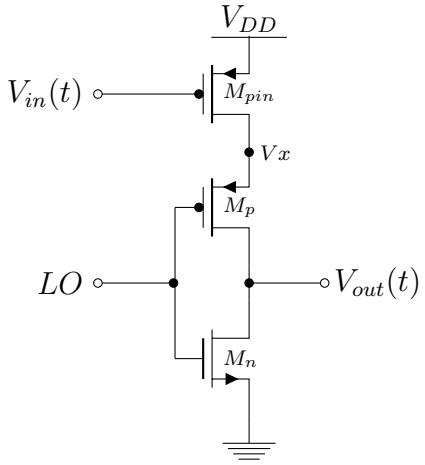

Figure 5.1: Proposed CMOS mixer circuit with transistor P in the input port.

port of the proposed mixer. Figure 5.1 shown the harmonic mixer with the transistor P labeled as M_{pin} at the input port. M_{pin} can be sized in function of the current which is intended to be delivered to the mixer if works in saturation. For the sizing of the transistor in the triode region, it is necessary that the resistance of this transistor be as small as possible, this with the aim of not degrading the time constant of the RC circuit seen from the input port ($V_{in}(t)$) to the output port ($V_{out}(t)$). To begin the design we propose to work with the propagation times of the mixer from high-to-low and low-to-high, these can be selected in function of the speed of the square wave at the input of the mixer and the duty cycle desired at the output. Expressions (5.1) and (5.2) are now used to size the harmonic mixer. The aspect ratio of such elements can be determined by means of

$$\left(\frac{W}{L}\right)_n = \frac{t_{PHL}\mu_n C_{ox}(V_{DD} - V_{TN})^2}{C_L V x} \tag{5.1}$$

$$\left(\frac{W}{L}\right)_p = \frac{t_{PLH}\mu_p C_{ox}(-V_{DD} - |V_{TP}|)^2}{C_L V x} \tag{5.2}$$

Where t_{PLH} and t_{PHL} are the propagation delays of the harmonic mixer from high-to-low and low-to-high, respectively; μ_p is the mobility of the wholes; V_{TN} and V_{TP} are the threshold voltages from M_n and M_p, respectively; V_{DD} is the bias voltage employed

Table 5.2: Dimensions of the transistors of the fabricated prototype.

Mixer			Input Buffer		
	Width(μm)	Length (μm)		Width (μm)	Length (μm)
M_{pin}	480	1.2	M_{pb1}	19.8	0.6
M_p	180	0.6	M_{nb1}	15	0.6
M_n	540	0.6	M_{pb2}	66	0.6
			M_{nb2}	30	0.6
			M_{pb3}	115.5	0.6
			M_{nb3}	45	0.6
			M_{pb4}	264	0.6
			M_{nb4}	120	0.6

meanwhile Vx is the DC voltage at source port of the M_p transistor; finally, C_L is the load capacitance seen by the mixer, which is compound by the self load of the circuit and the capacitance of the interconnection line. For dimensioning of M_{pin} we used (5.3), this expression is obtained from the propagation constant which is given by the sum of resistors of the M_{Pin} and M_p by C_L.

$$\left(\frac{W}{L}\right)_{pin} = \frac{C_L\,(Vx - V_{TH})}{\left((Vx - V_{TH})\,(\frac{W}{L})_p Cox\,\mu_p\tau - C_L\right)(V_{DD} - V_{in} - V_{TH})}\left(\frac{W}{L}\right)_p \tag{5.3}$$

where τ is the time required for the C_L to be charged, $(\frac{W}{L})_p$ is the aspect ratio of M_p. With the aim of reducing the mismatch the size of M_p is not designed with the minimum dimension allowed by the technology.

5.3 Experimental Results

Following all the considerations described in the previous section, the designed of a harmonic mixer for MICS was carried out and fabricated in a double poly, three metal

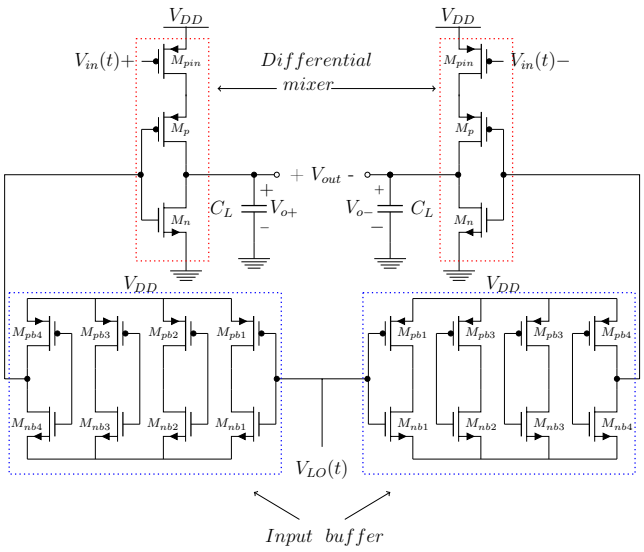

(a) Circuit diagram

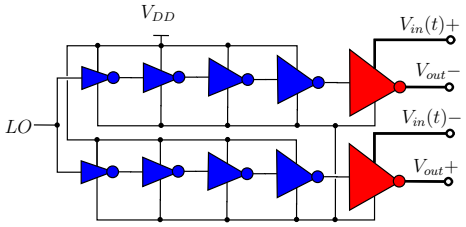

(b) Block diagram

Figure 5.2: Schematics of the fabricated prototype

layers, $0.5\mu m$ in CMOS technology from MOSIS foundry. Table 5.2 shows the dimensions obtained for the transistors of the harmonic mixer of Figure 5.2(a). Figure 5.2(b) shows the block diagram of the fabricated circuit. As can be seen, it consists of an input buffer which turns the sinusoidal input from the LO into a square wave signal with 50% duty cycle followed by the mixer.

The prototype area is $619.5\mu m \;\; X \;\; 236.5\mu m$ including the output pads. The prototype die photo is depicted in Fig. 5.3. As can be appreciated, the bias input, V_{DD}, the $V_{in}+$ and $V_{in}-$ input, the LO input and the ground are fed to the bond pads of the chip meanwhile the output nodes are placed on inner-pads labeled as $V_{out}+$ and $V_{out}-$. The die was attached to a printed circuit board (PCB) with an epoxy resin.

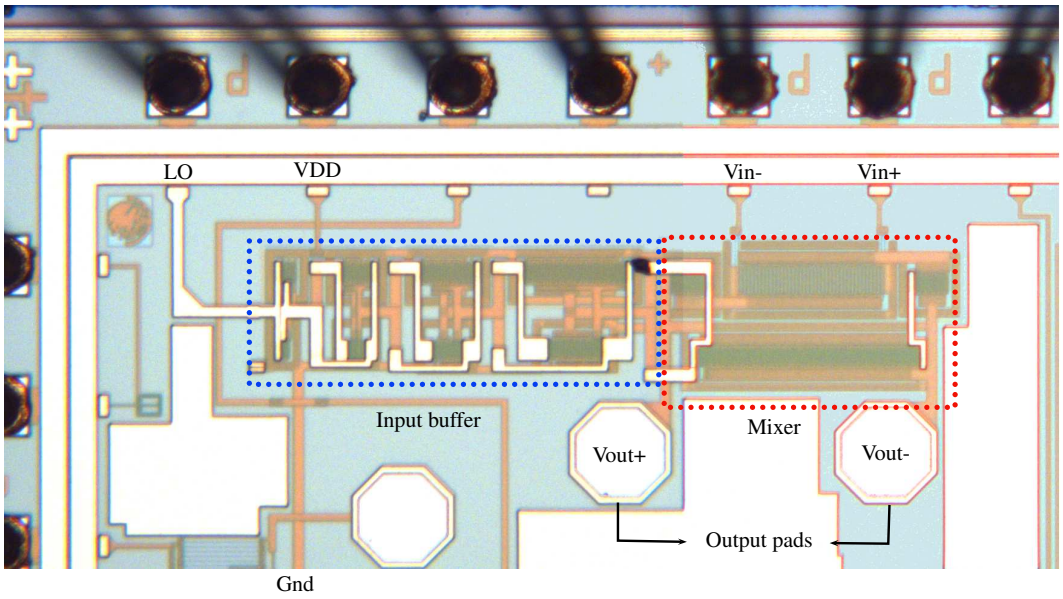

Figure 5.3: Prototype die photo.

The PCB was designed and fabricated quite straightforward with an standard FR4 material, which is shown in 5.4. Two SMA connectors are used to feed the LO and the BB signals. In order to generate the differential signal of V_{in}, it is used a balun *Coilcraft* ***WB2010-1-PCL***, which has a relation of the primary with the secondary of $1:1$, and a bandwidth of $0.04MHz$ - $175MHz$. In addition, three groups of poles are used to bias and to ground the circuit. Also, Two SMA connectors are used to measure the output signal. To alleviate the ground bouncing, capacitors in each bias point were placed on the PCB.

The Test-setup for the evaluation of the functionality of the mixer is shown in Figure 5.5. The source which consists of a Tektronix PWS4000, biases the circuit with $3.3V$. On the other hand, an Agilent E3614A source amends the DC level at which the signal enters the mixer (This same voltage is the one that enables variation of the conduction angle and the modulation of the output power); an Agilent 33250A function generator is responsible for generating the BB signal; in addition, a vector signal generator, Rohde & Schwarz SMBV100A-B106, prodece the LO signal (a drawback of this generator

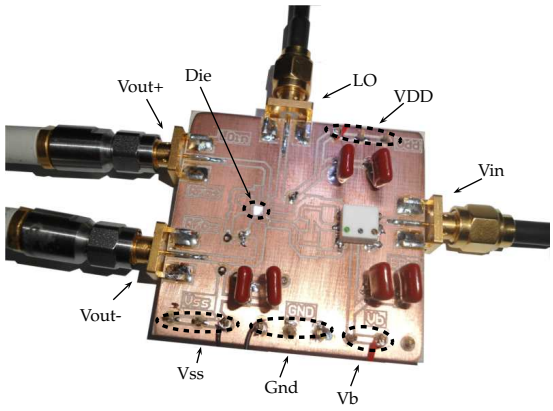

Figure 5.4: Evaluation test board.

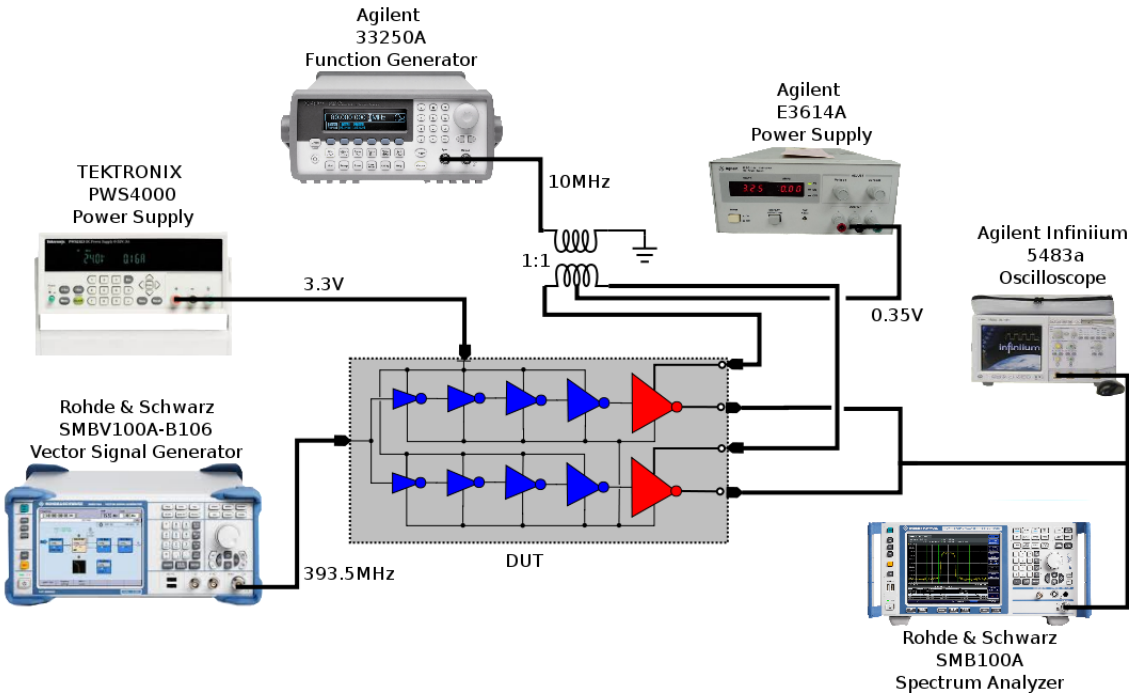

Figure 5.5: Prototyp test-setup.

is that it has not the capability to generate signals mounted on a DC level). Finally, to analyze the output signals in the time domain we used an Agilent oscilloscope 5483rd Infinitum, which was very useful to determine the duty cycle of the mixer as well as the maximum and minimum output voltage signals. Also, we use an spectrum analyzer

Table 5.3: Measured results of the harmonic mixer.

RF band	$402MHz$-$405MHz$
LO Frequency	$393.5MHz$
BB Frequency	$10MHz$
Power supply	$\pm 1.65V$
Power consumption	$28.2mW$
Conversion Factor	$-6.25dB$
IIP3	$28.3dBm$
Power output	$5dBm$ **@** $Vb = 1.9V$
Duty Cycle	46%-25%
Amplitude of BB	$660mV$

Rohde & Schwarz SMBV100A. For determining the power at the frequency of interest, and also the linearity.

In table 5.3 it is shown the most important characteristics of the prototype. As mentioned earlier, LO has a frequency of $393.5MHz$, while BB a frequency of $10MHz$. The polarization of the circuit is of $\pm 1.65V$. The modulation of the output power is achieved with a voltage control between $450mV$ to $1.9V$, obtaining a minimum power of output of $-28dBm$ and a maximum power of $5dBm$.

Figure 5.6 depicts the waveforms obtained in the characterization of the prototype for some voltage control values. As can be seen, as the voltage increases the amplitude of the pulse train varies periodically and also its duty cycle and, consequently, the power delivered to the load changes. The image shows the differentials signals along with their subtraction.

It is of major interest to examine the spectral content of the output signal in order to determine the harmonics and the IM prodcust produced by the harmonic mixer. Figure 5.7 shows the output spectrum of the single-ended mixer. As you can see the spectrum is repeated periodically, the LO signal is present and is the harmonic that

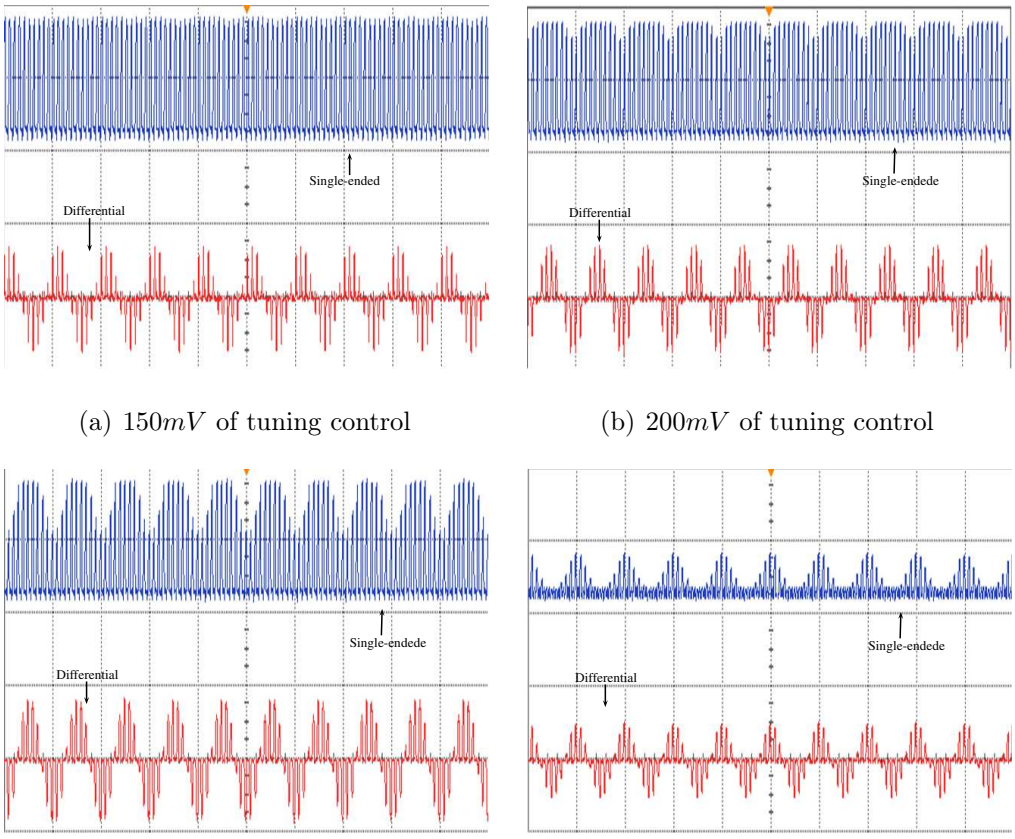

(a) $150mV$ of tuning control

(b) $200mV$ of tuning control

(c) $300mV$ of tuning control

(d) $650mV$ of tuning control

Figure 5.6: Output waveforms of the prototype

contains more energy. Furthermore, there are two third order intermodulacion products $(2\omega_{LO} \pm \omega_{BB})$. Similarly, Figure 5.8 depicts the output spectrum of the differential harmonic mixer. It can be seen that the only difference is the absence of the harmonic of LO. As anticipated in the analysis of Chapter Three, the main advantage of the differential mixer is the elimination of LO without the use of a resonant network. Therefore, in Figure 5.7 and 5.8, the Harmonics of the BB (@$10MHz$), the component of interest $(\omega_{LO} + \omega_{BB})$ (@$403.5MHz$), its image $(\omega_{LO} - \omega_{BB})$ (@$383.5MHz$) and the high order IM products $(n\omega_{LO} \pm \omega_{BB})$ (where n is $2, \ldots, \infty$) are shown. It is worthy to mention that in the differential mixer there may be a small presence of LO is due to the mismatch between the LO at the input of each inverter in the mixer. Therefore, a careful layout of the mixer must done to keep the LO as balanced as possible at the input of the mixer.

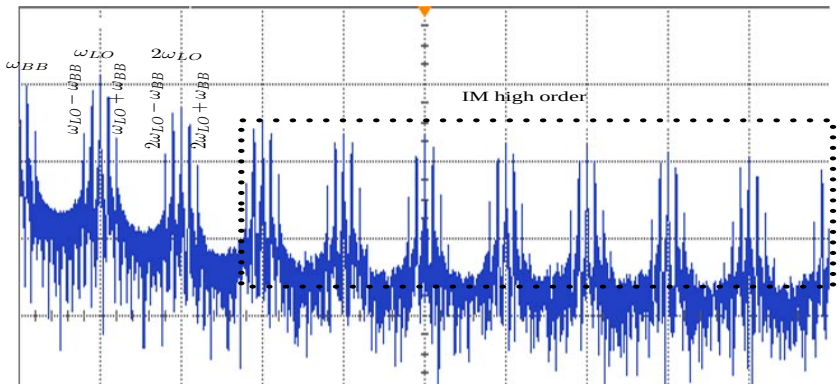

Figure 5.7: Output spectrum of single harmonic mixer

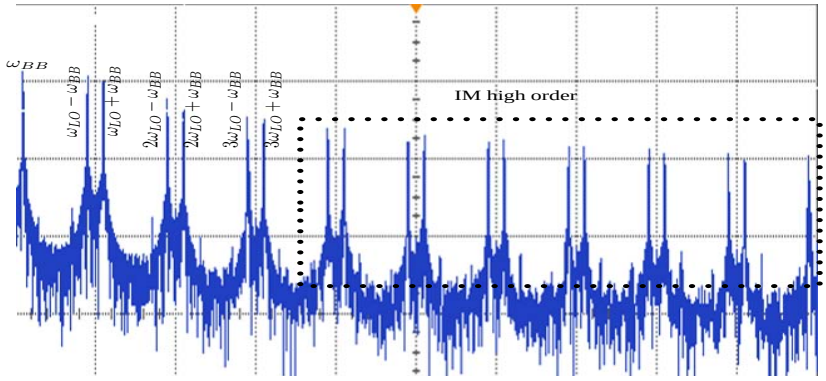

Figure 5.8: Output spectrum of diferential harmonic mixer

The linearity is one of the figures of merit to characterize a mixer. In Chapter Three, by mathematical analysis it was concluded that the mixer has a linearity of approximately $36dBm$. Linearity of the prototype was characterized by means of the two-tone test. The first tone is $\omega_{LO} + \omega_{BB}$ for the upconversion, and the second tone is IM3 $(2\omega_{LO} + \omega_{BB})$. After performing the linearity characterization we compared it with that obtained from the mathematical equation; such comparition is shown in the Figure 5.9, and it was found that the mixer has a very good performance in terms of linearity since the obtained was of approximately $29dBm$. Therefore it has a difference of $7dBm$ the which is due to the deficiencies in the test-setup. For example, bad welds,

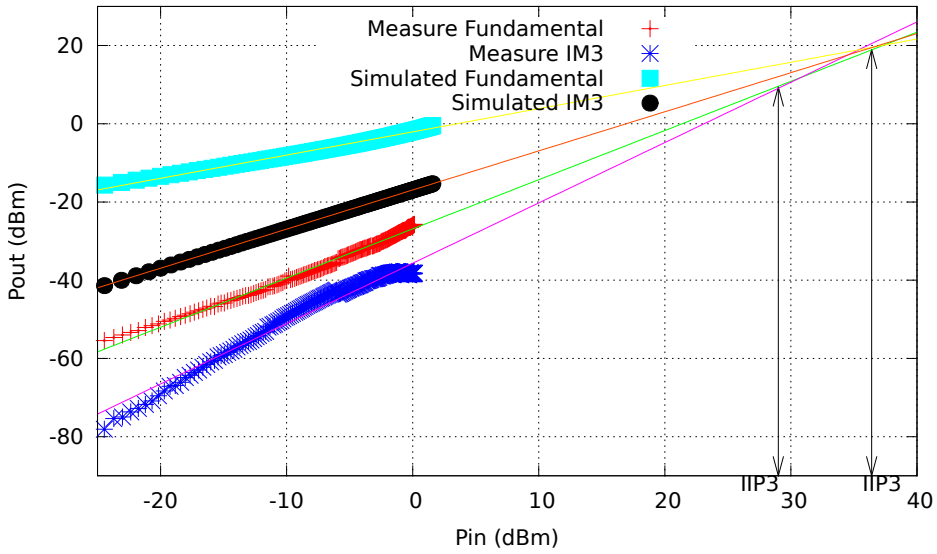

Figure 5.9: IIP3 characterization

manufacturing defective of the PCB, bonding wire and others.

One of the main contributions of this work is the possibility of modifying the conduction angle, this is achieved by modifying the DC level of BB. Therefore, Figure 5.10 illustrates the range attained. It goes from the 47% to 25% with a variation of Vb from $0V$ to $650mV$. This variation help us to modulate the output power of the $\omega_{LO} + \omega_{BB}$. The DC level of BB affects equally to the differential mixer and the single-ended mixer. Therefore, the conduction angle and duty cycle are the same for any of the two possibilities. Figure 5.11 shows the output power variation in function of Vb. One can see that the power modulation has a behavior practically linear between $-1.1V$ to $400mV$, whereas higher the value of Vb is the higher the power attained. This is because the transistor where the signal is injected changes its region of operation.

Finally, in Table 5.4 the most important features of the prototype are summarized.

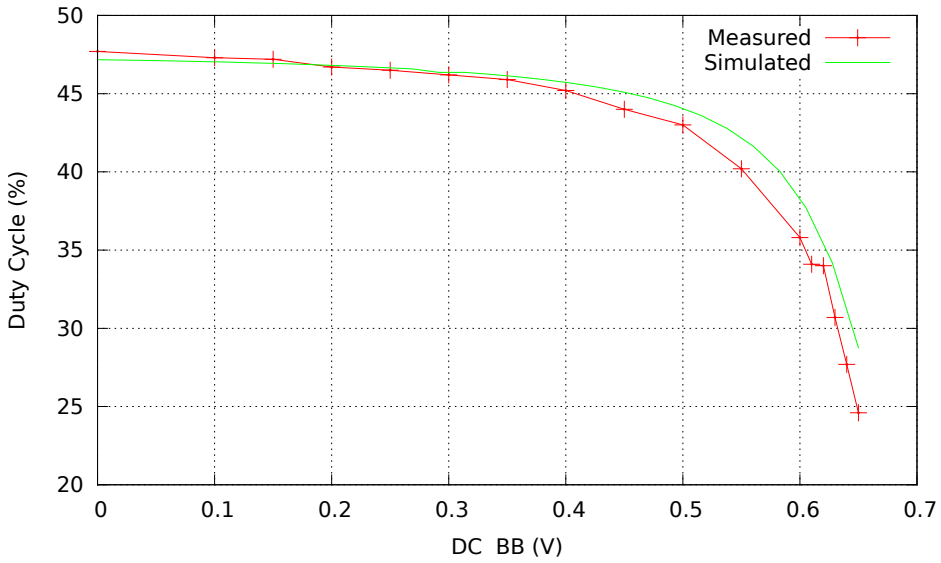

Figure 5.10: Duty cycle of the prototype for the whole tuning control range.

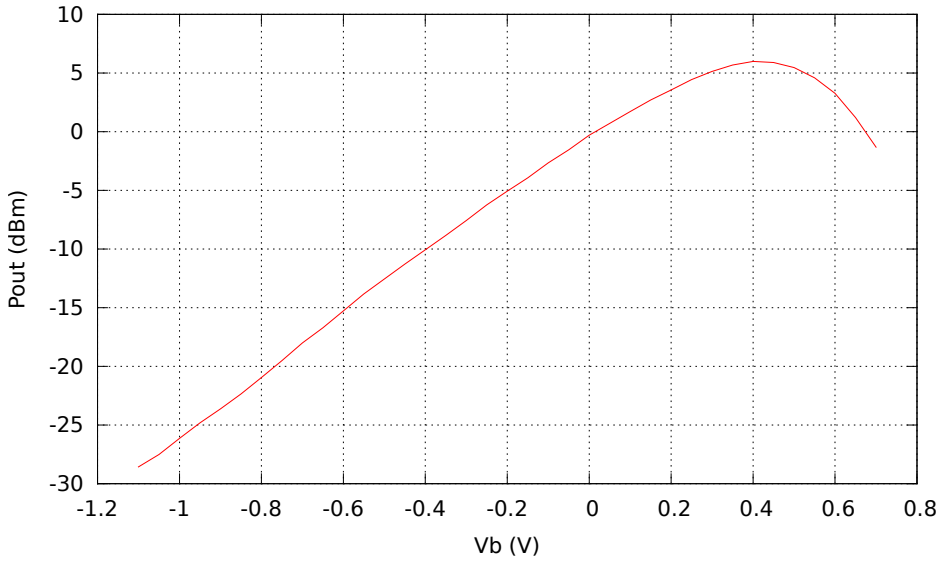

Figure 5.11: Output power of the prototype for the whole tuning control range.

5.4 Conclusion

The design and fabrication of the harmonic mixer was also realized but in a double poly three metal layers $0.5\mu m$ CMOS technology from MOSIS foundry. The fabricated

Table 5.4: Performance features of the prototype

Technology	ON Semiconductor $0.5\mu m$
RF Frequency	$402MHz$ - $405MHz$
LO Frequency	$393.5MHz$
BB Frequency	$10MHz$
Power supply	3.3
Power consumption	$28.2mW$
Conversion Factor	$-6.25dB$
IIP3	$28.3dBm$
Power output	$5dBm$ **@**$Vb = 1.9V$ -
Duty cycle	46% - 25%

prototype area was $619.5\mu m$ X $236.5\mu m$. The PCB used for measurements was designed and fabricated with an standard FR4 material. The circuit works with LO signal of $393.5MHz$ with a excursions of $\pm 1.65V$, while that BB has a frequency of $10MHz$ with amplitude of $660mV$. The circuit is biased with $\pm 1.65V$ and the f_{BB} is @$10MHz$. The modulation of the output power is achieved with a control voltage between $450mV$ to $1.9V$, obtaining a minimum power of output of $-28dBm$ and a maximum power of $5dBm$. Similarly, it was shown that the differential mixer and single-ended mixer have the same behavior in Linearity, Gc and modulation of the output power. According to the results obtained in the characterization of the prototype, we conclude that the behavior of the harmonic mixer follows the course anticipated in the synthesis of the mixer performed in Chapter Three.

Chapter 6

Summary and Conclusion

In this chapter, the thesis is summarized, the main conclusions are listed and finally the suggestions for future research are given.

6.1 Summary of the Thesis

Chapter 1

The mixer is a complex circuit whose important features include; Gain conversion, Noise Figure, Lineality, Port Isolation and Power Consumption. This five FOMs are important [3], however, the mixer is an element that generates a lot of distortion, therefore it is necessary to take special care if the mixer if it is used in broadband systems. Nevertheless, if it occupied in systems where the TX power is low, the NF is very important. In sum, before designing a mixer, it is necessary to know the requirements of the standard in which it is going to be placed, because there is a trade-off among each of the FOMs, which can not be ignored.

Chapter 2

The harmonic mixer is a variant of the passive mixer which has the advantage that the devices employed in its architecture do not contribute to the degradation of the linearity of the circuit in comparison to the active mixer. This is due to two main

reasons: first, because the mixer behaves like a resistive circuit, and these resistors have a linear behavior; therefore, the output current has a linear behavior; this is valid if LO has enough energy to completely turn on and off the transistors and its transitions are abrupt; on the other hand, the balanced mixer eliminates IM3, which alleviates the linearity because this harmonic is which more energy gives to the fundamental. This kind of mixer is reliable when the LO has not to perform at high frequencies. However, an special issue is the NF due to losses in the output port. Although the harmonic mixer has a minimum contribution of noise with respect to the active mixer.

Therefore, based on the information presented it can be concluded that the harmonic mixer may be used in broadband systems such as UWB or MBWA, because they have a good linearity performance. However, UWB has an effective isotropic radiated power transmitted to the receiver in the order of $-41dBm/Hz$ and a noise floor in the band in the order of $-84dBm/Hz$. These two data limited the conversion factor and have minimum losses. The losses reduce the energy of the signal, making it approaches to the noise floor level. In contrast, MBWA has a TX power of $43dBm/MHz$ and a noise floor within the band of $-174.5dBm$. This implies that MBWA has a higher dynamic range compared to UWB. Therefore, there are no complications if Gc has losses. In sum, it is necessary to know all the features and needs of the standard in order to propose the best design and performance.

Chapter 3

They are presented all the analyze of two topologies proposed harmonic mixer for obtained the five FORMs, both topologies are good, the main advantage that presents the differential architecture is that it cancels the LO. On the other hand, the single-ended mixer has a lower power consumption and a better NF. In addition, by changing the DC level at the input, the duty cycle at the output can be modified and consequently the spectrum of the signal is changed. This may be advantageus in applications where linearity demands are stringent. Some of the most salient features of the proposed mixer are summarized in Table 6.1.

Table 6.1: characteristics of the proposed mixer.

	Sibgle-ended	Differential
Linearity	$36dBm$	
Conversion Factor	$-3dB$	
Noise Figure	$2.7dB$ @ $W = 200\mu m$	$6.25dB$ @ $W = 200\mu m$
Isolation Ports	LO to BB $-20dB$ @ $1HGz$ (UMC) LO to RF $-18dB$ @ $1GHz$ (UCM) RF to LO $-20dB$ @ $1GHz$ (DCM) RF to BB $0dB$ @ $1GHz$ (DCM)	LO to BB $-\infty dB$ (UMC) LO to RF $-20dB$ @ $1GHz$ (UCM) RF to LO $-20dB$ @ $1GHz$ (DCM) RF to BB $0dB$ @ $1GHz$ (DCM)
Power variation of $\omega_{LO} \pm \omega_{in}$ with respect to the duty cycle	$9.5dB$ @ 50% *to* 5%	

We can see that the linearity achieved is $36dBm$ which is a good number as it indicates that the proposed mixer can work with large signal amplitudes and if working with small signals the $IM3$ shows very little energy. Concerning Gc, it is a typical value for a passive device. However, because the IP3 is high and consequently large signals at the input port can be used, the output signal of the mixer is away from the noise floor. In relation to the ports isolation, it can be seen that in the order of the GHz, there is a transference of approximately one hundred of the power of the unwanted signal. However, in the differential mixer the carrier is suppressed. Hence, LO is not present at the output of the mixer and consequently the ports isolation is, theoretically, perfect. One of the important contributions in this work is the variation of the output power in function duty cycle, considering that the maximum output power is at 50% of the duty cycle and reducing the duty cycle at 5% we have that the output power varies approximately $9.5dB$. This is helpful in systems where linearity is important, because when the output power is changed also the efficiency of the system is modified.

Chapter 4

The simulation in *Mentor Graphics® ICstudio* 2008.2*b* of the harmonic mixer for standard Bluetooth and UWB with the UMC 0.18μm Mixed Mode and RF CMOS technology was carried out. The first design presents two proposals of harmonic mixer in Bluetooth. Both proposals have identical performance in Gc with $-6.05dB$, IIP3 of $15.5dBm$ and a variation of the conduction angle from 40% to 7%. However, the differential mixer have NF of $9.73dB$ which is superior compared to the NF of $7.7dB$ of the single-ended mixer, but the principal advantages of the differential mixer is that removed all harmonics of f_{LO} and increases the dynamic range. The proposed mixer works with the third harmonic of the LO source, this helps to reduce the frequency of the LO to reach the Bluetooth band. The second design is for the UWB standard, the behavior of the proposed mixers for UWB have identical performance in Gc with $-6.63dB$, IIP3 of $16.26dBm$ and a variation of the conduction angle from 28% to 7%. However, the differential mixer have NF $8.6dB$ and NF of the single-ended mixer is $6.7dB$. The proposed mixer works with the fourth harmonic of the LO source, this helps to reduce the frequency of LO to reach the band UWB.

It can be seen that the NF of the mixer in Bluetooth is larger with respect to the mixer in UWB this is because the mixer that is designed for UWB has larger sizing, accordingly, it also provides a lower noise. It was shown that the conduction angle change helps to modify the output power of each of the harmonics. However, it is not advisable to use small angles, because this causes a slower propagation time and therefore more harmonics. We can conclude that the mixer proposed has good performance in terms of noise, linearity and conversion factor, the latter thanks to the manipulation of the conduction angle.

Chapter 5

The design and fabrication of the harmonic mixer was also realized but in a double poly three metal layers 0.5μm CMOS technology from MOSIS foundry. The fabricated prototype area was 619.5μm X 236.5μm. The PCB used for measurements was designed

and fabricated with an standard FR4 material. The circuit works with LO signal of $393.5MHz$ with a excursions of $\pm 1.65V$, while that BB has a frequency of $10MHz$ with amplitude of $660mV$. The circuit is biased with $\pm 1.65V$ and the f_{BB} is @$10MHz$. The modulation of the output power is achieved with a control voltage between $450mV$ to $1.9V$, obtaining a minimum power of output of $-28dBm$ and a maximum power of $5dBm$. Similarly, it was shown that the differential mixer and single-ended mixer have the same behavior in Linearity, Gc and modulation of the output power. According to the results obtained in the characterization of the prototype, we conclude that the behavior of the harmonic mixer follows the course anticipated in the synthesis of the mixer performed in Chapter Three.

6.2 Original Contributions

- In the analysis of the proposed harmonic mixers it was demonstrated that those have good performance in three of the five FOMs. All passive mixers present losses in its conversion factor which affects unfavorably the NF. However, the proposed single-ended mixer NF has a value of $2.7dB$, which can be considered a good number considering that the ideal value is $0dB$. The differential mixer has an NF of $6.25dB$, this was expected because the double number of active elements. With respect to the linearity, it was obtained for both mixers an IIP3 of $36dBm$, this is an excellent value. As a result, a large signal can be present at the input port, this helps the mixer output signal to be away from the noise floor. Both proposals have good ports isolation, which is inferior to $-20dB$ at $1GHz$. Furthermore, in the differential mixer, the LO is eliminated, which means that carrier feed through is not an issue in the upconversion case.

- One of the important contributions in this work is the variation of the output power in function of the duty cycle. This is helpful in systems where linearity is important, because when the output power is changed also the efficiency of the system is modified. For example, in the case of the TX, it is useful to increase the

output power of the mixer because this output is connected to a power amplifier (PA) which has the function of supplying the greatest amount of energy to the signal to be transmitted. However, the problem is that the energy supplied by PA may contains a huge distortion. Therefore, it is very useful that the mixer can control the output power of the harmonic of interest. On the other hand, at the RX is important to control the power of the harmonic of interest since it represents a control on the SNR. Therefore, increasing the output power also decreases the NF.

- In the literature there is already a mixer implemented with CMOS inverters, the architecture is called *H-Bridge Ring Mixer*. This topology simply eliminates some IM products and even harmonics. Furthermore using a differential LO signal complicates the implementation. In our proposal, by using a differential mixer we cancel the carrier without employing a differentially LO. Therefore, we can consider that the isolation port of $LO - to - V_{out}$ is perfect. However, for this to be true is necessary to take special care in designing the layout, otherwise LO can be suppressed to some extent but not totally erased.

- The design and simulation of the harmonic mixer was realized in UMC $0.18\mu m$ Mixed-Mode and RF CMOS $1.8V$ Twin-Well technology for two standards (Bluetooth and UWB). Furthermore, The design, fabrication and characterization of the harmonic mixer realized in a ON Semiconductor technology $0.5\mu m$. The results obtained in the UMC technology and in the characterization of the prototype indicate that the behavior of the mixer follows the curse anticipated in the synthesis.

- Table 6.2 details the results obtained. We see that the highest linearity obtained was for the MICS case with a value of 28.3dBm. The obtained NF is at an average level compared to others reported in the lietarture. Ours is the only approach which presents output power modulation.

Table 6.2: Comparison of different mixer topologies

Reference	This work	This work	This work	Jacob Pihl [21]	Eric A. M. Klumperink [28]	vincent J. Arkesteijn [29]	Sining Zhou [30]	E.De Backer [31]
Technology	UMC $0.18\mu m$	UMC $0.18\mu m$	ON Semiconductor $0.5\mu m$	$0.25\mu m$ CMOS	$0.18\mu m$	$0.18\mu m$	$0.18\mu m$	$0.25\mu m$ SiGe BiCMOS
Estandar	Bluetooth	UWB	MICS	-	-	-	-	-
RF Frequency	$2.4GHz$ - $2.485GHz$	$3.1GHz$ - $10.6GHz$	$402MHz$ - $405MHz$	-	-	-	$5.15GHz$ - $5.35HGz$ UNI band	$2MHz$ - $60MHz$
LO Frequency	$800MHz$	$772.5MHz$	$393.5MHz$	$2.1GHz$	$6GHz$	$1GHz$	-	-
BB Frequency	$10MHz$	$10MHz$	$10MHz$	-	-	-	-	-
Power supply	$1.8V$	$1.8V$	1.65	$1.8V$	$1V$	$1.8V$	-	$2.5V$
Power consumption	$35mW$	$10mW$	$28.2mW$	-	$0.49mW$	$200mW$	$17.5mA$	-
Conversion Factor	$-6.05dB$	$-6.63dB$	$-6.25dB$	$-7.1dB$	$8dB$	$25dB$	-	$-2.9dB$
IIP3	$15.5dBm$	$16.26dBm$	$28.3dBm$	$7dBm$	$6dBm$	$1dBm$	$-21dBm$	$20dBm$
Noise Figure	$8.03dB$	$7.1dB$	-	$6.8dB$	$25.8dB$	$6.5dB$	$5.3dB$	-
Power output	$-24dB$ @$Vb = 1V$	$-21.8dB$ @$Vd = 1V$	$5dBm$ @$Vb = 1.9V$	-	-	-	$29dB$	-
Duty cycle	40% - 7%	28% - 9%	46% - 25%	-	-	-	-	-

6.3 Recommendations for Future Work

- Chapter 3 presents the entire circuit analysis of the proposed circuits in order to get all the figures of merit. Therefore, are expressed all the design equations and if there is the need to know the performance of the proposed mixer with different CMOS technology, you only have to change the value of the mobilities, threshold voltages and oxide capacitances to get the performance with a different technology.

- Both the single-ended and differential mixers have good performance with respect to the figures of merit. However, it is recommend the use of the single-endedt mixer for the downconverter case. This is because the complexity and inconvenience of converting the RF signal to a differential mode.

- For Bluetooth and UWB designs, it is recommended to take into account the threshold voltage of the inverter gate. However, it is not convenient to design with angles lesser than 30% because this affects the slope of transition making it slower, which causes more IM products.

Bibliography

[1] G. Han and E. Sanchez-Sinencio, "CMOS transconductance multipliers: a tutorial," *Circuits and Systems II: Analog and Digital Signal Processing, IEEE Transactions on*, vol. 45, no. 12, p. 1550–1563, Dec 1998.

[2] B. Razavi, *Rf Microelectronics*. Prentice Hall, 1998.

[3] E. S. Sinencio, "Mixer," Analog and Mixed-Signal Center, TAMU, College Station, Texas 77843-3128 318E Wisenbaker Engineering Research Center, Tech. Rep., Oct. 2008. [Online]. Available: http://amesp02.tamu.edu/~sanchez/665%20Mixer%202008.pdf

[4] T. Lee, *The Design of CMOS Radio-Frequency Integrated Circuits*. Cambridge University Press, 2003.

[5] G. Vasilescu, *Electronic Noise and Interfering Signals: Principles and Applications*, ser. Signals and Communication Technology. Springer, 2005.

[6] H. S. Ramírez, "Diseño de mezcladores en if para un procesador gsm de frecuencia intermedia," Master's thesis, Instituto Nacional de Astrofísica Óptica y Electrónica, Luis Enrique Erro # 1, Tonantzintla, Puebla, México C.P. 72840 | Teléfono: (222) 266.31.00, May 2002.

[7] C. D. Hull and R. G. Meyer, "A systematic approach to the analysis of noise in mixers," *EEE TRANSACTIONS ON CIRCUITS AND SYSTEMS-I: FUNDAMENTAL. THEORY AND APPLICATIONS*, vol. 40, no. 12, pp. 909–919, Dec. 1993.

[8] L. Li and H. Tenhunen, "Noise analysis of monolithic rf balanced down conversion mixers," *Mixed-Signal Design, 2001. SSMSD. 2001 Southwest Symposium on*, pp. 70–75, Feb. 2001.

[9] B. Razavi, T. Aytur, C. Lam, F.-R. Yang, Kuang-Yu, R.-H. Yan, H.-C. Kang, C.-C. Hsu, and C.-C. Lee, "A uwb cmos transceiver," *IEEE JOURNAL OF SOLID-STATE CIRCUITS*, vol. 40, no. 12, Dec. 2005. [Online]. Available: http://www.ee.ucla.edu/~brweb/papers/Journals/R%26AetcDec05.pdf

[10] J. Griggs, P. Yin, Z. Wang, and N. S. Dogan, "Low-power medical implant communication service (mics) transceiver," Department of Electrical and Computer Engineering North Carolina A&T State University, Tech. Rep., 2007.

[11] J. Kardach. Bluetooth special interest group. [Online]. Available: https://www.bluetooth.org/en-us

[12] B. Leung, *VLSI for Wireless Communication*. Springer, 2011.

[13] M. Radmanesh, *Advanced Rf & Microwave Circuit Design: The Ultimate Guide to Superior Design*. AuthorHouse, 2008. [Online]. Available: http://booklens.com/matthew-m-radmanesh/advanced-rf-microwave-circuit-design

[14] A. Chenakin, *Frequency Synthesizers: Concept to Product*, ser. Artech House microwave library. Artech House, Incorporated, 2011.

[15] I. Glover, S. Pennock, and P. Shepherd, *Microwave devices, circuits and subsystems for communications engineering*. John Wiley & Sons, Ltd, 2005.

[16] B. Schiek, H.-J. Siweris, and I. Rolfes, *Noise in High-Frequency Circuits and Oscillators*, 1st ed. Wiley-Interscience, Jun. 2006.

[17] E. Carey and S. Lidholm, *Millimeter-Wave Integrated Circuits*. Springer, 2005.

[18] L. Besser and R. Gilmore, *Practical RF Circuit Design for Modern Wireless Systems*, ser. Artech House microwave library. Artech House, 2003, no. v. 1.

[19] C. J. Kikkert, *RF Electronics.* AWR Corp., 2009.

[20] K. Du and N. Swamy, *Wireless Communication Systems: From RF Subsystems to 4G Enabling Technologies.* Cambridge University Press, 2010. [Online]. Available: http://books.google.com.mx/books?id=5dGjKLawsTkC

[21] J. Pihl, K. Christensen, and E. Bruun, "Direct downconversion with switching cmos mixer," *Circuits and Systems, 2001. ISCAS 2001. The 2001 IEEE International Symposium*, vol. 1, pp. 117–120, May 2001.

[22] B. Razavi, "Design considerations for future rf circuits," in *ISCAS*, 2007, pp. 741–744.

[23] H. Hsu, R. Mehra, and R. Torres, *Análisis de Fourier*, ser. Colección de Teoría y Problemas con Solución. Fondo Educativo Interamericano, 1973.

[24] J. Uyemura, *Circuit design for CMOS VLSI.* Kluwer Academic Publishers, 1992.

[25] J. Rabaey, *Digital Integrated Circuits: A Design Perspective*, ser. Prentice Hall electronics and VLSI series. Prentice-Hall International (UK), 1996.

[26] "Umc 0.18μm 1p6m salicidemixed-mode/rf cmos model," Giga Solution Tech. Co., Ltd, Tech. Rep., 2003.

[27] P. Bradley and Z. Semicond, "Wireless medical implant technology - recent advances and future developments," *ESSCIRC (ESSCIRC), 2011 Proceedings of the*, pp. 37–41, Sep. 2011.

[28] E. A. M. Klumperink, S. M. Louwsma, G. J. M. Wienk, and B. Nauta, "A cmos switched transconductor mixer," *Solid-State Circuits, IEEE Journal*, vol. 39, no. 8, pp. 1231–1240, Aug. 2004.

[29] V. Arkesteijn, E. Klumperink, and B. Nauta, "A wideband high-linearity rf receiver front-end in cmos," *Solid-State Circuits Conference, 2004. ESSCIRC 2004. Proceeding of the 30th European*, pp. 71–74, Sep. 2004.

[30] S. Zhou and M.-C. Chang, "A cmos passive mixer with low flicker noise for low-power direct-conversion receiver," *Solid-State Circuits, IEEE Journa*, vol. 40, no. 5, pp. 1084–1093, May 2005.

[31] E. D. Backer, J. Bauwelinck, C. Melange, and E. Matei, "2.5 v passive cmos mixer with 20 dbm p1 db compression," *Electronics Letters*, vol. 44, no. 18, pp. 1067–1068, Aug. 2008.

[32] B. Razavi, *Dsign Of Analog Cmos Intgrtd Circuits*, ser. McGraw-Hill series in electrical and computer engineering: Circuits and systems. Tata McGraw-Hill, 2002.

[33] T. Sarkar, R. Mailloux, A. Oliner, and D. Sengupta, *History of Wireless*, 1st ed., ser. Wiley Series in Microwave and Optical Engineering. Wiley, jan 2006.

[34] H. Luediger and S. Zeisberg, "Uwb performance assessment based on recent fcc regulation and measured radio channel characteristics." IST Mobile Summit 2002, Jun. 2002. [Online]. Available: http://www.whyless.org/files/public/WP5_luediger_zeisberg_ist2002.pdf

[35] J.-S. Lee, Y.-W. Su, and C.-C. Shen, "A comparative study of wireless protocols: Bluetooth, uwb, zigbee, and wi-fi." The 33rd Annual Conference of the IEEE Industrial Electronics Society (IECON), Nov. 2007. [Online]. Available: http://eee.guc.edu.eg/Announcements/Comparaitive_Wireless_standards.pdf

[36] I. W. G. 802.20, "802.20 evaluation criteria," Sep. 2005. [Online]. Available: http://ieee802.org/20/P_Docs/IEEE_802.20-PD-09.doc

[37] B. Walke, S. Mangold, and L. Berlemann, *IEEE 802 Wireless Systems: Protocols, Multi-Hop Mesh/Relaying, Performance and Spectrum Coexistence*. Chichester Hoboken, NJ: John Wiley Sons, nov 2006.

[38] S. Smolskiy, L. Belov, and V. Kočemasov, *Handbook of RF, Microwave, and Millimeter-Wave Components*, ser. Artech House microwave library. ARTECH HOUSE Incorporated, 2012.

[39] T. Melly, NewAuthor2, NewAuthor3, and E. A. Vittoz, "An analysis of flicker noise rejection in low-power and low-voltage cmos mixers," *EEE JOURNAL OF SOLID-STATE CIRCUITS*, vol. 36, no. 1, pp. 102–109, Jan. 2001.

[40] J. Lerdworatawee and W. Namgoong, "Generalized linear periodic time-varying analysis for noise reduction in an active mixer," *IEEE JOURNAL OF SOLID-STATE CIRCUITS*, vol. 42, no. 6, pp. 1339–1351, Jun. 2007.

[41] W. Cheng, A. J. Annema, J. A. Croon, and B. Nauta, "Noise and nonlinearity modeling of active mixers for fast and accurate estimation," *IEEE TRANSACTIONS ON CIRCUITS AND SYSTEMS—I: REGULAR PAPERS*, vol. 58, no. 2, pp. 276–289, Feb. 2011.

[42] M. T. Terrovitis and R. G. Meyer, "Noise in current-commutating cmos mixers," *IEEE JOURNAL OF SOLID-STATE CIRCUITS*, vol. 34, no. 6, pp. 772–783, Jun. 1999. [Online]. Available: http://rfic.eecs.berkeley.edu/files/jssc_jun99_2.pdf

[43] H. Darabi and A. A. Abidi, "Noise in rf-cmos mixers: A simple physical model," *IEEE TRANSACTIONS ON SOLID STATE CIRCUITS*, vol. 35, no. 1, pp. 15–25, Jan. 2000.

[44] A. R. Petrov, "System approach for low l/f noise, high ip2 dynamic range cmos mixer design," *University/Government/Industry Microelectronics Symposium, 2003. Proceedings of the 15th Biennial*, pp. 74–77, Jul. 2003.

[45] J. Pedro and N. Carvalho, *Intermodulation Distortion in Microwave and Wireless Circuits*, ser. Artech House microwave library. Artech House, 2003.

[46] Y. Ding and R. Harjani, *High-Linearity CMOS RF Front-End Circuits*. Springer, 2005.

[47] H. Veendrick, *Deep-Submicron Cmos Ics: From Basics to Asics*. Kluwer, 2000.